Brigham Young University
Department of Electrical and Computer Engineering

459 Clyde Building
Provo, Utah 84602

Current Progress in Ku-Band Model Functions

A report by the NSCAT Science Working Team Subcommittee on Geophysical Model Functions

David G. Long
Committee Chair

August 1996

MERS Technical Report # MERS 96-002
ECEN Department Report # TR-L100-96.2

Microwave Earth Remote Sensing (MERS) Laboratory

Current Progress in Ku-Band Model Functions

a report by the

NSCAT Science Working Team
Subcommittee on Geophysical Model Functions

Release Version 2.0

August 1996

Current Progress in Ku-Band Model Functions

This report has been prepared by the

NSCAT Science Working Team Geophysical Model Function Subcommittee

for the NSCAT Project

Subcommittee Members

David G. Long (Chair)
Mark A. Donelan
Michael H. Freilich
Hans C. Graber
Harunobu Masuko
Willard J. Pierson, Jr.
William J. Plant (adjunct member)
David Weissman (adjunct member)
Frank Wentz

Subcommittee Charter

The NSCAT SWT Model Function Subcommittee will evaluate existing and new or proposed Ku-band model functions relating sigma-0 to vector winds and/or wind stress. The evaluation will consider the effects of other geophysical quantities (e.g., long waves, sea surface temperature). Emphasis will be placed on understanding and quantifying errors and error sources in the model function and the resulting error characteristics in the retrieved wind. The evaluation must include both science and practical implementation issues. As appropriate the subcommittee will recommend and/or endorse changes in the model function and its error analysis. The subcommittee will also consider providing inputs to the project-sponsored verification and validation activities. On an occasional basis the subcommittee will evaluate plans for other NASA-funded, related (but not necessarily NSCAT-funded) field activities.

Foreward

While wind scatterometry is a proven technique for measuring near-surface winds from space, it is an indirect technique requiring the use of a geophysical model relating the measured parameter, sigma-0, to the wind. Thus the accuracy of the inferred wind is dependent not only on the accuracy of the sigma-0 measurement (which falls within the purview of the radar engineer and which much be adequately defined for the geophysicists), but also on the accuracy of the geophysical model function. A quantitative analysis of the accuracy of the estimated winds requires a detailed knowledge of the model function and its uncertainties. Research since the development of the first Ku-band model function (known as SASS-1) has suggested that further refinements of the model function are desirable. To utilize scarce resources most effectively for model function refinement activities, it is appropriate to review the current state-of-the-art in Ku-band model function and, as users of the scatterometer data, make prioritized recommendations and suggestions for future model function refinement activities to support the NSCAT mission.

This second revision includes additional references and incorporates comments resulting from the May 1996 ADEOS/NSCAT SWT meeting in Pasadena.

Model function research is actively being pursued in many areas. Thus, this report is necessarily incomplete nor is the report without flaws. Additions and corrections to the text as well as additional bibliographic references are welcomed. Please send your comments and inputs to:

David G. Long, chair
NSCAT SWT Subcommittee on Geophysical Model Functions
Electrical and Computer Engineering Department
459 Clyde Building
Brigham Young University
Provo, Utah 84602
long@ee.byu.edu
(801) 378-4383

Table of Contents

Abstract/Summary

The SEASAT Scatterometer (SASS) first demonstrated that winds could be measured from space more than a decade ago. The success of this mission has lead to the development of several new scatterometers by the U.S. and other countries. In particular, a SASS follow-on scatterometer, the NASA Scatterometer (NSCAT), will be orbited aboard the Japanese Advanced Earth Observing Satellite (ADEOS) planned for launch in 1996.

Wind scatterometry is based on an indirect measurement technique and requires the use of a *geophysical model function* relating the measured parameter, the normalized radar cross-section (sigma-0), to the near-surface wind. The model function is the relationship between the wind velocity and the radar backscatter. Understanding of the model function requires a knowledge of *both* the relationship between the wind and the two dimensional geometry of the sea surface *and* the relationship of the surface geometry and sigma-0 at moderate incidence angles.

While a complete understanding of the model function remains illusive, existing empirical model functions have demonstrated that the accuracy of wind vectors derived from scatterometer measurements is suitable for a wide variety of global and mesoscale studies of wind dynamics, wind-driven ocean circulation, and air/sea interaction. To improve the accuracy of scatterometer-derived winds as well as to better understand the relationship between wind and waves, research into improved geophysical model functions continue.

This report reviews the current state-of-the-art in understanding and developing improved Ku-band geophysical model functions to support the NSCAT mission. Historical background and context within the NSCAT mission are briefly considered. Approaches to developing the geophysical model function, including empirical and dynamically-based approaches, are discussed. While the most successful model functions have been derived empirically [e.g., SASS-1 and the model of *Wentz* et al., (1984)], recent progress in dynamically-based functions is encouraging. We consider and compare several existing model functions and suggest criteria for the selection of a model function for processing NSCAT data.

As background for our recommendations for future model function research we consider the sensitivity of radar backscatter to the wind and other geophysical parameters and the problems of accurately measuring these parameters. In particular, we consider the still-open question of the fundamental variable controlling sigma-0: wind speed, wind stress, or u*, and suggest directions for future work in this area.

We consider an essential part of the development of the model function to be the determination of the modeling error, discuss possible approaches for evaluating the modeling error, and provide recommendations for use in processing NSCAT data. After discussing current and planned model function refinement activities, we make summary recommendations for future refinement efforts, particularly in regard to the NSCAT verification experiments.

I. Introduction

The oceans of the Earth work in concert with the atmosphere to control and regulate the environment. Fed by the sun, the interaction of land, ocean, and atmosphere produces the phenomenon of weather and climate. Only in the past half century have meteorologists begun to understand weather patterns well enough to produce relatively accurate, although limited, forecasts of future weather patterns. One of the limitations of predicting future weather is that meteorologists do not adequately know the *current* weather. An accurate understanding of current conditions over the ocean is required to predict future weather patterns. Until recently, detailed local oceanic weather conditions were available only from sparsely arrayed weather stations, ships along commercial shipping lanes and sparsely distributed ocean buoys. Knowledge of conventional meteorological conditions over most of the oceans remain unavailable.

The development of satellites for remote sensing has improved the situation significantly. Satellite remote sensing has the potential to provide measurements of local weather conditions with unprecedented frequency and spatial resolution. Of primary importance in the remotely sensed data is the determination of accurate, high resolution wind fields over the ocean's surface to support global weather forecasting, air/sea interaction studies and climate change programs. In 1978 the experimental SEASAT radar scatterometer (SASS) first demonstrated the ability to accurately infer vector winds over the ocean's surface from space. The success of SASS has lead to the development of additional scatterometer systems such as the NASA Scatterometer (NSCAT) and the ESA AMI scatterometer.

Wind scatterometers are active microwave instruments designed specifically to allow estimation of near-surface wind velocity (both speed and direction) over the ocean under near all-weather conditions. Principles of scatterometry, and the hardware and ground processing designs for NSCAT in particular, are described in *Naderi* et al. (1991) as well as many textbooks on remote sensing. In short, scatterometers allow estimation of ocean surface vector winds based on measurements of the backscatter cross-section of the sea surface at moderate incidence angles. Although the mechanisms responsible for the measured backscattered power under realistic oceanic conditions are not completely understood, dynamically-based theoretical analyses, controlled laboratory and field experiments, and measurements from previous spaceborne radars all confirm that the ocean's normalized radar cross-section at moderate incidence angles is substantially dependent on near-surface wind speed and azimuthal direction (with respect to the radar viewing geometry). Multiple spatially and temporally colocated measurements of radar cross-section, obtained from different viewing geometries, can thus be used to estimate wind velocity if the dependence between backscatter cross-section and environmental conditions are known for the particular radar and geometric parameters of the instrument. The relationship between backscatter cross-section and environmental parameters (chiefly wind velocity) for given radar/geometric parameters is known as the "Geophysical Model Function" and is the primary focus of this report.

At a given frequency the geophysical model function may be expressed as,

$$\sigma^o = f(|U|, \chi, ...; \theta, p) \qquad (1.1)$$

where σ^o is the normalized radar backscatter coefficient (sigma-0), $|U|$ is the wind speed, χ is the relative azimuth angle between the incident electromagnetic wave (see Fig. 1.1), "..." represents the (possibly small) effects of non-wind variables such as long waves, atmospheric stratification, water temperature, etc., θ is the incidence angle, and p is the polarization. In this context the terms "wind speed" and "wind direction" denote the magnitude and direction, respectively, of the wind-like vector quantity.

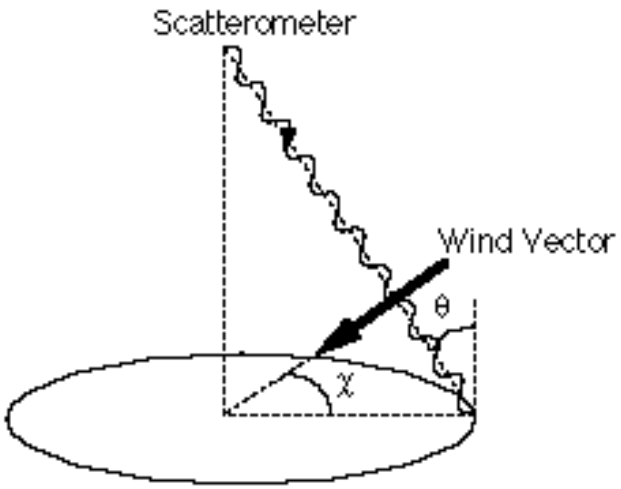

Figure 1.1. Geometric definition of the incidence θ and relative azimuth χ angles.

While geophysical model functions have been extensively studied since before the flight of SASS, there still remains significant room for model function refinement. This includes identification of any important subsidiary parameters [the "..." in Eq. (1.1)] as well as better understanding the basic functional form of the relationship between sigma-o and the wind velocity alone. The full definition of f in Eq. (1.1) must embody both of these aspects.

Calculation of the wind velocity from scatterometer measurements involves three distinct (but related) aspects:

1) acquisition of accurate, colocated measurements of the backscatter cross-section of the ocean from several different viewing geometries;

2) knowledge of the model function which is relationship between the backscatter cross-section, environmental conditions (principally wind velocity), and the radar parameters; and

3) determination, using an objective algorithm, of a (possibly set of) wind velocities consistent with both the set of backscatter measurements and the model function ("wind retrieval").

A separate step, known as ambiguity removal, may be required to select a unique wind direction from the set of wind velocities produced by wind retrieval.

Errors in the final retrieved wind velocities are dependent not only on the model function, but also on errors in the backscatter measurements themselves and details of the wind retrieval algorithm. The nonlinear natures of both the model function and the retrieval algorithms have thus far precluded the development of analytical expressions relating errors in the inputs (measurements and/or model function) to errors in the final retrieved winds. The challenges of scatterometry thus include development of robust wind retrieval algorithms and accurate characterizations of input error statistics, in addition to the more obvious difficulties associated with specifying an accurate model function and acquiring accurate backscatter measurements.

Model function accuracy thus cannot be meaningfully discussed and evaluated in isolation from the accuracy of the backscatter measurements and the details of the wind retrieval algorithms used to process the data. This report therefore first examines the expected error structure of the backscatter measurements to be acquired by the NSCAT instrument on the

ADEOS-I spacecraft. This is followed by an examination of the Maximum Likelihood retrieval algorithm selected for use in the baseline NSCAT ground processing system. While neither of these topics directly addresses the model function itself, the aims are to identify the types and magnitudes of measurement errors, and the ways in which *estimates* of both measurement and model function errors are used to weight the backscatter data in the wind retrieval processing.

The report then summarizes what is known analytically or through carefully controlled experiments regarding the dependence of centimetric waves and radar backscatter on environmental conditions (and viewing geometry). While theoretical and experimental studies have contributed greatly to the understanding of small-scale air-sea momentum transfer and wave generation by wind, it is clear that substantial gaps in our knowledge remain. In particular, it is apparent that backscatter is related to a host of environmental conditions (e.g., sea-surface temperature, surface tension due to films and contaminants, details of the long wave field, etc.), all of which must be measured independently if a perfect wind measurement is to be calculated from scatterometer data. Unfortunately, while winds constitute the *dominant* influence on backscatter and centimetric surface waves, present analytical understanding is insufficient to even allow the *relative* influences of the subsidiary geophysical effects to be quantified over the wide range of globally occurring conditions. We must, therefore, reluctantly conclude that although detailed process studies should continue to be vigorously pursued, it is unlikely that they will provide accurate, dynamically based scatterometer model functions that can be used operationally during the NSCAT time frame.

The flights of previous and ongoing spaceborne and airborne scatterometers have clearly demonstrated, however, that although perfect radar scatterometers may never yield *perfectly* accurate wind velocity estimates, scatterometers are the only demonstrated spaceborne instruments capable of measuring near-surface wind *velocities* with sufficient accuracy to contribute substantially to many studies in oceanography, meteorology, air-sea interaction, and climate change.

With this in mind the remainder of the report thus addresses a set of important, but tractable issues associated with defining the dominant influence of winds on backscatter (as a function of radar/geometry parameters) so as to:

1) allow accurate wind velocities (meeting the Science and Mission requirements) to be calculated from NSCAT backscatter measurements, using physically reasonable assumptions and resulting in measurements with minimal bias and small systematic errors;

2) allow reasonable estimates to be made of the uncertainties and errors in the model function, so that NSCAT winds can be calculated accurately using the baseline Maximum Likelihood estimation algorithm (described in the Appendix) as well as provide error estimates of the retrieved wind; and

3) allow the model function to be updated to reflect increased knowledge (e.g., the effects of selected, independently measurable subsidiary effects such as sea-surface temperature) without requiring redesign or even substantial revision of the wind retrieval algorithms.

In particular, the following questions are addressed are addressed in this report:

1) Of the published model functions based on actual aircraft and/or Ku-band satellite scatterometer measurements, which is the "best" (in the sense that the quantified accuracy and all required measurements/inputs will be available during the NSCAT

time period)? This model function will be used during the initial post-launch period prior to the development of a refined model function based on NSCAT data.

2) What known (and correctable) systematic inaccuracies in the "best" model function exist, and how can they best be remedied before the launch of NSCAT? (e.g., are present data sets sufficient to allow the fundamental wind quantity on which backscatter depends to be identified -- velocity, friction velocity, or vector wind stress? Similarly, are present data sets sufficient to allow the efficacy of low-order truncated Fourier series in azimuth to be evaluated?)

3) What analysis techniques should be developed or refined to allow quantitative estimates of model function uncertainty and statistics to be calculated using existing data or using NSCAT data acquired soon after the launch of ADEOS-I?

4) What auxiliary data sets should be acquired during the flight of NSCAT (and especially during its validation period to allow questions (2,3) to be answered?

A. Report Scope Limitation

This report considers the only current "state of the art" in Ku-band geophysical model functions with emphasis on applications connected with the NSCAT project. As a result, C-band models are not considered in any detail. However, very useful techniques have been developed for C-band data which can be used when NSCAT data becomes available.

B. References

Naderi, F. M., M. H. Freilich, and D. G. Long, "Spaceborne Radar Measurement of Wind Velocity Over the Ocean--An Overview of the NSCAT Scatterometer System", *Proceedings of the IEEE*, pp. 850-866, Vol. 79, No. 6, June 1991.

II. Ku-Band Model Function Background

In this report we are primarily interested in "operational" Ku-band model functions, i.e., tabulated or functional forms (with known coefficients) suited for use in wind retrieval from spaceborne scatterometer measurements. Thus, pure electromagnetic scattering models which require known surface profiles or other information unavailable for NSCAT wind retrieval are not considered. Operational model functions permit computation of sigma-0 from a wind or wind-like variable and (possibly) available auxiliary information.

For use in wind retrieval from NSCAT measurements, the model function must usable over an incidence angle range of approximately 15° to 65° and an azimuth angle range of 0° to 360° with both V and H polarization. Operational model functions considered in this report are identified in a later following section.

Because NSCAT is a follow-on to the Seasat mission, Ku-band operation at nearly the same frequency has been used rather than C-band like ERS-1/ERS-2. While C-band is less sensitive to atmospheric attenuation due to rain, Ku-band is much more sensitive to the wind (*Long et al.,* 1996).

A. General model function characteristics

While existing model functions differ in detail, the share many common features. These are summarized here and schematically illustrated in Fig. 2.1. First, at a fixed incidence angle all model functions predict an increase in sigma-0 with wind speed (at least for moderate wind speeds 3-15 m/s). The wind speed dependence of sigma-0 at a fixed incidence and azimuth angle is frequently expressed as a power-law. For a given wind speed, sigma-0 exhibits a biharmonic dependence on the wind direction. As discussed later, this feature of the model function is a driving in the retrieval of wind vectors from measurements of sigma-0

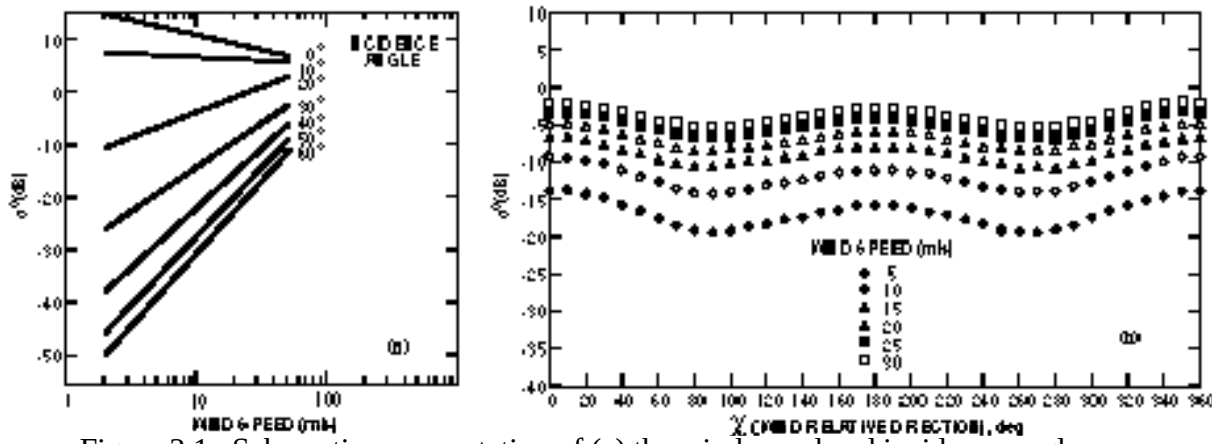

Figure 2.1. Schematic representation of (a) the wind speed and incidence angle dependence of the model function (at a fixed wind direction) and (b) the wind speed and direction dependence at a fixed incidence angle based on the SASS-1 model function.

B. Existing Model Functions

To date, the most successful Ku-band model functions have been empirically derived. While model function for high incidence angle sea clutter have existed for some time (e.g., *Wright,* 1968), the first model function widely used for Ku-band wind retrieval was SASS-1 (*Bracalente et al.,* 1980; *Jones et al.,* 1982; *Schroeder et al.,* 1982). Using the SASS-1 model function, SASS was determined to have met wind measurement accuracy

requirements of 2 m/s rms wind speed accuracy and 20° direction accuracy of the ambiguity closest to the true wind (*Stewart,* 1985).

Later, *Wentz* et al. (1984) developed a model function based on the statistics of the SASS data and some aircraft data. This model function has become commonly known as the Wentz or SASS-2 model function. While SASS-1 and SASS-2 differ in detail, they are qualitatively very similar. Further discussion of the differences between these and other models are given later.

Potentially operational model functions based on theoretical derivations include *Plant* (1986) and *Donelan and Pierson* (1987). Other models worth noting include *Chen et al.* (1992) and *Durden and Vesecky* (1985) although these are not "operational" model functions as defined above.

C. References

Bracalente, E., D. Boggs, W. Grantham, and J. Sweet, "The SASS1 Scattering Coefficient (sigma-0) Algorithm," *IEEE J. Oceanic Engineering*, Vol. OE-5, No. 2, pp. 145-154, April 1980.

Chen, K.M., A. Fung and D.E. Weissman, "A Backscattering Model for the Ocean Surface", *IEEE Transactions on Geoscience & Remote Sensing*, Vol. 30, No. 4, pp 811-817, July 1992.

Donelan, M. A., and W.J. Pierson, Jr., "Radar Scattering and Equilbrium Ranges in Wind-Generated Waves with Application to Scatterometry," *J. Geophys. Res.*, Vol. 92, pp. 4971-5029, 1987.

Durden, S.L., and J.F. Vesecky, "A Physical Radar Cross Section Model for a Wind Driven Sea with Swell", *IEEE J. Ocean. Engg*, Vol. OE-10, pp 445-451, October, 1985.

Jones, W. L., L. C. Schroeder, D. H. Boggs, E. M. Bracalente, R. A. Brown, G. J. Dome, W. J. Pierson, and F. J. Wentz, "The SEASAT-A Satellite Scatterometer: The Geophysical Evaluation of Remotely Sensed Wind Vectors Over the Ocean," *J. Geophys. Res.*, Vol. 87, No. C5, pp. 3297-3317, April 1982.

Long, D.G., R.S. Collyer, R. Reed, and D.V. Arnold, "Dependence of the Normalized Radar Cross Section of Water Waves on Bragg Wavelength--Wind Speed Sensitivity," *IEEE Trans. Geosc. and Remote Sens.*, Vol. 34, No. 3, pp 656-666, 1995.

Plant, W. J., "A Two-Scale Model of Short Wind-Generated Waves and Scatterometry," *J. Geophys. Res.*, Vol. 91, pp. 10735-10749, 1986.

Schroeder, L., et al., "The Relationship Between the Wind Vector and the Normalized Radar Cross Section Used to Derive Seasat-A Satellite Scatterometer Winds," *J. Geophys. Res.*, Vol. 87, No. C5, pp. 3318-3336, 1982.

R. H. Stewart, "Seasat Success Statement," JPL Publication D-2841, April 11, 1985.

Wentz, F. J., S. Peteherych, and L.A. Thomas, "A Model Function for Ocean Radar Cross-sections at 14.6 GHz," *J. Geophys. Res.*, Vol. 89, pp 3689-3704, May 20, 1984.

Wright, J. W., "A New Model for Sea Clutter", *IEEE Trans. Antennas and Prop.*, AP-16, p. 217, 1968.

III. Relationship of Wind Retrieval to the Model Function

The geophysical model function defined in Eq. (1.1) is a *forward* model, i.e., the radar backscatter, sigma-0, is expressed as a function of the wind vector. To "retrieve" a wind from measurements of sigma-0, the model must, in effect, be inverted to determine the vector wind. Because of the biharmonic nature of the model function with respect to wind direction, the model function can not be directly inverted since it would be double valued. Rather that directly inverting the model function, the wind vector is *retrieved* from multiple measurements of sigma-0 from different azimuth angles with the aid of an objective function. The accuracy of the wind estimate is determined not only by the geophysical model but also by the wind retrieval process. In this section the relationship between the model function and the wind retrieval process are explored. The effects of errors in the measurement of sigma-0 are first considered.

A. Sigma-0 measurement errors

The fundamental direct measurement obtained by scatterometer instruments is received power. Although the mathematical transformations required to convert these direct measurements into the apparent normalized radar cross-section of the ocean (sigma-0) are thoroughly understood from a physical standpoint, the calculations require knowledge of many spacecraft and instrument calibration parameters which are often not known perfectly. Thus, while errors in retrieved winds arise from inaccuracies in the specification of the model function, inaccuracies in the sigma-0 values derived from the scatterometer basic measurements also contribute significantly. This section describes the dominant sigma-0 errors. As noted above and discussed in more detail in the following section on wind retrieval, accurate specification of the statistical distribution of these errors is needed if the results of the maximum likelihood wind retrieval are to be properly interpreted (see Appendix A).

Probably the primary source of error in the sigma-0 "measurements" results from uncertainties in the values of parameters used to calculate sigma-0 from the received radar power measurements, and in particular the error in the determination of the attitude of the spacecraft (*Pierson*, 1989, 1990). This error is known in scatterometer jargon as "retrieval Kp" where the "retrieval" refers to the calculation of sigma-0 from the power measurements. While the precise value of the retrieval Kp is dependent on the (unknown) calibration errors in the instrument system and on spacecraft attitude control, the pre-launch retrieval Kp for NSCAT is estimated to <0.35 dB.

Pierson (1989) treated this source of variability (retrieval Kp) as an independent random variable for every backscatter estimate. As he points out, this is unrealisitic since the unknown attitude error is expected to remain roughly constant over fairly long segments of a given revolution and will depend upon the details of the spacecraft systems that control and adjust the attitude of the spacecraft. Treating the temporally correlated attitude errors incorrectly as uncorrelated between measurements can lead to biases in wind recoveries that are dependent on errors in the knowledge of spacecraft roll and pitch attitude. Unfortunately, biases in the retrieved winds due to attitude knowledge errors have not been studied thoroughly although *Long* (1991) has formulated the ML retrieval algorithm to incorporate correlation in the sigma-0 retrieval error.

The other major source of sigma-0 error is the communication noise (known in scatterometer jargon as "communication Kp" -- see Appendix A and *Long and Mendel*, 1991) inherent in the radar receiver and measurement strategy. In order to estimate the backscatter cross-section of the ocean surface, separate measurements of the "signal+noise" power (including backscattered power, 14 GHz emissions from the sea surface and the

intervening atmosphere, and instrumental noise) and "noise-only" power (including only 14 GHz emissions and instrumental noise) are subtracted to obtain an estimate of the backscattered power alone (related to sigma-0 via the radar equation). However, because both the "signal+noise" and "noise-only" measurements are realizations of random processes, the subtraction can lead to negative "signal" power estimates, particularly when the backscattered power is very low compared with the "noise" power. As discussed later in this report this may be a concern when the wind is not strong enough to generate the Bragg scattering ripples on the water resulting in very small sigma-0 values (see *Donelan and Pierson,* 1987).

The communication Kp is a function of the radar signal-to-noise ratio and therefore on the true value of sigma-0 (see Appendix A). For NSCAT the communication Kp ranges from approximately 0.02 at high SNR values (SNR > 10 dB) to over 1 at extremely low SNR values (SNR <-15 dB). For wind speeds greater than 4 m/s the SNR is generally good with corresponding communication Kp values typically less than 0.08.

B. Error structure due to retrieval process

There are no existing analytical techniques to determine the accuracy of the retrieved winds from estimates of the sigma-0 sampling variability. However, Monte Carlo simulations suggest that the wind velocity errors resulting from sampling variability of the backscatter estimates is small (*Long*, 1988). *Leotta and Long* (1989) used simulations of the NSCAT system to study the statistics of the errors in the estimated wind vectors (assuming a maximum likelihood (ML) wind retrieval algorithm and the *Wentz et al.* (1984) SASS-2 model function). The normalized wind speed error was found to be Gaussian with a variance dependent on instrument design parameters, and the wind direction errors were dependent on the true wind direction. They developed a scheme for predicting the rms wind direction error of the ambiguity closest to the true wind from the instrument design without extensive simulation.

Long (1991) expanded the error and noise modeling approach of *Long and Mendel* (1991) to incorporate correlated noise and retrieval error. Using the ML estimator, Monte Carlo simulations were performed with the ML algorithm and expected design values for the NSCAT instrument. Although the number of cases considered was limited, the results indicated that the wind direction error characteristics were not affected by correlation in the noise and retrieval error. However, the correlation of the noise and error resulted in increased mean wind speed error (bias) and reduced wind speed error variance. Unfortunately, the computation required for wind retrieval using the correlated noise model is significantly more than in the uncorrelated case. Further studies have not been completed because of the lack of suitably accurate estimates of the noise and retrieval error correlation coefficients. However, given sufficient data, it may be possible to estimate the correlation coefficients as well as the measurement biases using a maximum a posterior (MAP) estimation technique.

Recently, *Oliphant and Long* (1996a) derived the Cramer-Rao bound for scatterometer wind retrieval. The C-R bound provides an analytic lower bound on the wind estmate error when a maximum likelihood estimator is used. This bound can be useful for scatterometer design tradeoffs and analysis. For example, *Oliphant and Long* (1996a) were able to explain the variations in wind direction rms error observed in simulations. This variation is not the result of errors in the model function. The C-R bound suggests that this is less information in the sigma-0 measurements for wind aligned with the fore/aft beams.

Previously, the previous lack of an analytical technique for determining the accuracy of the retrieved winds has forced reliance on simulation. However, there are significant limits to simulation techniques. Since the same model function is generally used for generating

sigma_0 values from the wind as is used for retrieving the wind from the noisy sigma-0 measurements the simulations can give little insight into the geophysical modeling error (compare *Pierson*, 1989). Nevertheless, simulations can be useful in understanding the errors associated with the wind retrieval process.

B. ML versus other retrieval algorithms

The maximum likelihood wind retrieval algorithm is valid only if the probabilistic structure of the sample backscatter values is correct. The sample backscatter values in natural units are normally distributed random variables with the important property that the variance is a function of the true first moment. Thus if the expected value of the backscatter is known, the variance is also known, and the probability distribution function is a function of only one parameter. The maximum likelihood estimate maximizes the probability that the sample values were the result of the recovered wind speed and direction (see Appendix A).

The detailed application of the maximum likelihood estimate varies from implementation to implementation. In its pure form the ML estimator involves the natural logarithm of the standard deviation of the expected value (see Appendix A). Although the standard deviation of the backscatter sample enters into the theory, a modified maximum likelihood estimate where these terms in the maximum likelihood estimate have been omitted has been suggested by *Pierson* (1989, 1990). While there is no apparent theoretical advantage in this approach (there is a small computational savings), this approach has been successfully used with ERS-1 C-band data. However, it has recently been shown that a decision-theoretic technique for discarding extra ambiguities can be applied when an ML estimator is used (*Oliphant and Long*, 1996b). This technique can simplify ambiguity removal.

Chi and Li (1987) considered a number of other wind retrieval algorithms using the SASS-1 model function. They concluded that the ML algorithm was generally superior to other algorithms, resulting in the minimum RMS errors in the retrieved winds.

C. Geophysical modeling error

In order to place accurate bounds on the error in the retrieved winds knowledge of both the retrieval error and the geophysical modeling error is required. The modeling error may be defined as the variability in the observed sigma-0 for a given point in the model parameter space. By definition such variability is due to the effects of unmodeled geophysical parameters on sigma-0. Variability may also be due to spatial variability of model function parameters over the sigma-0 measurement footprint.

ML-based wind retrieval algorithms require knowledge (or at least a good estimate) of the variance of the sigma-0 measurements. The variance of the measurement may be computed from a combination of the known communication Kp, the retrieval error, and the modeling error (*Chi and Li*, 1988; *Long and Mendel*, 1991; *Long*, 1991; *Long and Skouson*, 1996). While the communication Kp can be analytically computed based on the instrument design parameters and the assumed model function, estimates of the retrieval error and the modeling error must be used to estimate wind performance accuracy. To estimate the accuracy of the wind retrieval process (and of the whole NSCAT system) Monte Carlo simulations have traditionally been used (*Long*, 1988). These simulations have played a crucial role in the design of the NSCAT instrument and will continue to play a crucial role in the development of future scatterometer systems.

Recently, *Oliphant and Long* (1996a) derived the Cramer-Rao bound for scatterometer wind retrieval. The C-R bound provides an analytic lower bound on the wind estmate error and is useful for scatterometer design analysis. Their results show that the wind estimate accuracy can be quite sensitive to the geophysical modeling error. Thus, any problems

estimating the modeling error may lead to poor design decisions and degraded wind measurement accuracy. Conversely, accurate modeling error estimates can lead to better design tradeoffs and improved measurement performance.

Unfortunately, suitable modeling error estimates for existing model functions are not presently available though an interesting new technique has recently been developed by *Johnson et al.* (1996). Because some estimate of the modeling error is required when making design tradeoff studies, the NSCAT project has adopted the value of 0.7 dB for all values of sigma-0 based on an estimate of the regression error observed in the development of the Wentz or SASS-2 model function (Wentz, personal communication). This value is assumed for both the SASS-1 and SASS-2 model functions. While this is the best available value it is highly unlikely that this value is correct for all regions of model parameter space.

It is hoped that estimates of the geophysical modeling error will be provided along with any refinements to the model function. Determination of the modeling error is the topic of Section VII. While the general subcommittee feels that the modelling error should be incorporated into the wind retrieval, W. Pierson voices the opinion that the modelling error term should not be used in the retrieval, reasoning that without the modelling error incorporated into the wind retrieval it will be easier to determine (i.e., model) the unmodelled error sources and thereby eliminate them (see Section VII).

D. References

Chi, C-Y and F.K. Li, "A Comparative Study of Several Wind Estimation Algorithms for Spaceborne Scatterometers," *IEEE Trans. Geosci. and Rem. Sens.*, Vol. GE-26, No. 2, pp. 115-121, March 1988.

Johnson, P.E., D.G. Long, and T.E. Oliphant, "Geophysical Modeling Error in Wind Scatterometry," *Proc. Int. Geosc. Rem. Sens. Sym.*, Lincoln, Nebraska, 27-31 May, pp 1721-1723, 1996.

Leotta, D., and D. G. Long, "Probability Distribution of Wind Retrieval Error Versus True Wind Vector and Swath Location for the NASA Scatterometer," *Proceedings of the International Geoscience and Remote Sensing Symposium*, pp. 1466-1469, Vancover, B.C., July 1989.

Long, D.G., and G.B. Skouson, "Calibration of Spaceborne Scatterometers Using Tropical Rainforests," *IEEE Trans. Geosc. and Remote Sens.*, Vol. 34, No. 2, pp 413-424, 1996.

Long, D. G., "The Scatterometer Measurement Model With Correlated Noise and Bias," Report prepared for the Jet Propulsion Laboratory, Pasadena, CA, 10 Sept. 1991.

Long, D. G., and J. M. Mendel, "Identifiability in Wind Estimation from Wind Scatterometer Measurements," *IEEE Trans. on Geosc. and Rem. Sens.*,Vol. 29, No. 2, pp. 268-276, 1991.

Long, D.G., "Documentation for the NSCAT Simulation Programs," Jet Propulsion Laboratory Internal Memo, 3343-88-177, Dec. 20, 1988.

Oliphant, T.E., and D.G. Long, "Cramer-Rao Bound for Wind Estimation from Scatterometer Measurements," *Proc. Int. Geosc. Rem. Sens. Sym.*, Lincoln, Nebraska, 27-31 May, pp 1724-1726, 1996a.

Oliphant, T.E., and D.G. Long, "Development of a Statistical Method for Eliminating Improbable Wind Aliases in Scatterometer Wind Retrieval," *Proc. Int. Geosc. Rem. Sens. Sym.*, Lincoln, Nebraska, 27-31 May, pp 1715-1717, 1996b.

Pierson, W. J., Jr., "Dependence of Radar Backscatter on Environmental Parameters," from G. L. Geernaert and W. J. Plant (eds), *Surface Waves and Fluxes*, Vol II, pp 173-220, Kluwer Academic Publishers, Netherlands, 1990.

Pierson, W. J., Jr., "Probabilities and Statistics for Backscatter Estimates Obtained by a Scatterometer," *J. Geophys. Res.*, Vol. 94, No. C7, pp 9743-9759, July 15, 1989.

IV. Model Function Derivation Approaches

There are a number of approaches to developing a geophysical model function. Unfortunately, our present understanding of radar scattering from wind-roughened seas and the detailed relationship between centimetric scale roughness and near-surface winds is insufficient to allow the construction of dynamically-based geophysical model functions (although as discussed below, a number of investigators have made attempts at this difficult problem). Thus, empirical approaches to developing model functions have historically had the greatest success.

In the following sections both analytic (dynamically-based) and empirical approaches are considered. Recent advances in understanding provide hope that a successful dynamically-based approach can eventually be developed.

A. Dynamically-Based Model Functions

One of the goals of the study of radar backscatter is to describe backscatter by means of a theoretical model of the extremely complicated ocean surface. A theoretical model function has two parts. One is the mathematical description of the air/sea interface which specifies the relation between wind and sea surface geometry on scales of 0.01-100 m. This range encompasses waves from short capillary to gravity waves including the dynamically important transition regions. The other component in the model function is the expression for the electromagnetic backscattering from the rough air/sea interface. Each of these components are considered in the following sections.

i. Wind-Wave Modeling

We first consider the limitations of wind-wave modeling. While most model functions assume linear wave models with Gaussian statistics, available scientific measurements of waves and backscatter from waves have made it evident that such models of the waves are inadequate. In particular, the linear Gaussian model fails to describe many features of a wind generated sea. Moreover, the variance spectrum alone is an inadequate representation of the wavy surface because nonlinear processes results in nonzero odd moments of sea-surface elevation. Thus a linear model cannot fully describe the geometrical properties of the sea surface. This is supported by measurements of the surface (*Huang* et al., 1990; *Wu* 1990). Further, measurements of wave slopes have shown that the probability density function is not Gaussian (*Hwang*, 1986). Stereo profiles of waves have also shown decidedly Stokes-like wave forms. Some progress has been in modeling of nonlinear waves, see, for example, *Barrick and Weber* (1977), *Huang and Tung* (1977), *Pierson* (1993), and *Weber and Barrick* (1977).

Moreover, waves in a wind generated sea break. Spilling breakers have been studied experimentally by *Banner and Fooks* (1985) and theoretically by *Wetzel* (1986), *Tung* et. al. (1987), and *Huang* et al., (1986). Breaking waves produce foam patches that roughen the sea surface by bubbles breaking at the surface, forming stalk like cylinders and fairly large water drops that fly through the air. This phenomenon is similar to a raindrop splash as described by *Wetzel* (1986). Ways to quantify the number of patches and the backscatter (or lack of it) from these patches are lacking. Foam patches are known to be strong emitters of microwave frequencies as sensed by passive microwave sensors. Conversely they may be strong absorbers of radar signals. The effects of foam are difficult to include in a theoretical model.

As discussed in detail in Section VI.C, there is disagreement concerning the effects of sea surface temperature on waves primarily responsible for Ku-band radar backscatter. Waves with wavelengths of 5 and 2 cm, which approximately correspond to the Bragg

wavelengths at C and Ku-band, are significantly attenuated by viscosity. Molecular viscosity doubles as the water temperature decreases from 30° to 0° C. *Donelan and Pierson* (1987) predicted that these wavelengths could not be generated at all unless a certain threshold temperature dependent wind speed was exceeded (see Section VI.C).

ii. EM Scattering

Models for EM scattering from a random surface is an important topic in scattering theory and a number of techniques have been developed. For application to scattering from the sea surface EM scattering models have been either based on the Bragg scattering-composite (two-scale) surface model (*Wright*, 1968; *Bass et al.*, 1968; *Valenzula*, 1978) or the more recently developed integral equation method. The latter approach seeks a more accurate estimate of the electromagnetic surface currents by solving the integral equation for this current iteratively. This surface current is then used to compute the scattered far-zone fields. The work of *Fung and Pan* (1987) discusses the evolution of this approach which recently has been augmented by a more realistic non-Gaussian surface statistical model to estimate the ocean radar cross section properties at Ku-band (*Fung and Lee*, 1982; *Chen et al.*, 1992; *Chen et al.* 1993). In particular, *Chen et al* (1993) has recently used the bispectrum of the surface wave field to understand the azimuthal modulation of sigma-0. EM scattering computed with the integral method is actively being investigated by several researchers though no operational model functions have been developed based on the method.

To date, most dynamically-based model functions have relied on a Bragg scattering-composite model for the sea surface. Since these models rely on simplified descriptions and the statistics of the sea surface it is difficult to completely divorce the discussion of the EM scattering from the surface description. As a result, the following discussion combines both EM scattering and surface modeling issues. To keep the discussion short, the derivations of the model functions are not given. Instead, the reader is referred to the appropriate references. The model functions discussed in the sections have very complicated forms.

Three model functions based on Bragg scattering-composite surface theory and various assumptions about the properties of the waves have been proposed (*Durden and Vesecky*, 1985; *Plant*, 1986; *Donelan and Pierson*, 1987). All three attempt to determine the dependence of the sigma-0 on wind and other parameters by developing a short wave spectrum, specifying the long wave field, modeling the interaction between the two, and averaging the sigma-0 over all surface tilts in order to produce the final model function. Plant specifies this model function only over the incidence angle range from about 20° to 70° using composite surface theory. Durden and Vesecky extend this range to 0° to 70° by including quasi-specular scattering at small incidence angles. Donelan and Pierson include both quasi-specular scattering at small incidence angles and scattering by wedges and breakers at high incidence angles in their work but present results primarily for the 20° to 70° range of incidence angles.

Durden and Vesecky (1985) specified the short wave omni-directional wavenumber spectrum using dimensional considerations. The corresponding spectrum for the long waves was taken to have the form of the classical Pierson-Moskowitz spectrum (*Pierson and Moskowitz*, 1964). The cutoff wavelength between long and short waves was varied between about 12 and 20 times the radar wavelength. The angular dependence of both long and short waves was taken to be a form specified by *Fung and Lee* (1982) (see also *Wu*, 1990). The interaction between long and short waves was modeled by a constant hydrodynamic modulation transfer function for all short wavenumbers so that only the ratio of long wave slope to its standard deviation contributed to this modulation. In averaging sigma-0 over long wave slopes, Durden and Vesecky assumed the long waves to have a

surface elevation distribution which is Gaussian and determined the standard deviation of this distribution from the long wave spectrum.

Plant (1986) specified the short wave spectrum by solving the short wave action balance equation using a WKB approximation for long wave effects. He found that it was possible to specify a form for the average short wave spectrum accurate to second order in long wave slope if a quadratic approximation to the interaction/dissipation functional was made. The angular dependence of this spectrum depended on the angular variation of the short wave growth rate and thus was poorly specified. A modulation transfer function which was a function of long and short wavenumber was used to model the long wave/short wave interaction. Since the short wave spectrum was modeled only to second order in long wave slope, Plant expanded the average over long wave slopes to this same order in calculating the final sigma-0. No long wave spectral form appears explicitly in this formulation since the mean-squared long wave slope is the only long wave parameter needed and it was taken from the work of *Cox and Munk* (1954) for a slick-covered surface (see also *Wu,* 1990). This procedure also made it unnecessary to specify a cutoff wavelength explicitly. In expanding the average over long wave slopes, Plant assumed that their distribution was Gaussian. Thus upwind/downwind asymmetry of the final sigma-0 was caused only by a second-order interaction between long wave tilting and the hydrodynamic modulation transfer function.

Donelan and Pierson (1987) specified the short wave spectral form by equating the average wind input to the average dissipation. This procedure is the same as that used by Plant if the effect of the long waves on the short waves is neglected. Donelan and Pierson specified the short wave spectrum in a manner similar to Durden and Vesecky. In specifying the average dissipation, Donelan and Pierson took account of viscous damping of the short waves, an effect omitted from the other two model functions. This caused a threshold wind speed for short wave generation to exist and resulted in a short wave spectrum which was identically zero above some wind-speed dependent transition wavenumber. As a consequence, the sigma-0 initially increased with wind speed. In calculating the average over long wave slopes necessary to determine sigma-0 Donelan and Pierson assumed that the wave slopes followed a Gaussian distribution but modified the distribution to allow tilting toward the antenna to intercept a larger fraction of the microwave beam than tilting away from the antenna. This effect was included in neither of the other models. Upwind/downwind asymmetry is affected in the Donelan and Pierson model by this effect as well as tilt/hydrodynamic modulation interaction effects. The parameters of the Gaussian distribution were calculated from the long wave spectrum and a cutoff wavelength of 40 times the microwave wavelength was assumed.

Some of the details of comparisons between the predictions of these models and data will be given in later sections. Here, however, it is relevant to point out that none of these models has enjoyed success in explaining the dependence of the sigma-0 on the wind vector. None adequately fits measured wind speed dependencies over the range desired for an adequate scatterometer model function. The Durden and Vesecky model employs an unusual drag coefficient which makes it difficult to fit to both wind speed and friction velocity. Both it and the Donelan and Pierson model have difficulty accounting for the observed upwind/downwind asymmetry of measured data. Evidence is mounting that a wind-speed dependent transition wavenumber above which the short wave spectrum begins to decrease rapidly does not exist. Wave tank measurements by *Jähne,* et al. (1990) indicate that short wave spectra do decrease more rapidly at very high wavenumbers than at lower wavenumbers but that the transition point is independent of wind speed. This cannot be explained by the Donelan-Pierson model which includes viscous effects. Furthermore, evidence is accumulating that, as the wind speed is increased, the sigma-0 rises more slowly at low wind speeds than this model predicts. For V-pol and moderate winds Plant's

model appears to provide good predictions of the azimuthal modulation at incidence angles of 40° to 60° (*Weissman,* 1990).

One weakness that is common to all of the two-scale models is that they appear to under predict the H-pol average sigma-0 by about 3 dB. The integral equation method developed by Fung (*Chen, Fung and Weissman*, 1992) solves this problem and also addresses the upwind/downwind asymmetry. It develops a procedure that gives more accurate estimates of the total tangential electromagnetic current at the rough surface boundary than could be obtained using the Kirchoff approximation. In addition, this study generalizes the previously universal practice (in studies of EM scattering) of assuming the surface statistics are Gaussian. The nonlinear nature of ocean wave interaction is shown to produce surface statistics that have third order moments and skewness. The theory incorporates these effects using the third order bispectrum function along with the usual second-order surface spectrum. These have parameters that can be related to the physical features of the ocean surface. Recent comparisons of this theory with the FASINEX data (*Weissman* et al., 1992) show that this approach solves the problem of accurately predicting the H-pol sigma-0. At a wind speed of 7 m/s, over an incidence angle range from 20° to 60°, both V-pol and H-pol theoretical predictions were excellent. However much more work needs to be done to assess the wind speed, friction velocity, and azimuth angle dependence over a wider range of values to develop useful operational model functions.

Finally, we note that breaking waves may also cause an upwind-downwind asymmetry in backscatter. The upwind-downwind asymmetry seems to be particularly strong for H-pol. Unfortunately, there is not enough information on this phenomenon to pursue modeling it theoretically (*Jessup*, 1990). Foam patches generated by breaking are known to be strong emitters of microwave frequencies as sensed by passive microwave sensors and may be strong absorbers of radar signals. The lack of physical models make the effects of foam difficult to include in a theoretical model.

The above discussion suggests that all of these scattering models need to include non-Gaussian sea-surface geometries to explain features of scatterometer data such as upwind/downwind asymmetry. The composite-surface models accomplish this by letting the short and long waves interact while the integral equation formulation requires a specification of the skewness of the surface wave slopes. These are probably equivalent formulations (when concerned with kilometer-size footprints) and indicate the level of detail about the air/sea interface which is required in order to establish a physically-based model function. In the face of these extreme requirements, it is natural to attempt to determine scatterometer model functions on an empirical basis. We turn to these approaches next.

B. Empirical Approaches

In this section we consider approaches for developing empirical model functions. These are classified by the primary source of data used to generate the model functions: satellite-, aircraft-, or tower-based instruments.

i. Satellite-Based Approaches

Two major approaches to developing model functions based primarily on satellite data have been proposed and are discussed below. The first can actually be considered a mixed technique since it also uses both spacecraft-based and aircraft-based measurements. The SASS-1 model function grew out of this approach. *Wentz* et al. (1984) exploited statistical properties of global winds to develop the SASS-2 model function and has recently modified his technique to use wind speeds based from SSM/I measurements. *Freilich and Dunbar* (1993a) have developed a technique for determining a model function which is based spaceborne scatterometer measurements and numerical weather prediction (NWP)

surface wind analyses. Each of these approaches and the resulting model functions are discussed in the following sections.

a. The SASS-1 Model Function

In preparation for the launch of the SEASAT scatterometer SASS, the two-scale scattering model developed by *Wentz* (1975; 1977) was applied to the problem of radar backscattering from the ocean. This model represented the sea surface by an ensemble of tilted flat facets on which small-scale roughness was superimposed. The *Cox and Munk* (1954) sun glitter observations were used to assign the tilt probability, which contained the high order moments of skewness and peakedness. The small-scale roughness was statistically represented by the capillary power spectrum derived by *Pierson and Stacy* (1973). The roughness amplitude was a function of the facet tilt in order to account for wave-wave modulation. The bistatic scattering coefficients were found by assuming each facet scattered independently according to small-scale perturbation theory (*Rice,* 1951).

The objective in originally applying the two-scale model to SASS was to develop an interpolation tool for the AAFE-RADSCAT aircraft backscatter measurements: while aircraft observations were at selected azimuth and incidence angles, SASS needed a model that covered all angles. The solution to this problem was to fit the two-scale model to the aircraft observations.

Unique values for the model parameters were found by fitting the model to the observations in a least-squares sense (*Wentz*, 1977; 1978). The derived parameters were reasonable with the residual rms error between the model and the aircraft observations was 0.7 dB. The model well represented the incidence angle roll-off, the strong alongwind-crosswind modulation, and the weaker upwind-downwind asymmetry. Groups at the University of Kansas and at CUNY also independently worked on the problem. Workshops were held to intercompare the various resutls. Following one of these workshops, a model was developed at CUNY that attempted to combine the best features from the three groups. It was called CUWENKAN (or CWK for short). Jones et al. (1992) show tables what intercompare the CWK model with Wentz's GHTBWK7.

The final SASS-1 model (*Schroeder* et al., 1982) is a refinement of the CWK results. This refinement consists of ensuring that both *G* and *H* were smoothly varying function of incidence angle for each azimuth angle. For a given polarization the SASS-1 model function expresses sigma-0 (in dB) as a power-law function of the wind speed *U*,

$$10\log_{10}\sigma^{o} = G(\theta,\chi) + H(\theta,\chi)\log_{10} U \qquad (4.1)$$

where θ is the incidence angle and χ is the relative wind direction. The G and H coefficients are tabulated every 2° in incidence and 10° in azimuth and exhibit biharmonic variation with azimuth angle. SASS-1 is defined over incidence angles of 0° to 70° though only incidence angles of 15° to 65° are need for processing NSCAT data. In SASS-1 sigma-0 is a monotonically increasing function of incidence angle

b. The Wentz (SASS-2) Model Function

Following the flight of SEASAT in 1978, *Wentz* et al. (1984; 1986) published a model function derived primarily from the statistics of the SEASAT scatterometer data. They assumed that the over the three-month lifetime of SEASAT, the wind vector exhibited a high degree of variability relative to the antenna look direction so that the probability distribution of two orthogonal components of the wind vector was a bivariate normal distribution. This yields a Raleigh distribution for the wind speed. The single parameter of this distribution (the mean global wind speed) was obtained from a climatological atlas. They then derived the model function necessary to obtain the statistical distribution of

sigma-0 values measured by the SEASAT scatterometer from this wind vector distribution. They found that by assuming a model function form which was a power law in wind speed and a three-term Fourier series in azimuth angle they could specify all parameters of the model function (except the parameter responsible for upwind/downwind asymmetry) from only the wind and sigma-0 statistics. The additional parameter was derived from aircraft data obtained by the NASA Langley Research Center. They denoted their model function "SASS-2" (known also as "Wentz") to distinguish it from the SASS-1 model function which was used to process the SEASAT data.

The SASS-2 model function expresses sigma-0 (in normal space) as (*Wentz* et al., 1984)

$$\sigma^o = A_0 + A_1 \cos\chi + A_2 \cos 2\chi \tag{4.2}$$

where the A coefficients are computed have modified power-law dependencies on wind speed,

$$A_0 = a_0 U^{\alpha_0} \tag{4.3}$$

$$A_1 = (a_1 + \alpha_1 \log U) A_0 \tag{4.4}$$

$$A_2 = (a_2 + \alpha_2 \log U) A_0 \tag{4.5}$$

The coefficients a_0, a_1, a_2, α_0, α_1, and α_2 are tabulated functions of incidence angle. Coefficients with 0 and 2 subscripts are derived directly from the statistics of SASS measurements while coefficients with a 1 subscript were derived from AAFE RADSCAT data. *Wentz* (1991) has developed a simplified form of this model function though it has not been widely used.

c. NWP analysis-based approach

Recently, *Freilich and Dunbar* (1993a) developed a technique for determining a model function via comparison of the sigma-0 measurements and numerical weather prediction (NWP) surface wind analyses. The lack of suitable NWP analyses during the SASS period precludes the use of SASS data with their method. However, the method has worked very well for C-band data (*Freilich and Dunbar*, 1992; 1993b). Their method is based on interpolation of an NWP surface wind analysis to each sigma-0 measurement location to generate a very large collocated set of sigma-0 measurements and surface winds which span the range of global conditions. The sigma-0 measurements are then binned by physical parameter and averaged to generate a model function with some appropriate smoothing. This approach has the advantage that it can include other non-wind parameters as well as estimate the modeling error (discussed in a later section).

The use of synoptic scale wind field analyses to produce a model function table without the need for an analytical form has both advantages and disadvantages. The method clearly is sensitive to systematic errors in the NWP surface wind analyses. As the NWP surface wind velocities are used to assign each backscatter measurement to a wind speed and azimuth angle bin, NWP errors that are a systematic function of wind speed will result in mis-assignment of backscatter measurements, and corresponding errors in the calculation of bin-averaged values that form the initial model function estimate. Random NWP velocity errors will also result in mis-assignment of backscatter measurements; however, as the random errors are not systematic as a function of, say, wind speed, to lowest order their effects are smaller. Random NWP errors, however, can result in systematic under predictions of upwind-crosswind and upwind-downwind modulations. Importantly, the accuracy of *individual* NWP analyses is of lesser importance than the overall systematic accuracy of the analyses -- in the absence of systematic wind-speed-dependent or

geographical-dependent errors, analysis errors (such as missing fronts and misplacing the centers of lows, etc.) can be considered to add only random errors.

In recognition of the sensitivity of the model function to the NWP data, the method as implemented relies upon multiple NWP analysis products (produced by independent operational centers), and includes iterations to identify and exclude synoptic-scale regions where the NWP analyses clearly do not exhibit the variability evident in the scatterometer measurements.

A full analysis of the empirical method requires quantitative determination of the magnitudes of realistic NWP errors, followed by determination of the sensitivity of the method to these systematic and random errors. Such a study is presently being conducted, involving both buoy-NWP comparisons (to quantify NWP analysis errors) and simulations (to quantify the sensitivity of the resulting model function to realistic NWP errors).

The Freilich and Dunbar method does depend on a functional form of the model function but results in a tabular function. A truncated Fourier series expansion can be used to smooth the azimuth response.

d. SSM/I-derived wind speed-based approach

The SSM/I is a multichannel microwave radiometer instrument flying aboard the Defense Meteorological Satellites. There are usually two SSM/I's in operation, each having a 1400 km swath which provides near-global coverage each day. The SSM/I's 37 GHz H-pol channel is sensitive to ocean roughness and foam and can be used to estimate the near-surface wind *speed.* The rms difference between SSM/I-derived winds and buoy winds is about 1.3 m/s (*Wentz*, 1992a). SSM/I winds have also been compared with ECMWF wind fields (*Halpern et al.*, 1994) and appear to be a reliable product. However, cloud cover can prevent wind retrieval, resulting in large regions without adequate coverage. Further discussion of the accuracy of SSM/I wind speeds is not considered in this report.

SSM/I-derived wind fields can be used to derive a geophysical model function for scatterometers (*Wentz*, 1992b). Using standard collocation techniques, a SSM/I wind speed can be assigned to each scatterometer sigma-0 measurement. By relating this wind speed to the sum of the scatterometer forward and after observations (the expected value of the sigma-0 sum depends only on wind speed, see *Freilich,* 1994), the wind speed dependence of sigma-0 can be determined. Once the wind speed dependence is determined, the wind direction dependence of sigma-0 is found from histograms of the forward minus the aft sigma-0 difference. Essentially this approach is the same as used for the Wentz model function (*Wentz et al.*, 1984), except that the wind speed is now known from the SSM/I rather than from global statistics. Knowing the wind speed greatly simplifies and enhances the Wentz method. This approach has recently been successfully applied to the C-band ERS-1 scatterometer (*Wentz*, 1992b). The functional form is similar to SASS-2.

ii. Model Functions Based on Aircraft Data

As previously indicated, the SASS-1 model was originally based on aircraft-data generated by the RADSCAT project (Advanced Applications Flight Experiment, at the NASA Langley Research Center) (*Schroeder* et al, 1984; *Schroeder* et al, 1985). The project provided an extensive range of sigma-0 values spanning a wide range of ocean wind conditions. These data have been very useful to the research community in studying both the physics of short wave growth and the air-sea interaction (*Durden & Vesecky*, 1985; *Donelan and Pierson*, 1987) and in the development of wind-retrieval algorithms.

The JPL scatterometer group continued the program of airborne Ku-band scatterometer measurements with 2 major field experiments that included extensive support with in-situ

sea surface, wind, and friction velocity measurements. In the winter of 1986, the Frontal Air-Sea Interaction Experiment (FASINEX) included the JPL AMSCAT scatterometer supported by wind and friction velocity measurements (*Li et al.,* 1989). Studies by Weissman combining the radar cross section and in-situ data have lead to the development of a ku-band model function in terms of friction velocity that may be capable of being used with NSCAT data (*Wiessman et al.,* 1994). The Surface Wave Dynamics Experiment (SWADE) on the Gulf Stream in the Winter of 1991 included both the JPL NUSCAT Ku-band and the University of Massachusetts C-band scatterometers. These wer supported by a wide variety of in-situ measurements. The measurements were combined to create a new generation of sea surface meteorological analyses based on a wide network of buoy measurements with a high resolution meteorological reanaysis (*Cardone et al.,* 1995). These provided the in-situ firction velocity estiamtes that could be compared with values computed from the Ku-band radar cross section and Wiessman's friction velocity algorithm. Such comparisons show excellent agreement between the radar and coincident meteorlogical values (*Wiessman,* 1995; *Wiessman et al.,* 1996), suggesting that at least the first steps in the generation of a practical friction velocity-based model function have been made.

iii. Wave tank studies

While no operational model functions have resulted from wave tank studies, wave tank studies have played an important role in advancing model function theories. Since the late 1960's many wave tank experimental programs involving microwave radar measurements have been undertaken. For the most part, each has been focused on a particular scientific question associated with the wind/wave interaction (and sometimes rain), with the radar either acting as a "probe" of the short wave spectrum, or as a monitor of long wave-short wave interactions with wind speed as a parameter. A recent study by *Keller, Keller and Plant* (1992) raises the issue of how well scatterometer model functions, which are intended to relate actual ocean conditions to the microwave radar cross section, perform in wave tank conditions over a wide range of wind speeds (and other parameter variations).

This experimental program investigated five model functions over a range of wind speeds from 0 to 25 m/s, with an X-band radar whose polarization and incidence angle could be varied. The model functions were: Donelan and Pierson, Durden and Vesecky, Plant, SASS-1 and SASS-2. The degree of agreement between the sigma-0 data and each model function varied with wind conditions and radar parameters. The physically-based model functions tended to produce more accurate predictions (*Keller, Keller and Plant,* 1992).

Wave tank data can be useful in validating observations made from aircraft and other data but wave tank data does have significant limitations. For example, properties of the measured sigma-0 values in the wave tank can be compared with the sigma-0 data collected in the FASINEX experiment which included high quality in situ measurements of winds and saves (*Weissman,* et al., 1992). The comparison assumes that the physical mechanisms that affect the sigma-0 properties at X-band are not appreciably different from those at Ku-band.

With the NRL wave tank setup similar to corresponding measurements with the airborne scatterometer during FASINEX, the 28° incidence angle (upwind looking) wave tank data can be compared with aircraft scatterometer measurements. The wind speed dependence of the wave tank data for both V-pol and H-pol can be approximated with power law functions of the wind speed. At 28°, both H-pol and V-pol NRL data can be fit by a function whose wind speed exponent is approximately unity (see Fig. 15 of *Keller, Keller and Plant,* 1992). This is noticeably different from the SASS-2 algorithm for 28° which is close to 1.5 in both cases. The FASINEX data results (*Weissman* et al., 1992) show a wind speed exponent (for neutral stability winds) of about 2 for both polarizations. It is

prudent to keep in mind that the FASINEX results are derived from a fairly small population of data points (but which were well supported with surface observations).

The strong differences between the 28° wave tank sigma-0 and the models derived from ocean data may be explained by the likelihood that the electromagnetic scattering mechanism at this incidence angle may be dependent on the longer, dominant ocean waves which do not exist in the wave tank. A related observation in the NRL results is that the ratio of V-pol to H-pol sigma-0 at 28 degrees is typically about 5 dB, but this ratio derived from ocean observations from FASINEX and the NASDA-RRL data is only about 0 dB at 30°. Again, the absence of long waves in tank data may be the reason for this difference. As a result, while wave tank data can be useful in some studies, it probably can not be successfully used to develop an operational model function.

iv. Tower Measurements

Over the years there have been a number of experiments to collect tower-mounted scatterometer data. Such experiments have yielded important insights into the details of the model function but no operational model functions based on tower data have been derived. In the following discussion we illustrate the insights into model function physics provided by tower-based measurements.

Several recent experimental programs have been carried out involving Ku-band radars on fixed towers that have produced sigma-0 measurements as a function of wind speed. The Tower Ocean Wave and Radar Dependence Experiment (TOWARD) was conducted near Mission Beach in San Diego, in the Spring of 1985. There were a variety of research investigations involved in this effort. One of the studies conducted by the Naval Research Laboratory was of the modulation transfer function and average radar cross section measured at Ku-band (V-pol) (*Keller and Plant*, 1990). These results were limited to lower wind speeds, below 9 m/s. The analysis of these cross section results has mainly been with respect to observing the effect of the relative angles between winds, wave propagation and radar look-direction. The wind speed dependence properties were compared with the SASS-II algorithm and the measured sigma-0 found to lie about 3 dB lower than the model predictions for winds from 2.5 to 9 m/s and upwind looks. Other important tower experiments include SAXON and SAXON-FPN.

A comprehensive tower radar experiment that produced very significant results relevant to the Ku-band model function was the Water-Air Vertical Exchanges Experiment (WAVES 87). Ku-band radar backscatter (at 14 GHz), wave, and environmental measurements were conducted from a research tower in Lake Ontario in the Autumn of 1987, for about six weeks (*Colton*, 1989). Both wind speed and friction velocity were measured as the averaged sigma-0 was recorded as a function of incidence angle (0°, 10°, 20°, 40°, 60°, and 80° off nadir) and azimuth angle over a 300° range). Over the course of this experiment, a wide range of wave, wind and environmental measurements were encountered and the analysis by Colton systematically explores their individual effects on the various properties of the Ku-band backscatter signature.

Among the findings of this investigation, we can examine the results of the regression analysis of the average sigma-0 versus both wind speed (neutral stability winds at 19.5 m/s) and friction velocity. On a log-log scale, the slope of the regression line equals the wind variable exponent. The wind speed exponents (for a power law wind function) for both 20° and 40° incidence angles are smaller for the friction velocity model function than that of the wind speed model function. This is consistent with a drag coefficient that is a function of wind speed. *Colton* (1995) has pointed out that over Lake Ontario the drag coefficient dependence on wind is appreciably stronger than in the open ocean because of the shorter, steeper wave fields. Therefore for a situation in which the winds at a location

in Lake Ontario were equal to an ocean region, the stress and friction velocity would be greater in the Lake.

Long et al. (1996a) also conducted an extensive experiment on Lake Ontario (Yscat95). Comparing the wind speed dependence of sigma-0 at a variety of frequencies, they found that compared to lower frequencies, Ku-band is the most sensitive to wind speed. *Long et al.* (1996b) found that the scattering statistics were log-normal and had general agreement with the composite model though improvements in wind-wave modeling were required.

Similarities and agreements between tower and aircraft radar measurements suggest that we can learn a great deal about the physics of scatterometry from airborne platform measurements from well-executed tower measurement programs such as WAVES 87 (*Colton*, 1989; *Donelan* et al. 1985). It is important to realize, however, that sigma-0 measurements from these relatively low-altitude platforms may exhibit much more variability than similar satellite measurements. The increased variability inherent in these measurements must be compensated by careful measurement techniques and adequate attention to the effects of fetch and integration times on the resulting data.

C. References

Banner, M. L. and C. L. Vincent, "On the Microwave Reflectivity of Small-Scale Breaking Water Waves," *Proc. R. Soc.*, London, Ser. *A, 399*, pp. 93-109, 1985.

Barrick, D.E., and B. L. Weber, "On the nonlinear theory for gravity waves on the ocean's surface. Part II: Interpretation and applications," *J. Phys. Oceanogr.*, Vol. 7, pp. 11-21, 1977.

Bass, F., I.M. Fuks, A.J. Kalmykov, I.E. Ostrovsky, and A.D. Rosenberg, "Very High Frequency Radiowave Scattering by a Disturbed Sea Surface, Parts I and II", *IEEE Trans. Antennas Propagat.*, AP-16, pp. 554-559 and 560-568, 1968.

Cardone, V.J., H. Graber, R. Jensen, S. Hasselmann, M. Caruso, "In Search of the True Surface Wind Field in SWADE IOP-1: Ocean Modeling Wave Modeling Perspective," The Atmospheric and Ocean System, Vol. 3, pp. 107-150, 1995.

Chen, K.M., A. Fung and D. E. Weissman, "A Backscattering Model for the Ocean Surface", *IEEE Transactions on Geoscience & Remote Sensing*, Vol. 30, No. 4, pp 811-817, July 1992.

Chen, K. S., A.K. Fung, and F. Amar, "An Empirical Bispectrum Model for Sea Surface Scattering," IEEE Trans. Geoscience and Remote Sensing, Vol. 31, No. 4, pp. 830-835, 1993.

Colton, M.C., W.J. Plant, W.C. Keller, and G.L. Geernaert, "Tower-based measurements of normalized radar cross section from Lake Ontario: Evidence of wind stress dependence," J. Geophys. Res., vol. 100, no. C5, pp 8791-8813, 1995.

Colton, M. C., "The Dependence of Radar Backscatter on the Energetics of the Air-Sea Interface," Ph.D. Dissertation, Naval Postgraduate School, Monterey, CA, Dec. 1989.

Cox, C. and W. Munk, "Statistics of the Sea Surface Derived From Sun Glitter", *J. Mar. Res.*, Vol. 13, 198-227, 1954.\

Davidson, K.L., D.E. Weissman, E. vanHalsema, and R. Onstott, "Costal Applications of Scatterometer Wind Algorithms," *Oceans'95 Conf. Proc.*, San Diego, California, (Oct. 9-12, 1995)

Donelan, M. A., and W.J. Pierson, Jr., "Radar Scattering and Equilbrium Ranges in Wind-Generated Waves with Application to Scatterometry," *J. Geophys. Res.*, Vol. 92, pp. 4971-5029, 1987.

Donelan, M.A., J. Hamilton, and W.H. Hui, "Directional Spectra of Wind-Generated Waves", *Phil. Trans. R. Soc. Lond. A*, Vol. 315, pp. 509-562, 1985.

Durden, S.L., and J.F. Vesecky, "A Physical Radar Cross Section Model for a Wind Driven Sea with Swell", *IEEE J. Ocean. Engg*, Vol. OE-10, pp 445-451, October, 1985.

Freilich, M. H., and R. S. Dunbar, "Derivation of Satellite Wind Model Functions Using Operational Surface Wind Analyses: An Altimeter Example," *J. Geophys. Res.*, Vol. 98, No. C8, pp. 14633-14649, 1993.

Freilich, M. H., and R. S. Dunbar, "A C-band Scatterometer Model Function from ERS-1 and Global Surface Analysis Data," ADEOS/NSCAT Science Team Meeting Report, pp. 245-255, 1992.

Freilich, M. H., and R. S. Dunbar, "A Preliminary C-band Scatterometer Model Function for the ERS-1 AMI Instrument," *Proc. First ERS-1 Symposium*, ESA Sp-359, pp 79-84, 1993.

Fung, A. K., and K. K. Lee, "A Semi-Empirical Sea Spectrum Model for Scattering Coefficient Estimation", *IEEE Journal of Oceanic Eng,*. Vol. OE-7, No. 4, 1982.

Fung, A. K., M. R. Shah, and S. Tjuatja, "Numerical Simulation of Scattering from Three Dimensional Randomly Rough Surfaces," *IEEE Trans. Geosci. and Remote Sens.*, Vol. 32, No. 5, pp. 986-994, Sept. 1982.

Fung, A. K., and G.W. Pan, "A Scattering Model for Perfectly Conducting Random Surfaces: I. Model Development", *Int. J. Remote Sensing*, Vol. 8, No. 11, pp 1579-1593, 1987.

Halpern, D., A. Hollingsworth, and F.J. Wentz, "ECMWF and SSMI Global Surface Wind Speeds," *J. Atmospheric and Oceanic Technology*, 1994.

Huang, N. E., L. F. Blivern, S. R. Long, and C-C Tung, "An Analytidcal Model for Oceanic Whitecap Coverage," *Journal of Physical Oceanography*, Vol. 16, No. 10, pp. 1597-1604, 1986.

Huang, N. E., C-C Tung, and S. R. Long, "The Probability Structure of the Ocean Surface," *The Sea: Ocean Engineering Science*, pp. 335-366, Vol. 9, John Wiley and Sons, Inc., 1990.

Huang, N.E., and C.-C. Tung, "The influence of the directional energy distribution on the nonlinear dispersion relation in a random gravity wave field," *J. Phys. Oceanogr.*, Vol. 7, pp. 403-414, 1977.

Hwang, P., "Surface Slope Measurements with a Wave Follower in TOWARD 84/86," Rept. No. ORE 86-3, *Ocean Research and Engineering*, Oct. 1986.

Jähne, B., and K.S.Riemer, "Two-Dimensional Wave-Number Spectra of Small-Scale Water Surface Waves", *J. Geophys. Res.*, 95, C7, 11531-11,546, 1990.

Jessup, A., W.C. Keller and K. Melville, "Measureemnts of Sea Spikes in Microwave Backscatter at Moderate Incidence," J. Geophys. Res., Vol. 95, No. C6, pp. 9679-9688, 1990.

Li, F., W. Large, W. Shaw, E.J. Walsh, and K. Davidson, "Ocean Radar Backscatter Relationship with Near-Surface Winds: A Case Study During FASINEX," *J. Phys. Oceanogr.*, Vol. 19, pp. 342-353, 1989.

Long, D.G., R.S. Collyer, R. Reed, and D.V. Arnold, "Dependence of the Normalized Radar Cross Section of Water Waves on Bragg Wavelength--Wind Speed Sensitivity," *IEEE Trans. Geosc. and Remote Sens.*, Vol. 34, No. 3, pp 656-666, 1996a.

Long, D.G., R. Reed, and D.V. Arnold, "Statistics of Radar Backscatter from Wind Waves," *Proc. Int. Geosc. Rem. Sens. Sym.*, Lincoln, Nebraska, 27-31 May, pp 1475-1477, 1996b.

Masuko, H., K. Okamoto, M. Shimada and S. Niwa, "Measurement of Microwave Backscattering Signatures of the Ocean Surface Using X-Band and Ka-Band Airborne Scatterometers", *J. Geophys. Res.*, Vol. 91, No. C11, pp 13,065-13,083, November 15, 1986.

Pierson, W. J., Jr., "Dependence of Radar Backscatter on Environmental Parameters," from G. L. Geernaert and W. J. Plant (eds), *Surface Waves and Fluxes*, Vol II, pp 173-220, Kluwer Academic Publishers, Netherlands, 1990.

Pierson, W. J., Jr, "Oscillatory Third OrderPerturbation Soutions for Sums of Interacting Long Crested Stokes Waves in Deep Water," *J. Ship Reseach*, June 1993.

Pierson, W. J., Jr. and L. Moskowitz, "A Proposed Spectral Form for Fully Developed Wind Seas Based on the Similarity Theory of S.A. Kitaigorodskii", *J. Geophys. Res.*, Vol. 69, No. 24, pp. 5181-5190, 1964.

Pierson, W. J., and R. A. Stacy, "The Elevation, Slope, and Curvature Spectra of a Wind Roughened Sea Surface," *NASA Contr. Rep. 2247*, 122 pp., National Technical Information Service, Springfield VA, 1973.

Plant, W. J., "A Two-Scale Model of Short Wind-Generated Waves and Scatterometry," *J. Geophys. Res.*, Vol. 91, pp. 10735-10749, 1986.

Rice, S. O., "Reflection of Electromagnetic Waves from Slightly Rough Surfaces," *Commun. Pure Appl. Math.*, Vol 4, pp 351-378, 1951.

Schroeder, L. C., W.L. Jones, P.R. Schaffner and J.L. Mitchell, "Flight measurements and analysis of AAFE RADSCAT wind speed signature of the ocean", NASA Technical Memorandum 85646, January 1984.

Schroeder, L., D.H. Boggs, G. Dome, I.M. Halberstam, W.L. Jones, W.J. Pierson, and F.J. Wentz, "The Relationship Between the Wind Vector and the Normalized Radar Cross Section Used to Derive Seasat-A Satellite Scatterometer Winds," *J. Geophys. Res.*, Vol. 87, No. C5, pp. 3318-3336, 1982.

Tung, C-C, M. ASCE, and N.E. Huang, "Spectrum of Breaking Waves in Deep Water," *Journal of Engineering Mechanics*, Vol. 113, No. 3, pp. 293-302, 1987.

Valenzuela, G. R., "Theory for the interaction of electromagnetic and oceanic waves-A review," *Boundary Layer Meteorol., 13*, 61-85, 1978.

Weissman, D.E., "The Response of Microwave Cross Sections of the Sea to Wind Fluctuations," in review *J. Geophys. Res.*, 1994.

Weissman, D.E., K.L. Davidson, R.A. Brown, C.A. Friehe and F. Li, "The Relationships Between the Microwave Radar Cross Section and Both Wind Speed and Stress: Model Function Studies Using Frontal Air-Sea Interation Experiment Data," *J. Geophys. Res.*, Vol. 99, No. C5, 1994.

Weissman, D.E., F.K. Li, S. Lou, S.V. Nghiem, G. Neumann, R.E. McIntosh, S.C. Carson, J.R. Carswell, H.C. Graber, and R.E. Jensen, "Measurements of Ocean Surface Stress Using Aircraft Scatterometers," in review, *J. Atmos. Ocean. Tech..*, Jan. 1996.

Weissman, D.E., and W.J. Plant, "Calculations of the Microwave Radar Cross Section Dependence on Wave Height and Slope Skewness," *Oceans'90 Proceedings*, Washington, D. C., 24-26 Sept., 1990.

Weber, B.L., and D.E. Barrick, "On the nonlinear theory for gravity waves on the ocean's surface. Part I: Derivations," *J. Phys. Oceanogr.*, Vol. 7, pp. 3-10, 1977.

Wentz, F.J., "A Two-Scale Scattering Model for Foam-Free Sea Microwave Brightness Temperature," J. Geophys. Res., Vol 80, No. 24, pp. 3441-3446, 1975.

Wentz, F.J., "A Two-scale Scattering Model With Application to the JONSWAP '75 Aircraft Scatterometer Experiment, NASA Contractor Report 2919, 122 pgs., Dec. 1977.

Wentz, F. J., S. Peteherych, and L.A. Thomas, "New Algorithms of the Microwave Measurements of Ocean Winds with Application to SEASAT and SSM/I," *J. Geophys. Res.*, Vol. 91, pp 2289-2307, 1986.

Wentz, F. J., L.A. Mattox, and S. Peteherych, "A Model Function for Ocean Radar Cross-sections at 14.6 GHz," *J. Geophys. Res.*, Vol. 89, pp 3689-3704, May 20, 1984.

Wentz, F. J., "A Simplified Wind Vector Algorithm for Satellite Scatterometers," *J. Geophys. Res.*, Vol. 8, No. 5, pp 697-704, 1991.

Wentz, F. J., "Measurement of Oceanic Wind Vector Using Satellite Microwave Radiometers," I*EEE Trans. Geoscience and Remote Sensing*, Vol 30. No. 5, pp. 960-972, 1992a.

Wentz, F. J., "Intercomparison of ERS-1 Winds with SSM/I Winds", *1992 ADEOS/NSCAT Science Team Meeting Report*, pp 309-320, 1992b.

Wetzel, L., "On Microwave Scattering by Breaking Waves," in O. M. Phillips and K. Hasselmann, *Wave Dynamics and Radio Probing of the Ocean Surface*. pp. 273-284, 1986.

Wright, J. W., "A New Model for Sea Clutter", *IEEE Trans. Antennas and Prop.*, AP-16, p. 217, 1968.

Wu, J. "Mean Square Slope of the Wind-Disturbed Water Surface, Their Magnitude, Directionality and Composition," *Radio Science,* Vol. 25, No. 1, pp 37-48, Jan-Feb 1990.

V. Analysis and Comparison of Existing Model Functions

In this section we compare and analyze several model functions. We limit our comparison to "operational" model functions as previously defined. The model functions for Ku-band that are considered are the SASS-1, SASS-2 (*Wentz* et al. 1984), *Donelan and Pierson* (1987), and *Plant* (1986) models.

The ultimate tests and comparison metrics for model functions relate to the accuracies of the retrieved vector winds. However, as noted above, scatterometer wind retrieval is a highly nonlinear process, and it is difficult to relate changes in the model function to changes in retrieved vector winds in simple, yet accurate ways. The issue is compounded by the multi-dimensional parameter space (wind speed, relative azimuth, incidence angle) required by fan-beam scatterometer model functions. The tabular, non-analytic nature of some model functions adds further complexity.

A number of methods for comparing the performance of model functions have been developed but no single method is acceptable for all users. While most model function comparisons have been based on the comparison of retrieved winds with conventionally measured winds, other comparisons have been based on the RMS error and other statistics of the predicted and observed sigma-0 values have also been used.

In the following subsections we compare various models using published results and analysis and comparisons suggested by members of the subcommittee. Other analysis techniques and results are described elsewhere in this report. Overall, the committee feels that the best existing model function is SASS-2.

A. Comparisons using sigma-0 and comparison winds

Woiceshyn et al. (1986) provide the most comprehensive discussion of the limitations of the SASS-1 model function. Their results suggested an inconsistency between the model functions for each polarization (discussed in 5.C). They also compared the performance of SASS-1 and SASS-1 precursor model functions using wind data collected during JASIN and from NDBO buoys of the U.S. coast. They noted that winds retrieved using SASS-1 were biased approximately 1 m/s low. Reduced sensitivity of sigma-0 to the wind speed was noted for wind speeds less than 4 m/s and greater than 15 m/s suggesting that the simple power-law relationship used for SASS-1 does not adequately model the correct wind speed dependence of sigma-0. It should be noted that the wind speed bias noted for SASS-1 is corrected in SASS-2 (*Wentz*, 1984) and that SASS-2 exhibits a convexity in the wind speed dependence of the sort suggested by *Woiceshyn* et al. (1986).

B. Model function properties and comparisons using aircraft data

The Frontal Air-Sea Interaction Experiment (FASINEX) provided a unique data set with coincident airborne scatterometer measurements of the ocean surface radar cross section (at Ku-band) and a wide variety of precise environmental measurements including measurements of the wind stress. This data provides an opportunity to compare the relationship of aircraft-derived sigma-0 to both the near surface wind and the wind stress. These data have been analyzed to create new algorithms for both wind speed and surface friction velocity (square root of the kinematic wind stress) and to better understand the air-sea variables that have the strongest influence on the radar cross section. Studies of data from FASINEX indicate that the sigma-0 has a different dependence on friction velocity than on wind speed. The difference between sigma-0 models using these two variables depends on both the polarization and the incidence angle. FASINEX sigma-0 data span 10 different flight days. The wind speeds ranged from 2 to 20 m/s. Stress measurements were inferred from ship-board instruments and from aircraft flying at low altitudes, closely

following the scatterometer. A wide range of radar incidence angles and environmental conditions needed to develop algorithms fully are available from this experiment.

Weissman (1990) conducted a detailed comparison of the predictions of Plant's theory with these airborne sigma-0 measurements obtained during FASINEX (*Li* et al., 1989), which were supported by an excellent set of in-situ wind and wave data (*Friehe* et al., 1991). This study emphasized analysis of the azimuth properties of the data and the theory at incidence angles of 40° and 50°, at several different wind speeds (up to 13 m/s). The successes of this theory were for V-pol; both magnitude and azimuth dependence. The H-pol azimuth dependence could be interpreted with this theoretical model; the strong upwind-to-downwind difference could be predicted with the modulation transfer function in the sigma-0 calculation. The critical issue was that the absolute magnitude of the measured H-pol sigma-0 was typically 3 dB higher than the theory could predict for winds in the 6 to 13 m/s range. Also in this paper, there was data from a 13 m/s wind day for which there was 60° incidence angle data. Again the V-pol theory worked well, but H-pol was too low.

In a later study, the wind speed and friction velocity dependence of Plant's model at 40° and 50° incidence was assessed. The only case in which the predictions give good agreement with the data is for V-pol, at winds less than 10 m/s. For other conditions at these incidence angles, the predictions are appreciably lower, with a weaker sensitivity to wind than the data displays.

A more recent study by *Weissman*, et al. (1994) develops functional fits to the wind and friction velocity for both V-pol and H-pol, for incidence angles from 20° to 50°. Since the SASS-2 model function has been accepted as the best and most comprehensive for its purpose, the Weissman study follows the SASS-2 practice of representing the azimuthal variation of the sigma-0 with a 3 term, truncated Fourier series. At a fixed polarization and incidence angle, the coefficients of this series (usually labeled as A_0, A_1, A_2) are treated as functions of each of the wind variables, analyzed independently. Comparisons of the measurements with the SASS-2 (or, Wentz) model function predictions and with power-law fits of A_0 to the data have been made.

The comparisons of the FASINEX aircraft sigma-0 with the SASS-2 model function (for wind speed only) show the following:

1. For 40° and 50° incidence the average normalized radar cross section, A_0, has been used with this model function to estimate winds. These estimates are within an RMS error of less than 2 m/s from the *in-situ* winds. The relative errors are largest at wind speeds above 10 m/s. At these higher wind speeds the SASS-2 algorithm often under-predicts A_0 by about 1 to 2 dB. This can lead to wind inferences as much as 3 m/s too high. However, a simple "tuning" of A_0 by changing the power-law parameters can reduce this RMS error by a factor of two. At incidence angles of 20° and 30° there is greater scatter in the data about the SASS-2 and power law fits. The wind estimates in these case can have an RMS error of 2-3 m/s. However, changes in the numerical values of the power-law parameters, using the FASINEX results, can reduce these errors significantly.

   These FASINEX results support the widely held view that the SASS-2 algorithm is credible for many conditions. However, they also demonstrate that there is a need for improvement, and where these improvements should be made.

2. The Fourier series coefficients associated with the azimuthal variation display important features. The term associated with upwind/downwind differences (A_1/A_0) displays a wide variability and scatter about the SASS-2 formula. In many cases these data have a "running average" which decreases more steeply with

increasing wind than the SASS-2 model predicts. The data associated with the crosswind term (A_2/A_0) tends to have only moderate scatter and usually tends to lie close to the SASS-2 function in most case.

Another important finding of the FASINEX scatterometer analysis is that the data appear to confirm what had been suspected by some researchers: the functional fit of the A_0 data with increasing wind speed is often better (i.e., a higher level of correlation) for a power-law function of friction velocity than for a function of wind speed (U_{10}). The data analysis of *Weissman*, et al. (1994) provides specific information on the exact function parameters and the degree of correlation with both wind speed and friction velocity. Present indications are that a separate scatterometer model function for friction velocity may be preferable for oceanographic applications that require estimates of this variable. This would bypass the error-prone technique of using wind speed estimates and a mathematical model of the neutral stability drag coefficient to estimate u*.

Comparisons between the Wentz (SASS-2) model for A_0 and the value derived by *Weissman* et al. (1992) from FASINEX data are remarkably similar. Since Wentz's wind exponents were computed using an assumption about the form of the probability density function for global neutral stability winds, it would be interesting to compare the sensitivity of his model to changes in the probability density function. Such an analysis might lead to interesting observations about the global statistics of the 19 m neutral stability wind (U_{19N}) and u*. This is being pursued by D. Weissman.

C. Self consistency

The self consistency of model functions can be evaluated without the use of comparison data. For example, *Woiceshyn* et al. (1986) and *Sylvester et al*. (1989, 1990) examined the consistency of the model functions for the different polarization. *Woiceshyn* et al. (1986) colocated sets of pairs of H- and V-pol sigma- measurements. Graphing the wind speeds recovered from the H-pol measurements versus the wind speed recovered from the V-pol measurements revealed that the two polarizations did not yield consistent wind speeds, particularly at high wind speeds. At both low and high wind speeds, H-pol winds were consistently higher than V-pol winds. The SASS-1 model function yields self-consistent wind speeds only over mid-range wind speeds.

Using the same SASS data *Sylvester et al*. (1989, 1990) variously examined the scatter of the maximum H-pol versus the maximum V-pol and minimum H-pol versus minimum V-pol sigma-0 values. Based on these scatter plots and the statistics of the sigma-0 measurements, *Sylvester et al*. (1989, 1990) concluded that both the SASS-1, Plant, and Donelan and Pierson models were, in general, inadequate. They showed that the SASS-2 model has properties that agree most closely with the actual data based on the scatter of the actual data compared with the predicted scatter of the model.

D. Comparisons in model parameter space

Freilich and Dunbar (1993) present an example of a model function comparison approach designed to simply span the full parameter space while remaining independent of both wind retrieval technique and the precise formulation (tabular or analytic) of the models being compared. The approach involves calculating the azimuth Fourier series for sigma-0 at each location on a regular grid defined by wind speed and incidence angle (e.g., a 2 term series is illustrated in Eq. (4.2). The values of each coefficient (A_n) in the Fourier series define a surface in (speed, incidence angle) space, which can be easily presented as a contour plot. Multiple models can be compared, coefficient by coefficient, by overlaying the contours. In practice, significant model function differences can be examined for

moderate incidence angles by comparing contour plots for the general wind speed dependence (A_0 versus. speed and incidence angle), upwind/crosswind modulation (A_2 or normalized A_2/A_0 versus speed and incidence angle) and normalized upwind-downwind sensitivity (A_1/A_0 in the speed, incidence angle plane).

To illustrate Freilich and Dunbar's approach the SASS-I and SASS-2 model functions are compared in Figs. 5.1-5.3. A standard table of sigma-0 as a function of wind speed |U|, incidence angle θ, and relative azimuth χ was constructed for each model function based on analytic forms and coefficients provided in the literature. Coefficients of the Fourier cosine series in azimuth were calculated for each (|U|,θ) pair.

Figure 5.1 shows the surfaces defined by the A_o for each model over the range $3<|U|<20$ m/s and $16°<\theta<58°$. In both models, A_o is a decreasing function of incidence angle, with a greater incidence angle sensitivity at low wind speeds than at higher winds. The model functions predict very similar A_o for $\theta<30°$, but they increasingly diverge at higher incidence angles and particularly at low wind speeds.

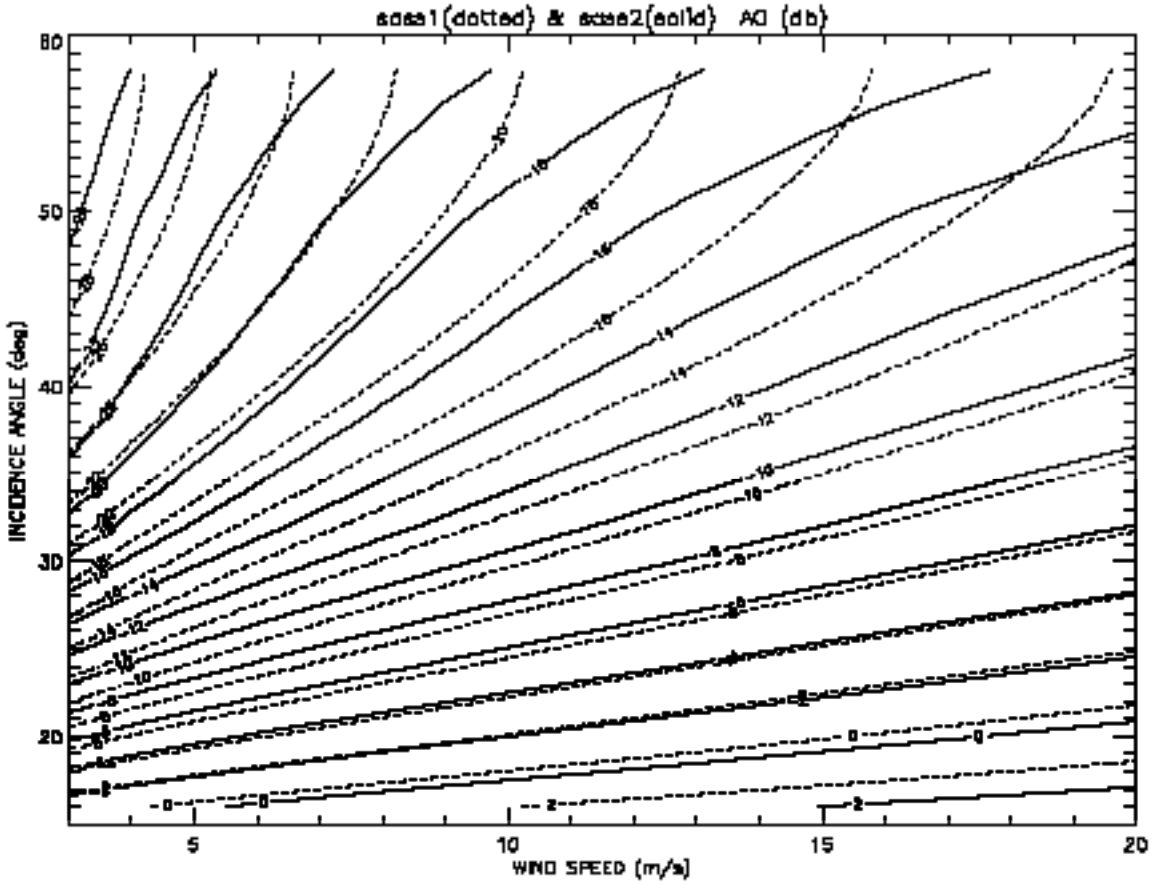

Figure 5.1. Comparison contour plot of A_0 for SASS-1 and SASS-2.

Figure 5.2 compares surfaces of upwind/crosswind modulation (defined here as the dB ratio of sigma-0 at $\chi=0°$ to sigma-0 at $\chi=90°$). Both models predict generally increasing

upwind/crosswind modulation with increasing incidence angle at fixed wind speed, and decreasing modulation with increasing wind speed at fixed incidence angle. However, the detailed shapes of the surfaces are significantly different for the two model functions, especially at low wind speeds.

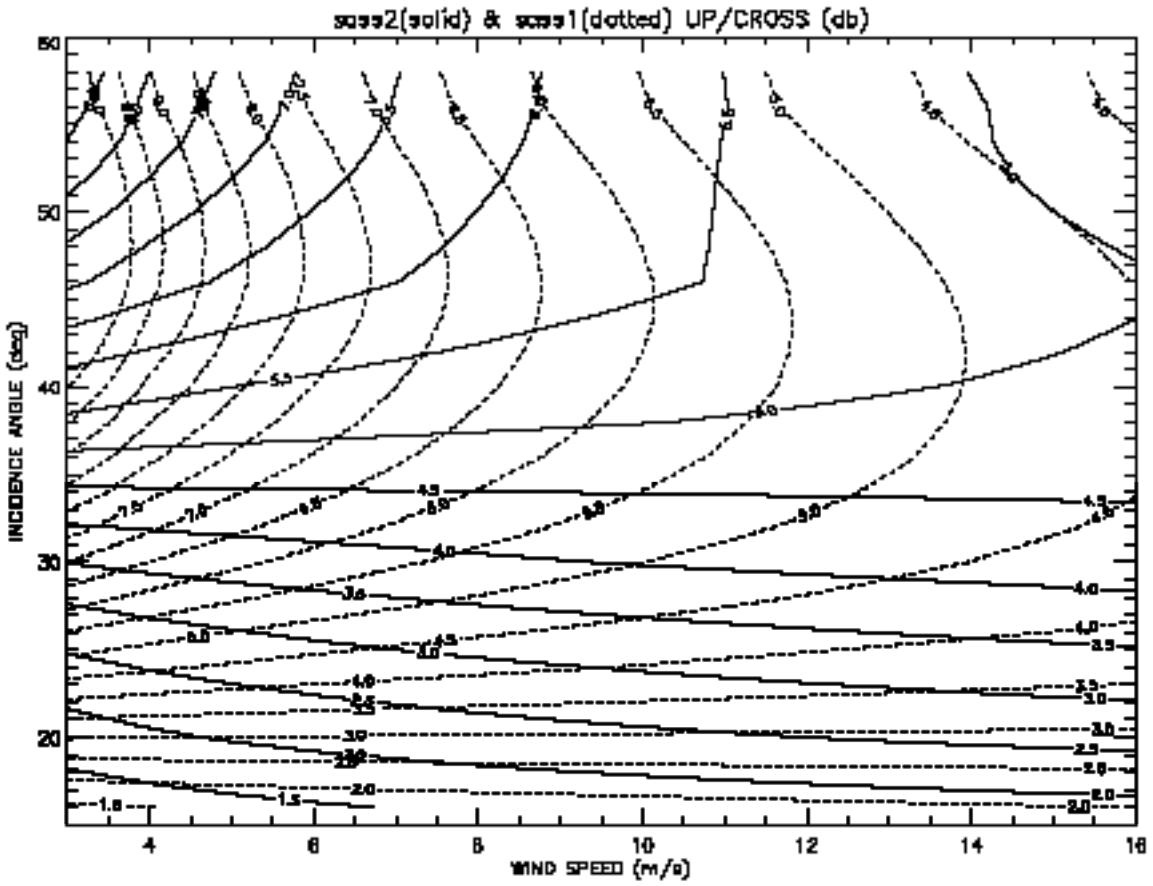

Figure 5.2. Comparison contour plot of upwind/crosswind ratio for SASS-1 and SASS-2. The ratio (in dB)is defined as the ratio of sigma-0 at χ=0° to sigma-0 at χ=90°

Finally, upwind/downwind ratios (in dB) (defined here as the dB ratio of sigma-0 at χ=0° to sigma-0 at χ=180°). are presented in Figure 5.3. As expected from the different data sources used in the derivations of the two models and previous discussions, both the relative shapes and the absolute magnitudes are significantly different between the two model functions. The differences are particularly large for θ>30°.

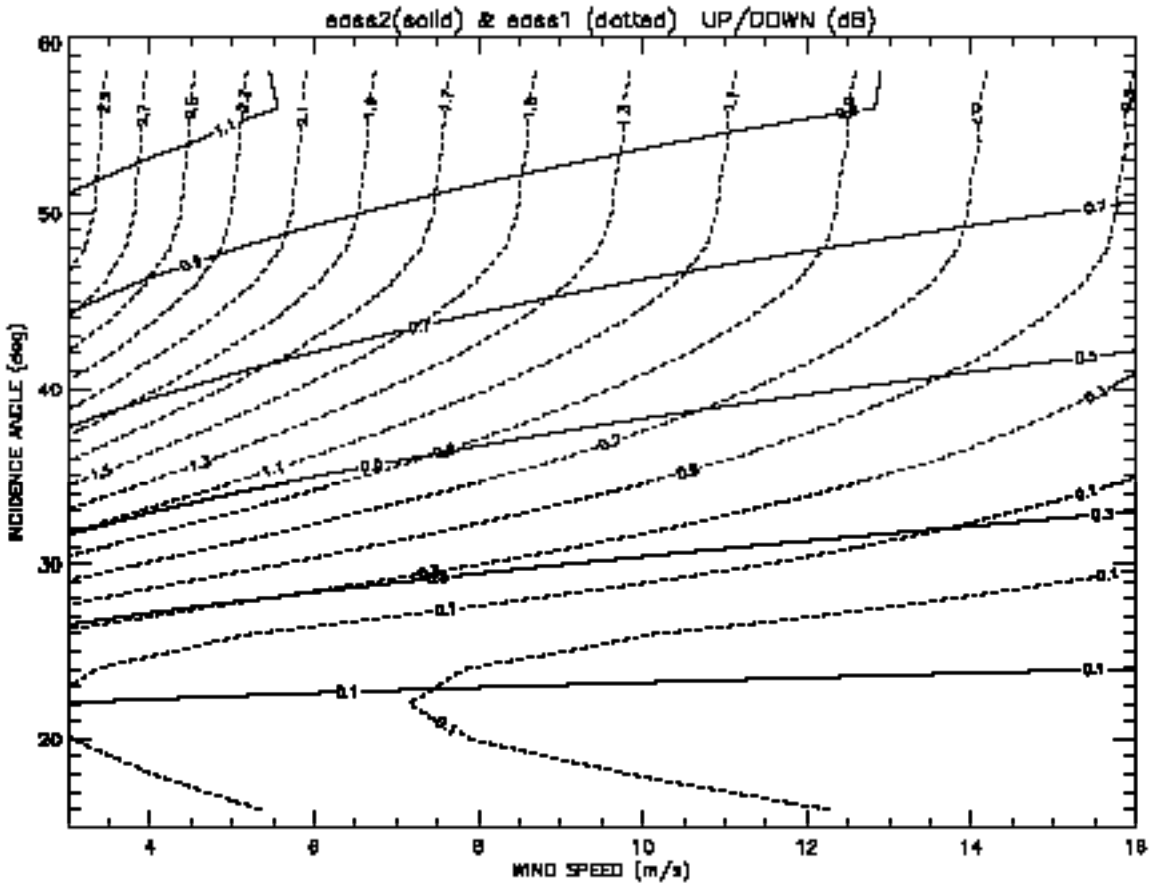

Figure 5.3. Comparison contour plot of the upwind/downwind ratio of SASS-1 and SASS-2.The ratio (in dB) is defined as the ratio of sigma-0 at $\chi=0°$ to sigma-0 at $\chi=180°$

E. Locations of Azimuth Minima

The normalized radar backscattering cross sections for each polarization, σ°_{VV} and σ°_{HH}, are a function of wind speed (or perhaps the friction velocity), incidence angle, wind direction. Various functional forms for these model functions have been given in the literature. As of now, there have been two different analytical forms for the C-band V-pol model function based on the availability of actual data. *Freilich and Dunbar* (1993) have developed a method that avoids expressing the model function analytically. It produces a table that replaces the analytical form and thus is not limited by the following considerations.

Recent results (*Li et al*. 1988) reveal inconsistencies between empirical model functions and the azimuthal variation of sigma-0. This is due, in part, to the functional form of the azimuth angle variation. For a given wind speed incidence angle and polarization, sigma-0 varies as a function of the wind direction. The most general representation, with no jump discontinuities for the purpose at hand, is a function that uses sines and cosines as the orthogonal basis as given by Eq. (5.1) below. In principle, but not in practice, *N* can be very large for an analytic expression for sigma-0 as a function of the relative azimuth angle.

For a fixed wind speed and incidence angle,

$$\sigma^o(\chi) = A_0 + \sum_{n=1}^{N} A_n \cos n\chi + B_n \sin n\chi \qquad (5.1)$$

where A_o, A_n, and B_n are functions of the wind speed and incidence angle.

Most model functions assume azimuthal symmetry, i.e., $\sigma^o(\chi) = \sigma^o(-\chi)$ so that the B_n in Eq. (5.1) are zero. This model for the azimuthal variation of sigma-0 (with small N) has been widely used. The SASS-1 model contained terms equivalent to N=7 fitted to the logarithm of the backscatter. *Schroeder, et al.* (1984, 1985) fitted Eq. (5.1) to the AAFE circle flight data with N=2. *Britt and Schroeder* (1984) fitted the AAFE circle flight data to Eq. (5.1) with N=4. Unfortunately, for small N, this approach may yield unrealistic secondary maxima and minima for some wind speeds, incidence angles, and directions as evident in *Wentz et al*. (1994) where the H-pol sigma-0 is negative for some low winds for relative azimuth angles near 90° and 270°.

Note that when B_n=0 in Eq. (5.1), the minima of $\sigma^o(\chi)$ are at exactly cross-wind only when A_1=0 (see Appendix D). *Li et al.* (1988) showed, using aircraft data from FASINEX (see previous discussion), that the minima of $\sigma^o(\chi)$ do not always occur at cross wind. The results of the modeling work presented in *Chen et al* (1993) suggest that this off-crosswind minima may be the result of the skewness of the surface waves. This is a key area of current research.

Liu and Pierson (1994) have made an extensive analysis of the locations of the azimuthal minima for C-band. Additional analysis for Ku-band is contained in Appendix D.

Freilich and Dunbar (1993) have developed a method that, in principle, can avoid expressing the model function analytically by produces a model function table that replaces the analytical form. The Freilich and Dunbar approach is thus particularly appealing for generating a post-launch model function. However, they did use a low-order Fourier Series expansion of the form of Eq. (5.1) to generate a C-band model function.

F. Recommendations

Based on the analyses presented the literature and here, we conclude that the SASS-2 model function represents the best existing operational model function. At this time, we recommend that it be used as the baseline model function for use in NSCAT wind retrieval.

A possible implication for future NSCAT activities resulting from Weissman's analysis is that two model functions could be developed for the analysis and application of satellite data. One for the wind speed (U_{10}) and another for friction velocity (u*). The question of the utility of additional, auxiliary data from other sensors (e.g., radiometers) to improve the u* algorithm remains open.

Further research into the location of the azimuth minima of $\sigma^o(\chi)$ and the use of the location of the azimuth minima as metric for model function comparisons is warranted.

G. References

Chen, K.S., A.K. Fung, and F. Amar, "An Emperical Bispectrum Model for Sea Surface Scattering," IEEE Trans. Geoscience ang Remote Sensing, Vol. 31, No. 4, pp 830-835, 1993.

Freilich, M. H., and R. S. Dunbar, "Derivation of Satellite Wind Model Functions Using Operational Surface Wind Analyses: An Altimeter Example," *J. Geophys. Res.*, Vol. 98, No. C8, pp 14633-14649, 1993.

Freilich, M.H.,"Satellite Scatterometer Comparisons with Surface Measurements: Techniques and SEASAT Results," *Proceedings of a Workshop on ERS-1 Wind and Wave Calibration*, 2-6 June 1986, pp. 57-62, (ESA SP-262, Sept. 1986).

Friehe, C. A., W. J. Shaw, D. P. Rogers, K. L. Davidson, W. G. Large, S. A. Stage, G. H. Crescenti, S. J. S. Khalsa, G. K. Greenhut, and F. Li, "Air-Sea Fluxes and Surface Layer Turbulence Around a Sea Surface Temperature Front," J. Geophys. Res., Vol. 96, No. C5, pp 8593-8609, May 15, 1991.

Keller, M.R., W.C. Keller and W.J. Plant, "A Wave Tank Study of the Dependence of the X-band Cross Sections on Wind Speed and Water Temperature", J. Geophys. Res., Vol. 97, No. C4, pp 5771-5792, 1992.

Li, F. , F., W. Large, W. Shaw, E.J. Walsh, and K. Davidson, "Ocean Radar Backscatter Relationship with Near Surface Winds: A Case Study During FASINEX, J. Phys. Oceanogr., 12, 342-353, 1989.

Liu, Y., and W. J. Pierson, "Comparisons of Scatterometer Models for the AMI on ERS-1: The Possibility of Systematic Azimuth Angle Biases of Wind Speed and Direction," I*EEE Trans. Geosci. Remote Sens.*, Vol. 32, No. 3, pp. 626-635, May 1994.

Weissman, D. E., "Dependence of the Microwave Radar Cross Section on Ocean Surface Variables: Comparison of Measurements and Theory Using Data From the Frontal Air-Sea Interaction Experiment," J. Geophys. Res., Vol. 95, No. C3, pp 3387-3398, Mar 15, 1990.

Weissman, D. E., K.L. Davidson, R.A. Brown, C.A. Friehe and F. Li, "The Relationships Between Microwave Radar Cross Section and Both Wind Speed and Stress: Model Function Studies Using Frontal Air-Sea Interation Experiment Data," *J. Geophys. Res.*, Vol. 99, No. C5, 1994.

VI. Sigma-0 Sensitivity to Geophysical Parameters

The purpose of this section is to consider the sensitivity of sigma-0 to geophysical variables. Chief among these, of course, is wind. However, as previously discussed, other geophysical parameters (e.g., long waves) may also affect sigma-0. Since the sensitivity of sigma-0 to geophysical parameters must be evaluated by comparison of the sigma-0 measurements to measurements of the geophysical variables. Unfortunately, both the measurements of sigma-0 and the geophysical parameters have errors. While the former is primarily a radar problem, the latter is a geophysical problem and it is appropriate that we consider the determination of the "ground-truth."

Because the geophysical measurements to which the sigma-0 measurements are compared also have errors we first consider the issues involved with comparison data when applied to scatterometer model function refinement. The sensitivity of sigma-0 to wind speed and wind stress are then addressed followed by a discussions of a possible low wind speed cutoff and a high wind speed saturation in the model function. Long waves and rain effects are also briefly considered. As discussed in the section summary the subcommittee concludes with reservations that "the scatterometer measures U_{10}."

A. The problems of comparison data

The problem of "ground truth" comparison data is that there is no ground and there is no truth. There are data on the winds and the wind stress over the ocean that can be compared to the winds and wind stress inferred from backscatter data. These data are varied in both quantity and quality.

i. Data sources

While not limiting data sources to this list, typical comparison conventional data consist of:

1) The routine reports by ships without anemometers of estimates of the wind speed and directions.

2) The routine reports by ships with anemometers of measurements of the wind speed and direction.

3) The routine reports of wind speed and direction by United States National Data Buoys every ten minutes, with supplemental data of great value.

4) The routine reports of wind speed and direction by data buoys deployed by other nations.

Some remotely-sensed comparison data include:

1) SSM/I-derived wind speeds.

2) The outputs of GCMs.

Directly measured wind stress is not routinely reported. The various experiments *Large and Pond* (1981), *Geernaert et al.* (1987, 1988), and *Donelan* (1990) that have measured wind stress disagree with one another as to the relationship of the stress to the time averaged wind at 10 m, or at any other height. The use of SSM/I-derived wind speeds and GCM outputs were previously discussed. In the following we address concerns with the interpretation and quality of conventional data.

ii. Quality of wind data

The study by *Pierson* (1990) that compared the wind reports from items 1 to 4 above found that the ship reports were highly questionable and essentially concluded that the wind reports by data buoys were the only data useful enough for comparison to the winds recovered by a scatterometer (based on NDBC buoy data).

The GOASEX experiment during SEASAT, *Jones et al.* (1982), *Schroeder et al*. (1982) and *Brown et al*. (1982) illustrates the difficulty of using conventional winds to validate scatterometer winds. If the errors and biases of the conventional winds produce uncertainties of plus or minus 2 or 3 m/s in speed and ±30° in direction, validating design goals for a scatterometer becomes impossible.

The difficulties in defining the synoptic scale wind field over an oceanic area at present are well illustrated by the recent LEWEX experiment (*Beal*, 1991). A number of analysis centers that used the same data base produced wind fields that disagreed with each other by substantial amounts. This complicated the interpretation of the wave spectra produced from these wind fields.

Pierson suggests a straightforward way to determine how well the synoptic scale winds from conventional analyses agree with measured winds. Every synoptic scale analysis yields a wind speed and direction by interpolation at each location of a data buoy. Each National Data Buoy reports the winds for 10 minute averages continuously. A synoptic scale average of the measured wind (*Pierson*, 1983) representative of a scatterometer super observation can be obtained from each data buoy, which would permit a direct comparison between the synoptic scale wind and the measured wind.

iii. Comparison data wind stress vs. wind speed measurement

The anemometer heights on the various data buoys vary. It is necessary to refer all winds to a common height and to what has been termed the effective neutral wind speed described below. The calculation of the effective neutral wind speed requires the use of the Monin-Obukhov - R. H. Brown planetary boundary layer model, which in turn require a drag coefficient.

The drag coefficient is one of the most elusive quantities in boundary layer theory. There are several dozen proposed equations of the form, $CD = A + B|U|$. Those who believe that the Buckingham PI theorem can solve all problems (See *LeMehaute* (1990) for a discussion of dimensional analysis) are distressed by this equation, but few have tried to do otherwise.

To confound the problem even more, there have been a number of papers that report a relationship between the wind stress and properties of the waves at the time the winds were measured, *Blake* (1991), *Donelan* (1982), *Geernaert* (1990). Several agree that the wind stress decreases with increasing wave age and wave height since one is correlated with the other. They do not agree as to details, however. *Toba et al*. (1990) give exactly the opposite conclusion.

The one favorable feature of these results is that the variation of wind speed with height, say from 10 m to 19.5 m, for most stability conditions is rather insensitive to the value of the drag coefficient. The calculated stresses can differ by large amounts but the wind speed differences at, say, 10 m for winds measured at, say 19.5 m, or conversely, differ by rather small amounts when different drag coefficients are used. The influence of varying wave properties on the variation of wind speed and direction versus height has been investigated in only a limited way.

iv. Wind reference height

The use of a 19.5 m reference height began with a series of three back to back papers by *Moskowitz* (1964), *Pierson and Moskowitz* (1964) and *Pierson* (1964). The well-known proposed spectral forms for fully developed wind seas were based on data obtained by the Tucker Shipborne Wave Recorder operated on British weather ships. These ships had anemometers mounted at a height above the waves as reported in feet which converted to 19.5 meters. The authors at that time had considerable trepidation in converting the reported winds in knots to meters per second and to a height of 10 meters because of the variety of drag coefficients then available (see *Neumann and Pierson*, 1966). Various wave forecasting models that resulted were then based on winds for an anemometer height of 19.5 m.

The reference anemometer height of 10 m was chosen a long time ago and thought to best represent the anemometer heights on ships and the wind that best corresponded to the Beaufort estimates. However, very few ships at sea have anemometers at 10 m and the air flow around the ship is distorted. The little data on the subject has failed to show that correcting a ship reported wind for anemometer effects makes the result more accurate. For a counter view see *Cardone and Carre* (1980).

There would be little difficulty in referring the wind to either 10 or 19.5 m, but there is a substantial difference in wind speeds for high winds that needs to be considered. The objective of ±2 m or 10%, whichever is worse, is more difficult to meet for the higher anemometer height.

v. The "effective" neutral wind in the marine boundary layer

The wind speed and direction measured by an anemometer may not equal the wind speed and direction recovered by a model function, even if the model function and the measured wind are correct. The time averaged wind varies as a function of elevation over the ocean and can be represented by the theory of *Monin and Obukhov* (1954) for the first 10 to 30 meters, or so, above the mean sea surface. The variation of wind with height calculated from Monin Obukhov theory merges with Ekman theory and the effects of the thermal wind so as to be able to describe the wind up to the gradient wind level.

Monin Obukhov theory accounts for the effects of atmospheric stability by means of the Monin Obukhov length, which yields a departure from the logarithmic wind profile depending upon atmospheric stratification. The actual wind speed at an elevation of 10 meters above the mean sea surface can be either greater than or less than the speed calculated for a neutrally stratified wind profile depending upon the Monin Obukhov length.

The SEASAT SASS winds were compared with the effective neutral wind because this wind describes the variation of the wind with elevation for the first few meters (one or two) above the sea surface where the Monin Obukhov effects are small. An assumption about the relationship between the wind stress and the wind at 10 m is needed, but once this is made the procedure is to use the wind measured at a known anemometer height, calculate the wind profile from the theory, which determines u_* and then calculate the wind at 10 meters (or as for SEASAT 19.5 meters) for a neutral profile. The difference between the measured wind at 10 m and the effective neutral wind, which is obtained from a model function, can be substantial for areas of warm air advection, and moderate wind speeds where the atmosphere is stable and for areas of strong cold air advection where the atmosphere is unstable.

The calculated wind stress and the friction velocity can differ by substantial amounts depending upon the assumed relationship between the wind and the friction velocity, but the effective neutral wind will not differ by very much for the different assumptions.

vi. Atmospheric stability and air/sea temperature difference

As discussed in the following section, the scatterometer measures a wind-like variable. However, we are generally interested in either the wind vector or the wind stress vector. Since the wind vector at some reference height and the wind stress are affect by the atmospheric stability which, in turn, is affected by the air/sea temperature difference, these become significant to the geophysical modeling problem.

There are considerable disagreement on the effects of sea surface temperature on radar backscatter. The general belief is that radar backscatter depends on ocean surface waves near the Bragg wavelengths which are affected by viscosity and surface tension. Viscosity changes roughly by 50% for the natural range of sea surface temperature and should be a more important factor than surface tension which changes by only 5% (*Liu*, 1984; *Stewart*, 1985). The effects have been examined using theory, laboratory experiments and from satellite data, but no clear conclusions have been reached.

Lleonart and Blackman (1980) introduced the factors of viscosity and surface tension into their formulation of wave spectra and postulated, through dimensional argument, that the spectral density of capillary waves $\phi = C\nu^{1/2}$, where ν is the kinematic viscosity and C is invariant with viscosity. Backscatter increases with wave and viscosity decreases with increasing temperature; however, the formulation of Lleonart and Blackman implies that the backscatter would decrease with increasing temperature. *Liu* (1984) examined the relationship between SEASAT scatterometer wind speed residual and sea surface temperature using bin-averaged ship reports. The comparison over the east North Atlantic and the west North Pacific, where dense ship reports are available, implies that backscatter decreases with increasing temperature when the wind speeds are low. The study by *Freilich* (1986) on a similar relationship, completed with more vigorous statistical techniques and using individual buoy data, yields excellent agreement.

There is a strong argument, however, for decreasing wave spectra with increasing viscosity based on the belief that viscosity acts as a damping of dissipating force. In the model of *Donelan and Pierson* (1987), the capillary spectra $\phi = A - B\nu^{1/n}$, where A and B are invariant to viscosity and n is to be determined, has been interpreted as a support of increase in backscatter with sea surface temperature (e.g., Woiceshyn et al., 1986), which is true if *n* is positive. Donelan and Pierson also postulated a temperature dependent threshold wind speed for capillary waves to form. In a laboratory experiment to validate this postulation, *Kahma and Donelan* (1988) also found that the rms slope of capillary waves increases with water temperature which implies that the spectral density would also increase with temperature. *Zheng et al.* (1996) measured X-band radar return over a water tank with mechanically generated waves and found large increases of the backscatter coefficient with temperature and postulated that capillary waves depend on kinematic viscosity to the -8/3 power.

Keller et al. (1989) and *Keller* et al. (1992) found no systematic dependence of C-band backscatter on sea surface temperature in both field experiments in the North Sea and in laboratory studies. Recently, T. Liu (unpublished results) compared backscatter coefficients from the ERS-1 scatterometer and wind fields from numerical weather prediction models from the National Meteorological Center and sea surface temperatures from AVHRR over the global ocean. Preliminary results show no significant dependence of the residual backscatter coefficient on sea surface temperature.

Imperfect model function and inaccurate observations of wind and temperature made it difficult to isolate the temperature effect from the scatterometer measurements, in the presence of much stronger variabilities due to wind, incidence angle, and polarization. The applicability to natural conditions of laboratory results, particularly those using mechanically generated waves without energy input from wind, is also a major concern. The sea surface temperatures available are bulk temperatures whose variability may be quite different from the skin temperature which affects the capillary waves. It is clear that there is no agreement between satellite data and laboratory data and between satellite data and theory. However, except for the results of *Zheng et al.* (1995), sea surface temperature appears to be a secondary factor, with effects much smaller than primary factors related to wind.

B. Wind stress versus wind speed

Although it is beyond doubt that σ^o is sensitive to some characteristic of the wind in the boundary layer, it is not clear exactly what is the most appropriate choice. Is it the friction velocity - presumably with the direction of the stress vector - or is it some "neutral'" wind at 19 m, 10 m, 1 cm? In order to discuss the problem at all it is necessary to acknowledge that variations in σ^o come from several sources including: (a) Bragg scattering from wind-generated centimetric waves, (b) wedge and corner scattering from slope discontinuities due to very steep and breaking waves, (c) scattering from turbulent whitecaps, (d) Bragg scattering from parasitic capillaries. Clearly the wind dependencies of these various scattering mechanisms are different: in the usual moderate wind speed range of 5 to 15 m/s, various empirical results indicate that the wind speed dependence of σ^o for Ku-band is roughly quadratic for (a) and cubic for (b) and (c) -- virtually nothing is known about (d).

Ultimately the problem may be resolved by a complete coupled dynamical model for the air-water boundary layers and the scattering from the resulting surface. In the meantime, we must rely on emperical observations and simplified models such as Bragg scattering.

Let us consider Bragg scattering from wind-generated centimetric waves only, since this is believed to be the principal component of σ^o at moderate wind speeds (at least for vertical polarization). Insofar as first order Bragg scattering is the dominant component of sigma-0, the key question is what wind related parameter is most closely correlated with the spectral density of waves near the Bragg wavenumber. The stress is supported by a broad region of the spectrum, corresponding to waves of length 2 cm to several meters. A reasonable rule of thumb is that those waves having phase speed less than 5 times the friction velocity carry the stress. Calculations, based on the little we know of the high wavenumber part of the spectrum, indicate that the capillary waves support very little of the stress. Thus at Ku-band the Bragg waves provide an indication of the roughness height at one end of the spectrum of roughness. They do not reflect the "integral" overall roughness, and therefore their connection with the total stress is tenuous.

Consider the effect of adding a mono-molecular layer of some surfactant to a water surface under the action of wind stress. The surfactant film attenuates the high wavenumber waves and may entirely eliminate the Bragg waves at the high end of the spectrum. If only a small quantity of surfactant is added, some of the roughness elements remain but the Bragg scatters, and hence sigma-0, are greatly reduced. The stress will be reduced also but typically by only a factor of 2 or so (*Mitsuyasu and Honda*, 1982). If enough surfactant is added to eliminate all the wind-waves, sigma-0 will drop to near zero, but the stress will drop to its smooth wall value (*Mitsuyasu and Kusaba*, 1986), which is only about a factor of 2 or 3 smaller than its nominal value.

These thought experiments suggest that "the scatterometer measures stress" can not be completely correct. Nonetheless, surface stress may well be the wind parameter most closely related to sigma-0. The other popular choices of wind parameter are the wind speed at the WMO recommended height of 10 m or at the nominal ship mast height of 19.5 m. Both of these wind parameters would actually increase for a given geostrophic wind and a film-smoothed surface, while σ^o decreases. There is no escaping the fact that σ^o reflects the scattering from a narrow wavelength range and u*, U_{10}, $U_{19.5}$ etc., are all determined by the total roughness of the surface, which involves a very wide range of wavelengths.

The only completely consistent way to correlate σ^o with surface variables necessarily includes: a complete scattering theory; knowledge of the non-locally generated waves - "swell"'; knowledge of surface properties that affect the local generation such as viscosity, currents, surface dilational modulus; knowledge of atmospheric stability. Although considerable work is being done on the subject, a full scattering theory has not yet been developed. Furthermore, much of the required knowledge of surface properties may not be easily acquired from satellites. In view of these shortcomings, how should sigma-0 be interpreted?

In a purely wind generated sea, if conditions are steady and homogeneous over the upwind fetch, the spectrum of waves is self similar and the distribution of "roughness elements" over the wave spectrum depends on the wave age. In these circumstances, a measure of the roughness height in one part of the spectrum (1 cm to 5 cm) may very well yield a good estimate of the stress provided the wave age is not widely different from its open ocean range of 0.5 to 0.83 and the surface is clean. If the wave age is known, from measurements or modeling, then even tighter estimates are possible. The presence of non-locally generated wave systems can alter the stress and refined stress estimates are possible if the non-local wave systems are measured or accurately predicted by numerical models. These "long waves" are dealt with below. For the moment we will assume a purely locally generated sea and see how σ^o may be exploited to yield the best estimate of surface wind properties. The following information is assumed to be available: σ^o, and sea surface temperature, T_w. The following relationships are assumed to be established:

$$\sigma^o = f\,(u^*, T_w, c_p/U_{10})$$

where c_p/U_{10} is the wave age. The following procedure is then applied:

1. From the σ^o and Tw values and the assumed full development value of wave age ($c_p/U_{10} = 0.83$), the magnitude of the stress is determined (the direction is discussed elsewhere).
2. The roughness length Z_0 is estimated from *Charnock* (1955) using 0.014 for the "constant", i.e.
$$Z_0 = 0.014\ u^{*2}/g.$$
3. The neutral wind speed at 10 m is determined from the "law of wall",
$$U_{10} = u^*/\kappa\ \ln(10/Z_0).$$
4. The wave age of the wind sea is computed, c_p/U_{10}, and the roughness length is adjusted. The wind speed at 10 m is recomputed.

C. Low wind speed cutoff and water temperature

It has been argued (*Donelan and Pierson*, 1987) that viscous dissipation will suppress the short wave length Bragg scatterers at low wind speeds. Waves with wavelengths of 5 and

2 cm, which approximately correspond to the Bragg wavelengths at C and Ku-band, are significantly attenuated by viscosity. However, molecular viscosity doubles as the water temperature decreases from 30° to 0° C. *Donelan and Pierson* (1987) predicted that these wavelengths could not be generated at all unless a certain threshold temperature dependent wind speed was exceeded. This would result in very small (or zero) backscatter values (see Appendix E).

An experimental study of the generation of waves by light winds made by *Kahma and Donelan* (1988) suggested that water temperature has a strong effect on the frequency spectrum of the Bragg waves. Data were acquired for a fixed water temperature and for two fixed frequencies. Increasing the wind speed from a very low value showed a two order of magnitude jump in the spectral variance at a certain wind speed that could correspond to the hypothesized threshold speed. Separate variations of the wind speed and the water temperature showed that the spectrum for the water with a higher temperature was higher than the spectrum for a lower temperature.

Keller, et al. (1992) reported that they could not find this effect in a laboratory study of backscatter from waves with water of different temperatures. The measured backscatter values did, however, decrease rapidly for low winds. Recent laboratory results by *Plant and Donelan* (Appendix E) suggest a temperature dependent wind speed cutoff. Initial results from a tower experiment on Lake Ontario seem to confirm these results (*Long*, personal communication).

Unpublished results of a study at the University of Delaware (*Zheng et al.*, 1995) also support the idea that backscatter is water temperature dependent. Mechanically generated waves were produced and the 10.25 GHz radar backscatter measured. The mean square detected voltage (a measure of the uncalibrated backscatter power) was measured for a range of water temperatures from 5° C to 30° C at two antenna angles. The variation in the mean squared voltage with water temperature was significant and was estimated to correspond to a factor of 4-7 change in the backscatter. For light winds this would be non-negligible. A more detailed discussion of some of the effects described above has been given by *Pierson* (1990).

Although the satellite data does not support this view, some recent airborne measurements during the Surface Waves Dynamics Experiment yield clear evidence of it (*Carson,* 1992 - personal communication). He points out that the large scale spatial averaging of satellite data make it difficult to find consistent low wind speed returns. A further problem is that mechanical anemometers on buoys in very light winds will tend to yield low averages of the wind due to intermittent stopping and starting of the anemometer.

It is clear that wind speed or stress estimation at low winds from satellite scatterometers will benefit from a fuller understanding of wind variability on scales less than 50 km. Very little is known about this, but significant effort was put into gathering data in this area during the Surface Wave Dynamics Experiment (SWADE). A combination of buoy records at various horizontal spacings and aircraft flight tracks between buoys may be very helpful in this regard.

It is worthwhile to consider a recent, unpublished observation. In a recent experiment the JPL NUSCAT scatterometer was flown in conjunction with *R. McIntosh's* Ku-Band radar system. A key difference between the two systems is the measurement integration time. While McIntosh's radar system appeared to have observed a strong low wind speed cutoff, these were not seen by the NUSCAT system. This may illuminate a possible explanation for why the cutoff is not observed in spaceborne data: while the cutoff may be real when the wind speed is uniformly low over the illuminated region, the variability of low winds (particularly over a large region corresponding to kilometer-sized footprint) is such that the

observed sigma-0 is dominated by the response of the surface with local winds above the cutoff. Further research is needed in this area.

D. High wind speed saturation

The wind speed (or stress) dependence of σ^o is related to the spectral density of the Bragg scatterers, at least at low and moderate wind speeds. Various microwave backscattering experiments seem to show that the spectral levels of these waves are sensitive to wind. *Wu* (1990) has summarized the wind speed dependence of sigma-0 at a particular Bragg wavelength k as $\sigma^o(k) \sim U^n$. He finds that the summary of all available data in the Bragg wavelength range of 0.87 cm to 70 cm suggest a variation of wind sensitivity given by:

$$n = 0.23\ k^{1/3}, \quad \text{kin m}^{-1}.$$

The wind sensitivity varies from roughly $U^{0.5}$ to $U^{2.5}$ over the wavelength range covered. Taken at face value, this implies a monotonic wind dependence over a wide range of wind speeds. In fact the data were gathered in the usual rather restricted range of field data --- about 5 m/s to 20 m/s. It seems unlikely that the spectral levels will increase indefinitely with wind speed. Rather, at sufficiently high winds the high wavenumber spectra will become fully saturated and show no further appreciable wind dependence. The large tank wavenumber spectra of *Jähne and Riemer* (1990) are very revealing in this regard. Their downwind wavenumber spectra for one decade on either side of the capillary-gravity transition are reproduced in Figure 6.1. The variation in wind sensitivity with wavenumber is apparent. While the short gravity waves on the left of the diagram show only weak sensitivity, the capillary-gravity region unfolds under the action of the wind providing, in this tiny corner of the wave spectrum, the essential key to scatterometry. The purely capillary waves to the right of the diagram are quite wind-sensitive but are also strongly attenuated by viscosity.

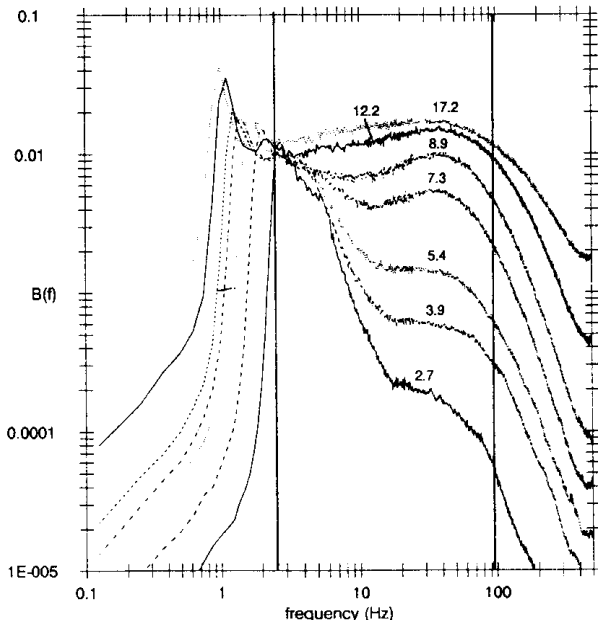

Figure. 6.1. Reproduction of Fig. 7 from *Jähne and Riemer* (1990) showing a large-tank wavenumber spectra for various values of U_{10} at 90 m fetch.

The ordinate of Figure 6.1 is the spectrum times k^4 --- *Phillips*' (1958) degree of saturation. A vertical slice through Figure 6.1 at any wavenumber reveals the tendency to saturation at the highest wind speeds. The saturation level increases from gravity to capillary gravity waves in a manner that suggests that the limiting process is wave breaking, as originally suggested by *Phillips* (1958). If this were so, the asymptotic spectral dependence in both short gravity and capillary ranges would be as γk^{-4} but the degree of saturation γ would be somewhat greater for capillary waves --- roughly proportional to the square of the ratio of their limiting steepness, i.e., ~3. Of course, the purely capillary waves are limited by viscosity and the wave-breaking asymptote is never reached but the tendency is apparent.

This saturation of the Bragg scatterers is predicted by *Donelan and Pierson* (1987) (see their Figure 3). Unfortunately, observations of saturation of sigma-0 at high wind speeds are not common and the dominance of other (besides Bragg) scattering mechanisms at high wind speed may offset the saturation of the Bragg scatterers. While it does appear that sigma-0 versus wind does roll-off at least somewhat for high wind speeds, this effect is not understood.

E. Long waves

The results of *Colton* (1989) and others suggest that modulation of the short waves by long waves may affect the response of sigma-0 versus wind (see previous discussions). However, further research in this area is required to fully understand this effect. Recent results from the ONR/NRL sponsored High Resolution Remote Sensing (HIRES) program suggest that wave-current interaction modulate the long and short waves yield large sigma-0 values. Such interactions are prevalent in regions of large horizontal shear such as the Gulf Stream, the Kuroshio and Algulhas currents and with large surface features such as eddies and rings.

There is also a substantial growth in evidence that the presence of waves on the ocean surface influence the determination of wind stress. Experimental results have shown that the aerodynamic drag coefficient depends on sea state, because the roughness of the sea surface is coupled to waves (for a detailed review see *Donelan*, 1990). Such a relationship might be intuitive from studies of fluid flow over solid walls, but in practice a description of the sea surface roughness is complicated by the fact that waves are mobile and constantly evolving in space and time (*Donelan* et al., 1993). A sea which contains relatively higher slopes (compared with a fully developed situation, possibly caused by short time and/of spatial fetches) has been observed to cause a higher drag coefficient. This usually influences the small scale roughness and can be expected to affect the backscatter.

An experiment conducted from a tower in the Gulf of Mexico (*Keller* et al., 1985) studied the dependence of the backscattered power on long wave slope for stable and unstable atmospheric conditions. For narrow bands of moderate wind speed (6-8 m/s and 8-10 m/s) at 40° incidence, v-pol, and stable stratification, clear evidence of a proportional increase in the upwind radar cross section with long wave slope was observed. However, this is not the case when a colder atmosphere resulted in an unstable boundary layer. Here, at moderate winds, no effect of wave slope could be detected in the backscatter.

Recent airborne Ku-band measurements during SWADE (*Nghiem* et al., 1993) found strong effects of sea state on the azimuthal signature of the radar backscatter under light wind (< 4 m/s) conditions. No significant long wave effects were observed for high (12 m/s) wind conditions.

A fully developed sea contains a range of long waves. However, the long wave spectrum is different in a developing sea. A simple measure of the difference between a fully developed sea and the waves that are possibly present at the time of the scatterometer measurements is the wave age which is defined by the ratio of the linear phase speed of the spectral peak to the 10 m wind speed. Without direct measurements this quantity can be estimated from wave forecasting models. Sensitivity studies reported by *Janssen and Woiceshyn* (1992) and *Woiceshyn and Janssen* (1992) for C-band data show that the residual scatter in the wind speeds from ERS-1 AMI data can be reduced by taking this parameter into account.

While progress is being made in interpreting the wide range of ocean, lake, and wave tank studies on the dependence of small scale roughness on longer waves, more research is needed to understand this relationship further.

F. Rain

The effect of rain on the waves may invalidate the use of backscatter data to measure winds where it is raining. In a series of carefully controlled tank experiments *Bliven* et al. (1988a; 1988b; 1993a; 1993b) have shown that rain modifies the surface geometry producing rain-generated small-scale waves, attenuating existing wind-generated waves due to rain-generated turbulence, and modifying the momentum transfer from the atmosphere to the ocean due to water stratification. The net result is that for a given wind speed, sigma-0 tends to increase with the rain rate. However, the net effect decreases as the wind speed increases. Further, *Bliven and Giovanangeli* (1993) have shown that rain hitting a water surface causes circular ripples to radiate from each impact forming an isotropic pattern with the same radar signature at all directions. This suggests that that rain will effect the directional retrieval of the wind. *Atlas* (1994) describes this effect for L-band and review the subject by means of an extensive list of references.

The presence of rain drops in clouds also affects the observed sigma-0 due do the attenuation and scattering of the Ku-band signal as it passes through the clouds. Using simulation, *Spencer and Shimada* (1991) have demonstrated that the attenuation by rain dominates at low radar incidence angles and high wind speeds. Volume scattering from cloud-borne raindrops is significant at high incidence angles and low wind speeds.

To correct for the attenuation of Ku-band signals by liquid atmospheric water, *Moore, et al.* (1982) used SMMR brightness temperatures to calculate the attenuation based on available models of cloud drop distributions. Kristina Katsaros and her colleagues have greatly advanced the use of SMMR and SSM/I data to find quantitative values for the integrated water vapor distribution and rainfall rates near fronts and in extra tropical cyclones. For Ku-band, areas of rain located from SMMR data, or postulated by continuity near fronts, should be considered suspect and used with caution. Pertinent references include *McMurdie and Katsaros* (1991), *Katsaros and Brown* (1991), and *McMurdie and Katsaros* (1992).

G. Summary and recommendations

Even a casual reading of this section reveals that there are a great many areas of uncertainty and controversy in geophysical model function sensitivity to various environmental parameters. It is probably useful to remind the reader that these effects are generally second-order and that operational model functions such as SASS-2 are good to at least first order.

i. Wind stress

Members of the subcommittee are of the general opinion that there should be no recommendation for the calculation of wind stress until such time as there is a broader consensus on the subject. Until such time we will support that "the scatterometer measures U_{10}."

ii. Comparison and supporting data

The following is a list of comparison and supporting data which the committee feels will be useful to support post-launch model function studies. As research ideas naturally evolve, this list may need to be expanded. We feel this list provides a useful starting point.

1) Other instruments onboard ADEOS need to be described and documented for the science team. Appropriate data products will need to be co-located with NSCAT data for use and disseminated to the science team.

2) As discussed in the following section data from all available moored data buoys deployed on the world oceans will be needed. All reports, whether continuous, hourly, or six hourly, are desired.

3) Global synoptic scale analysis from various meteorological centers will be needed on daily (or more frequent) basis.

4) Ship reports with reported dew points. These will be used with buoy data to compute the effective neutral winds.

5) Sea surface temperature fields predicted by meteorological centers and/or measured by SSM/I.

6) Appropriate data from other spacecraft sensors such as SSM/I, altimeters, etc.

7) Cloud imagry.

8) Wave height data from meteorological centers and/or altimeters.

W. Pierson has suggested that the project prepare daily maps of the locations of negative (and/or very small) sigma-0 values and the locations of very large Kp values.

iii. Bouy comparison data

We note that the analysis reported by *Pierson* (1990) was based on fairly old data. It might be useful to repeat the study by Pierson with a more up-to-date data base. Reliable wind data are much more available now than they were during SEASAT. There are 17 (or more) National Data Buoys in deep water and 6 Canadian buoys in the North Atlantic (See *Hamilton*, 1992, and *Gilhousen*, 1990). The 23, or more, operational data buoys can serve as a comparison data base for both the C-band scatterometer on ERS-1 and NSCAT on ADEOS. The operational data buoys from other nations will also be useful. They should be identified, especially the Japanese buoys, and ways to ensure that their data will be obtainable should be initiated. Data from other national buoy systems should be consistent with the NDBC in order to be combined with the NDBC data.

A data file similar to the one laboriously obtained for SEASAT by M. Freilich should be formed that consists of all of the data obtained by a data buoy including wave data for one hour before to one hour after an NSCAT measurement and of all of the "raw" and processed NSCAT data for a large radius around the buoy.

Pierson suggests a straightforward way to determine how well the synoptic scale winds from conventional analyses agree with measured winds. Every synoptic scale analysis

yields a wind speed and direction by interpolation at each location of a data buoy. Each National Data Buoy reports the winds for 10 minute averages continuously. A synoptic scale average of the measured wind (*Pierson*, 1983) representative of a scatterometer super observation can be obtained from each data buoy, which would permit a direct comparison between the synoptic scale wind and the measured wind.

The effect of differences in wind direction will be somewhat messy, but nevertheless revealing. The methods described by *Pierson* (1990) could be used. The pairs of wind speeds can be used to make a scatter plot. One ventures to predict that the relationship between the two wind speeds will be of the form

$$V_{SYNOPTIC} = V_0 + A\, V_{BUOY} \tag{6.1}$$

where V_0 is greater than zero and A is somewhat less than one. Moreover, it is quite possible that the correlation coefficient will be high. If the scatterometer winds have a high correlation with the winds from the synoptic scale analyses, an inversion of Eq. (6.1) as in Eq. (6.2) and arbitrarily renaming the variables will yield scatterometer winds that agree better with the measured winds than they do with the synoptic scale winds. These scatterometer winds can then be used to produce an improved synoptic scale analysis.

$$V_{SCAT(B)} = (V_{SCAT(S)} - V_0)/A \tag{6.2}$$

for $V_{SCAT(S)} > V_0$ and $V_{SCAT(B)} = 0$ otherwise.

Various members of the subcommittee feel that at the present time, the best way to validate the winds obtained by scatterometry seems to be to compare them with winds directly measured by data buoys. The data can be concurrent in space and time. The variability of the conventional winds can be taken into consideration.

I. References

Atlas, D., "Footprints of Storms at Sea: A View from Spaceborne Synthetic Aperture Radar," *J. Geophys. Res.*, Vol. 99, No. C4, pp 7961-7970, 1994.

Beal, R. C., *Directional ocean wave spectra*. John Hopkins University Press, 1991.

Blake, R. A., "The dependence of wind stress on wave height and wind speed," *J. Geophys. Res.*, Vol. 96, No. C11, pp. 20,531-20,545, 1991.

Bliven, L. F., J. P. Giovanangeli, and G. Norcross, "A Study of Rain Effects on Radar Scattering From Water Waves," Preprint volume. Seventh conference on Ocean-Atmosphere Interaction Jan. 13 to Feb. 5, 1988 Anaheim, Calif. *Amer. Meteor. Soc., 1988.*

Bliven, L. F., and G. Norcross, "Effects of Rainfall on Scatterometer Derived Wind Speeds," *Proceedings of the International Geoscience and Remote Sensing Symposium*, Edinburg, Scotland 13 to 16 Sept. 1988, ESA SP 284 (IEEE 88 CH 2497.6), 1988.

Bliven, L. F., H. Branger, P. Sobieski, and J-P Giovanangeli, "An Analysis of Scatterometer Returns from a Water Surface Agitated by Artificial Rain: Evidence that Ring-Waves are the Main Feature," in press, 1993.

Bliven, L. F., and J. P. Giovanangeli, "An Experimental Study of Microwave Scattering from Rain- and Wind-Roughened Seas," Int. J. Remote Sensing, Vol. 14, No. 5, pp. 855-869, *1993.*

Brown, R. A. "On a Satellite Scatterometer as an Anemometer," *J. Geophys. Res.*, Vol. 88, No. C3, pp. 1663-1673, Feb. 1983.

Colton, M. C., "The Dependence of Radar Backscatter on the Energetics of the Air-Sea Interface," Ph.D. Dissertation, Naval Postgraduate School, Monterey, CA, Dec. 1989.

Donelan, M., F. Dobson, S. Smith, and R. Anderson, "Dependence of Sea Surface Roughness on Wave Development," *J. Geophys. Res.*, Vol. 23, pp. 2143-2149, 1993.

Donelan, M.A., "The Dependendence of the Aerodynamic Drag Coefficient on Wave Parameters, in *Proceedings of the First International Converence on Meteorology and Air Sea Interaction of the Coastal Zone*, pp. 381-387, American Meteorological Society, Boston, MAss., 1982.

Donelan, M. A., and W.J. Pierson, Jr., "Radar Scattering and Equilbrium Ranges in Wind-Generated Waves with Application to Scatterometry," *J. Geophys. Res.*, Vol. 92, pp. 4971-5029, 1987.

Freilich, M.H., "Satellite Scatterometer Comparisons with Surface Measurements: Techniques and Seasat Results", *Proc. Workshop ERS-1 Wind and Wave Calibration*, ESA SP-262, 57-62, 1986.

Geernaert, G. L. "Variation of the Angle Between the Surface Layer Wind Vector and the Wind Stress Vector and its Dependence on Thermal Stratification and Advection," *J. Geophys. Res., 9*, 8215-8220., 1988.

Gilhausen, D. B., E. A. Meindl, M. J. Changery, P. L. Franks, M. G. Burges, D. A. McKittrick, "Climatic summaries for NDBC buoys and stations," U. S. Dept. of Commerce NOAA NWS, National Data Buoy Center, NSTL, Miss. 39529, 454 pp., 1990.

Hamilton, G., "Measurement of long period low amplitude swell in the western North Atlantic Ocean," *J. Atmos. Ocean Tech.*, pp. 645-658., 1992.

Jähne, B., and K.S. Riemer, "Two-Dimensional Wave-Number Spectra of Small-Scale Water Surface Waves", *J. Geophys. Res.*, 95, C7, 11531-11,546, 1990.

Janssen, P., and P.M. Woiceshyn, "Wave Age and the Scatterometer Retrieval Algorithm," pp. 141-143, in Attema, E., *ERS-1 Geophysical Validation: Workshop Proceedings*, European Space Agency ESA-WPT-36, Paris, France, Workshop at Penhors, Bretagne, France, April 27-30, 1992.

Jones, W. L., L. C. Schroeder, D. H. Boggs, E. M. Bracalente, R. A. Brown, G. J. Dome, W. J. Pierson, and F. J. Wentz, "The SEASAT-A Satellite Scatterometer: The Geophysical Evaluation of Remotely Sensed Wind Vectors Over the Ocean," *J. Geophys. Res.*, Vol. 87, No. C5, pp. 3297-3317, April 1982.

Kahma, K.K. and M.A. Donelan, "A Laboratory Study of the Minimum Wind Speed for Wind Wave Generation," J. *Fluid Mech.*, vol. 192, pp 339-364, 1988

Keller, M.R., W.C. Keller and W.J. Plant, "A Wave Tank Study of the Dependence of the X-band Cross Sections on Wind Speed and Water Temperature", *J. Geophys. Res.*, Vol. 97, No. C4, pp 5771-5792, 1992.

Katsaros, K.B., and R. Brown, "Legacy of the SeaSat Mission for Studies of the Atmosphere and Air-Sea-Ice Interactions," *B. Am. Meteor.*, Vol. 72, No. 7, pp 967-981, 1991.

Keller, M.R., W.C. Keller, and W.J. Plant, "A Wave Tank Study of the Dependence of X Band Cross Sections on Wind Speed and Water Temperature," *J. Geophys. Res.*, Vol 97, pp. 5771-5792, 1992.

Keller, W.C., V. Wismann, and W. Alpers, "Tower-based Measurements of the Ocean C Band Radar Backscattering Cross Section," *J. Geophys. Res.*, Vol 94, pp. 924-930, 1989.

Keller, W.C., W. Plant, and D. Wismann, "The Dependence of X-band Microwave Sea Return on Atmospheric Stability," *J. Geophys. Res.*, Vol 90, No. C1, pp. 1019-1029, 1985.

Large, W. and S. Pond, "Open ocean momentum flux measurements in moderate to strong winds," *J. Phys. Oceanogr.*, Vol. 11, pp. 324-336, 1981.

LeMehaute, B. and D. Hanes, eds., *The Sea, 9, Ocean Engineering Science*, John Wiley, New York, 239-292, 1990.

Liu, W. T., "The Effects of the Variations in Sea Surface Temperature and Atmospheric Stability in the Estimation of Average Wind Speed by Seasat-SASS", *J. Phys Oceanogr.*, vol. 14, pp. 392-401, 1984.

Lleonart, G.T., D.R. Blackman, "The Spectral Characteristics of Wind-Generated Capillary Waves," *J. Fluid Mech.*, vol. 97, pp.455-479, 1980.

McMurdie, L.A., and K.B. Katsaros, "Satellite-Derived Integrated Water-Vapor Distribution in Oceanic Midlatitude Storms: Variation with Region and Season," *M. Weath. Rev.*, Vol. 119, No. 3, pp 589-605, 1991.

Mitsuyasu, H., and Honda, "Wind-Induced Growth of Water Waves," J. Fluid Mec., Vol. 123, pp. 425-442, 1982.

Mitsuyasu, H., and Kusaba, "A Note on the Momentum Transfer from Wind to Waves," J. Geophys. Res., Vol. 90, No. C2, pp. 3343-3345, 1985.

Moore, R. K., A. H.Chaudhry, and I. J. Birrer, "Errors in Scatterometer-Radiometer Wind Measurement Due to Rain," *IEEE J. Oceanic Engineering*, Vol. OE-8, No. 1, pp 37-48, Jan 1983.

Moskowitz, L., "Estimates of the power spectrums for fully developed seas for wind speeds of 20 to 40 knots," *J. Geophys. Res.*, Vol. 69, pp. 5161-5179, 1964.

Neumann, G. and W. J. Pierson, *Principles of Physical Oceanography,* Prentice Hall, Englewood Cliffs, New Jersey, 1966.

Nghiem, S., F. Li, H. Lou, and G. Neumann, "Ocean Remote Sensing with Airborne Ku-band Scatterometer, *OCEANS 93 Proceedings*, Vol. I, pp. 20-24, Victoriea, BC, Oct. 18-21, 1993.

Phillips, O.M., Spectral and Statistical Properties of the Equilbrium Range of Wind-Generated Gravity Waves," *J. Fluid Mech.*, Vol. 156, pp. 501-531, 1985.

Pierson, W. J., Jr., "Dependence of Radar Backscatter on Environmental Parameters," from G. L. Geernaert and W. J. Plant (eds), *Surface Waves and Fluxes*, Vol II, pp 173-220, Kluwer Academic Publishers, Netherlands, 1990.

Pierson, W. J., Jr. and L. Moskowitz, "A Proposed Spectral Form for Fully Developed Wind Seas Based on the Similarity Theory of S.A. Kitaigorodskii", *J. Geophys. Res.*, Vol. 69, No. 24, pp. 5181-5190, 1964.

Pierson, W. J., "The measurement of the synoptic scale wind over ocean," *J. Geophys. Res.*, Vol. 88, No. C3, pp. 1683-1708, 1983.

Schroeder, L., D.H. Boggs, G. Dome, I.M. Halberstam, W.L. Jones, W.J. Pierson, and F.J. Wentz, "The Relationship Between the Wind Vector and the Normalized Radar Cross Section Used to Derive Seasat-A Satellite Scatterometer Winds," *J. Geophys. Res.*, Vol. 87, No. C5, pp. 3318-3336, 1982.

Spencer, M., and M. Shimada, "Effect of Rain on Ku-Band Scatterometer Wind Measurements," *Proceedings of the International Geoscience and Remote Sensing Symposium*, 1991.

Smith, S. D., "Wind stress and heat flux over the ocean in gale force winds," *J. Phys. Oceanogr.*, Vol. 10, pp. 709-726, 1980.

Stewart, R. H., *Methods of Satellite Oceanography,* Univ. of Calif. Press, Los Angeles, 1985.

Sylvester, W. B., W. J. Pierson and S. R. Breitstein, "Techniques for evaluating the performance of models of radar backscatter from the ocean surface: Suggestions for their improvement," *Proceedings: IGARSS '89*, 12th Canadian Symposium on Remote Sensing, Vancouver, Canada, July 10-14, 1989.

Sylvester, W. B., W. J. Pierson and S. R. Breitstein, "Further results on techniques for evaluating the performance of models of radar backscatter from the ocean surface: Suggestions for their improvement," *Proceedings: IGARSS '90*, Remote Sensing Science for the Nineties; 10th Annual International Geoscience and Remote Sensing Symposium, Library of Congress No. 89-82170, 2149-2156, 1990.

Toba, Y., N. Iida, H. Kawamura, N. Ebuchi, and I.S.F. Jones, "Wave Dependence of the Sea-Surface Wind Stress," J. Phys. Oceanogr., Vol. 20, No. 5, pp. 705-721, 1990.

Woiceshyn, P.M., and P. Janssen, "Sensitivity Study--Scatterometer Retrievals with Wave Age Parameters," pp. 133-139, in Attema, E., *ERS-1 Geophysical Validation: Workshop Proceedings*, European Space Agency ESA-WPT-36, Paris, France, Workshop at Penhors, Bretagne, France, April 27-30, 1992.

Woiceshyn, P.M., M.G. Wurtele, D.H. Boggs, L.F. McGoldrich, and S. Peteherych, "The necessity for a New Parameterization of an Empirical Model for Wind/Ocean Scatterometry," J. Geophys. Res., vol. 91, pp. 2273-2288, 1986.

Zheng, Q., Z-H Yan, N.E. Huang, V. Klemas, and J. Pan, "The Effects of Water Temperature on Radar Scattering from the Ocean Surface," in review, *Global Atmosphere and Ocean Science,* May 1995.

VII. Estimation of the Modeling Error

A. Model function uncertainty

Although much effort has been expended in the search for accurate model functions relating backscatter cross-section (sigma-0) to near-surface wind-like quantities (such as velocity, stress, friction velocity, etc.), all historical satellite and in situ data sets exhibit large data scatter. This scatter far exceeds that expected from uncertainties in instrument calibration and random fluctuations in the surface geometry. A critical part of any complete model function investigation program is the quantification of the observed data scatter as a function of at least the primary variables: wind speed (or some scalar related to the magnitude of a wind-like vector quantity), direction, incidence angle, polarization, and frequency.

Model function uncertainty analyses have direct applications in the areas of instrument design/processing and data assimilation, as well as for model function studies aimed at defining the relationship between backscatter and geophysical variables of interest. Simulation of instrument performance is vital for verifying proper design and for performing necessary tradeoffs. All simulations for scatterometers require input sets of realistic backscatter measurements, corresponding to "true" (noise-free) values defined by a deterministic geophysical model. To simulate "actual" measurements, variability due to unmodeled geophysical effects, must be accounted for. This variability is the modeling error and may include random or systematic error. In principle, the magnitude of the simulated "noise" (as a function of the primary variables) can best be established through analysis of scatter from actual data (either satellite-, tower-, or aircraft-based). The sensitivity of the wind estimates to model function errors can be analytically evaluated using the Cramer-Rao bound (*Oliphant and Long*, 1996). Fortunately, due to the measurement geometry and the Ku-band model function, NSCAT is expected to have much less sensitivity to random model function errors than the C-band ERS-1 scatterometer (*Oliphant and Long*, 1996).

Most present scatterometer wind retrieval algorithms involve using the measured backscatter values to set coefficients in predetermined models with the aim of minimizing a defined error norm (*Chi and Li* 1988; *Long and Mendel*, 1991). However, both the measurements themselves and the predetermined model function (the two principal components of the error norm) have errors. The error norm must thus be normalized by the expected errors in order for the minimization to be carried out in a consistent manner. Knowledge of the magnitudes of the expected errors of both components is required. Similarly, most direct assimilation schemes require error estimates for the backscatter measurements.

More directly, detailed analysis of the scatter and distributions of backscatter data as a function of parameter space can be used to identify systematic errors in potential model functions and to suggest the effects of unmodeled, non-wind geophysical phenomena (such as the long wave field, SST, etc.). Many studies have attempted to perform such analyses through analysis of errors in retrieved WINDS (e.g., *Woiceshyn* et al. 1986, *Liu and Large* 1981 and *Freilich* 1986 all examined the effects of SST [discussed in more detail below]; etc.). However, owing to the nonlinearity of the wind retrieval process and the geometry of "3-stick" spaceborne scatterometers (where backscatter measurements from the mid-beam are obtained at a different incidence angle than from the fore- and aft-beams), inversion of measured wind errors to obtain quantitative estimates of systematic model function errors is difficult at best (see, however, *Johnson et al.* (1996)); further, the nonlinearity of the retrieval process precludes analytic estimation of the wind velocity errors

as a function of random errors in the backscatter measurements (compare *Leotta and Long,* 1988).

Johnson et al. (1996) applied a new technique to estimate the model function uncertainty. They explictly included the model function uncertainty in the form of the normalized standard deviation (Kpm) explicitly in the ML objective function and minimized the objective function for both wind velocity and Kpm. They estimated Kpm and the uncertainty of their estimate for C-band model functions, finding a larger than expected model function error. They are currently working on a Ku-band Kpm estimate (personal communication).

B. Approaches

One of the most promising approaches to analysis of model function uncertainty involves examination of sigma-0, rather than wind velocity, distributions. A direct investigation along these lines, employed recently by *Freilich and Dunbar* (1993) (described previously) involves characterization of each backscatter measurement as to its geophysical and radar conditions; the multi-dimensional parameter space spanned by the model function is then divided into small volume elements (e.g., wind speed, incidence angle azimuth angle), and the sigma-0 measurements are assigned to appropriate bins.

A fully empirical model function (with no a priori assumed functional dependencies) results from suitably averaging the measurements in each individual volume element of parameter space. Model function uncertainty can be estimated directly (and as a function of parameter space) by characterizing the distributions of measurements about the "mean" in each volume element of the parameter space.

Systematic errors in the model function owing to unmodeled geophysical effects can be identified if each sigma-0 measurement is characterized by more geophysical variables than the parameter space on which they are binned (e.g., the binned parameter space may include wind speed, azimuth, and incidence angle, while each backscatter measurement may additionally be characterized by wave conditions, atmospheric stratification, SST, etc.). If the distribution about the "mean" of sigma-0 data in each bin is correlated significantly with one or more unmodeled variables, the model function based on the low-order parameter set is deficient and the additional variables must be added to the parameter space. Likewise, the issue of the primary dependency of backscatter (actual wind velocity, stress, friction velocity, neutral stability speed at a defined level, etc.) can be addressed in statistically rigorous fashion by determining which variable results in the smallest variance of the sigma-0 measurements throughout the parameter space.

Clearly, solution of the complete problem requires an exceptionally large and extensive data set owing to the large parameter space of importance for scatterometry. The technique of Freilich and Dunbar uses surface analyses produced by operational numerical weather prediction forecast/analysis systems as the correlative "data"; errors and uncertainties introduced by the operational forecasting process must therefore be identified and, insofar as possible, eliminated from the analysis. On the other hand, if large numbers of sigma-0 measurements are available in each bin in parameter space, many of the long-standing uncertainties of scatterometry can be addressed. As an example, based on collocations of ERS-1 scatterometer data with surface wind analyses, the azimuthal modulation of sigma-0 at each wind speed and incidence angle can be examined to determine whether natural or dB units should be used, and whether a low-order truncated Fourier series results in systematic errors or greater error variance than does a "double-cosine" function as proposed by *Wentz* (1991).

Another approach to the model function development, with application to the uncertainty issue, has been proposed independently by *Sylvester et al.* (1989, 1990), *Cavanie* (1986),

and *Stoffelen and Anderson* (1992). These authors examine joint distributions of sigma-0 at various azimuth/incidence angles defined by the measurement geometry of the instrument (and, in the case of the *Sylvester et al.* studies, by the polarization sampling strategy). For geometry's with symmetry about the axis perpendicular to the satellite subtrack (true for the two-stick SASS, the symmetric 3-stick ERS-1 AMI, and for the fore- and aft-beams of the proposed NSCAT instrument), all measurements should fall on manifolds in the space defined by orthogonal axes corresponding to the sigma-0 values of each beam if backscatter is a function ONLY of a single wind-like vector. Histograms of measurements in this space can thus be constructed (at each incidence angle) without use of any correlative data. Whereas most historical interest in this approach has focused on defining the centroid of the measurements in the multi-dimensional space (essentially, empirical model function determination), the variances of the joint distributions can be used to address uncertainty directly.

C. Spatial variability in the wind over the measurement footprint

A spaceborne scatterometer such as NSCAT makes a measurement of sigma-0 over a resolution element footprint. For NSCAT the sigma-0 footprint size is nominally 25 km^2. The measured sigma-0 is the average sigma-0 over the resolution element, weighted by the antenna pattern and the coefficients of the radar equation. Because the underlying wind field has variability at all scales, there will be variations in the wind vector over the 25 km^2 footprint. Given a model function relating the wind vector at a point to sigma-0 there may be significant variability in the observed sigma-0, *even if the relationship between sigma-0 and the wind was exact and without uncertainty*.

The magnitude of this contribution to the observed scatter in the wind observed by a spaceborne scatterometer can be estimated using the following approach: A simple model based on a k^{-n} power-law roll-off in the wind spectrum, simulated high-resolution wind fields is generated. Then, using candidate geophysical model functions and Monte Carlo simulation, the variance of the observed sigma-0 versus the average wind vector over the resolution element can be computed. Preliminary calculations of this contribution indicate that it may be significant compared to the currently assumed 0.7 dB modeling error.

D. Recommendations

As a subcommittee we strongly recommend that future model function development activities include estimates or bounds on the modeling error as a function of the model parameters, if possible.

E. References

Stoffelen, A., and D.L.T. Anderson, "ERS-1 Scatterometer Calibration and Validation Activities at ECMWF: The Quality and Characteristics of the Radar Backscatter Measurements, *Proc. European 'International Space Year' Conference*, Munich Germany, 30 Mar. - 4 Apr., 1992.

Freilich, M. H.,"Satellite Scatterometer Comparisons with Surface Measurements: Techniques and SEASAT Results," *Proceedings of a Workshop on ERS-1 Wind and Wave Calibration*, 2-6 June 1986, pp. 57-62, (ESA SP-262, Sept. 1986).

Chi, C-Y and F.K. Li, "A Comparative Study of Several Wind Estimation Algorithms for Spaceborne Scatterometers," *IEEE Trans. Geosci. and Rem. Sens.*, Vol. GE-26, No. 2, pp. 115-121, March 1988.

Johnson, P.E., D.G. Long, and T.E. Oliphant, "Geophysical Modeling Error in Wind Scatterometry," *Proc. Int. Geosc. Rem. Sens. Sym.*, Lincoln, Nebraska, 27-31 May, pp 1721-1723, 1996.

Leotta, D., and D. G. Long, "Probability Distribution of Wind Retrieval Error Versus True Wind Vector and Swath Location for the NASA Scatterometer," *Proceedings of the International Geoscience and Remote Sensing Symposium,* pp. 1466-1469, Vancover, B.C., July 1989.

Liu, W. T., and W. G. Large, "Determination of Surface Stress by Seasat-SASS: A Case Study with JASIN Data," J. Phys. Ocean., Vo;. 11, No. 12, pp. 1603-1611, 1981.

Long, D. G., and J. M. Mendel, "Identifiability in Wind Estimation from Wind Scatterometer Measurements," *IEEE Trans. on Geosc. and Rem. Sens.,*.Vol. 29, No. 2, pp. 268-276, 1991.

Oliphant, T.E., and D.G. Long, "Cramer-Rao Bound for Wind Estimation from Scatterometer Measurements," *Proc. Int. Geosc. Rem. Sens. Sym.*, Lincoln, Nebraska, 27-31 May, pp 1724-1726, 1996a.

Sylvester, W. B., W. J. Pierson and S. R. Breitstein, "Techniques for evaluating the performance of models of radar backscatter from the ocean surface: Suggestions for their improvement," *Proceedings: IGARSS '89,* 12th Canadian Symposium on Remote Sensing, Vancouver, Canada, July 10-14, 1989.

Sylvester, W. B., W. J. Pierson and S. R. Breitstein, "Further results on techniques for evaluating the performance of models of radar backscatter from the ocean surface: Suggestions for their improvement," *Proceedings: IGARSS '90,* Remote Sensing Science for the Nineties; 10th Annual International Geoscience and Remote Sensing Symposium, Library of Congress No. 89-82170, 2149-2156, 1990.

Wentz, F. J., S. Peteherych, and L.A. Thomas, "A Model Function for Ocean Radar Cross-sections at 14.6 GHz," *J. Geophys. Res.*, Vol. 89, pp 3689-3704, May 20, 1984.

Woiceshyn, P. M., M. G. Wurtele, D. H. Boggs, L. F. McGoldrick, and S. Peteherych, "The Necessity for a New Parameterization of an Empirical Model for Wind/Ocean Scatterometry," *J. Geophys. Res.*, Vol. 91, No. C2, pp 2273-2288, Feb. 1986.

VIII. Current/planned model function refinement activities

A. NASA-funded

This section was not available by the report release deadline. A separate report will consider NSCAT calibration and validation efforts and should address NASA-funded model function refinement activities.

B. ONR-funded

The Office of Naval Research (ONR) has active programs in microwave remote sensing of the ocean both in its Contract Research Program and at the Naval Research Laboratory. While most of these programs deal with issues which can potentially impact scatterometry, few of them are specifically devoted to developing an improved model function for use in scatterometry. The one ONR-funded research program which does have this explicit objective is the NRL/APL-UW air-sea interaction blimp project. Below we will describe this project in some detail after outlining other programs which are related to, but not specifically aimed at, the development of a scatterometer model function.

Accelerated Research Initiatives (ARI) are five-year programs organized by ONR to carry out research in areas selected for special emphasis. Among ongoing and planned ARI's, three contain components relevant to scatterometer model function development. The Surface Wave Processes ARI was divided into two experiments, SWAPP on the west coast and SWADE on the east coast. While SWAPP is primarily aimed at understanding mixed layer deepening in the ocean, the objective of SWADE is to understand wind wave growth and equilibrium in the open ocean. As part of SWADE, many high-quality wind stress measurements were made from buoys and surface ships off the east coast of the US near Wallops Island. NASA funded the JPL C-130 aircraft carrying the JPL NUSCAT and the UMass C-Band scatterometer to fly during the experimental phase of SWADE in 1990 in order to collect backscatter data for comparison with these surface measurements. The NRL P-3 aircraft also flew during this experiment with a scatterometer onboard. These data are presently under analysis. The High-Resolution ARI is a joint ONR/NRL research program aimed primarily at understanding mesoscale effects which can be imaged with high-resolution microwave systems. An initial experiment was conducted in September, 1991 in the Gulf Stream off Cape Hatteris and a second will take place in the same location in mid-1993. During the first experimental period, surface flux measurements were made from ships, buoys, and from a towed catamaran while backscattering cross sections were measured by NRL using a Ku-Band scatterometer with a rotating antenna. Thus data exist from this experiment with which a scatterometer model function can be investigated. The 1993 experiment will again provide an opportunity for comparison of backscattering data with surface flux measurements. Present plans call for both the NRL P-3 and the US-LTA blimp to carry scatterometers during this experiment. Further information about the blimp program will be given below. Finally, a third ARI, the Marine Boundary Layer ARI, is present in the planning stages. This ARI will be aimed at understanding variability in the ocean and atmospheric boundary layers and will provide extensive measurements of surface conditions, probably in a region off the west coast of the US. While no aircraft work is presently planned as part of this ARI, the opportunity for comparing backscattering cross sections with the extensive surface measurements will probably attract scatterometers with alternate sources of funding.

In recent years, ONR has also funded, at least in part, two other major experiments having scatterometry components. The FASINEX experiment took place in 1986 in the subtropical convergence zone southwest of Bermuda. The primary purpose of this experiment was to examine the effect of sea surface fronts on the atmospheric and oceanic

boundary layers. As part of this experiment, NRL and JPL flew scatterometers over the frontal areas under investigation. Atmospheric flux measurements were made from two surface ships as well as from the NRL P-3 and NCAR Electra aircraft. Comparison of these scatterometer and flux data have resulted in several papers to date which study various aspects of the scatterometer model function (*Li et al.* 1988, 1989; *Weissman*, 1990, *Weissman et al.*, 1992). These studies indicate that cross wind minima may not lie 180 degrees apart, that backscatter cross sections correlate better with surface stress than with surface fluxes, and that cross sections respond to variations in surface water temperature in a complex manner which relates to atmospheric stability. More recently, ONR has conducted the SAXON-FPN experiment near the German research platform FPN in the North Sea. The primary purpose of this experiment was to examine the accuracy of present theories of SAR imagery of ocean waves. Again, however, a scatterometry component existed within the experiment, the primary phase of which took place in November, 1990. The NRL P-3 aircraft again flew with its scatterometer over the research platform which was instrumented with two sonic anemometers and a fast humidity sensor as well as a variety of microwave systems. Results from this experiment should be forthcoming shortly and should show how microwave backscatter at a variety of frequencies responds to the wind.

In addition to these major, multi-institutional research programs, ONR also funds a variety of smaller research programs at individual institutions. Among these are programs to develop improved theories of microwave scattering from rough water surfaces at JPL and at VPI&SU. Several other programs at ORI, SIO, WHOI, and UMass are aimed at providing either images or spectra of the small scale structure of the sea surface in order to provide input to scattering models. Additional programs at WHOI, NRL, SIO, and ORINCON are investigating the effect of surfactants on short surface waves and microwave backscatter. Finally, ONR continues to support wave tank measurements of microwave scattering at a variety of frequencies in the NRL wind wave tank. Although none of these individual efforts are specifically aimed at developing a scatterometer model function, all should provide input which can enhance such development.

One program which ONR supports along with NASA is specifically geared toward scatterometer model function development. This is an air/sea interaction blimp project being carried out jointly by NRL and APL-UW (*Blanc* et al., 1989). The objective of the program is to compare long-term records of microwave backscatter with surface flux measurements made simultaneously at the same location. By operating from a blimp, these measurements can be made free from the distorting influence of a platform, over deep water, over a long period of time, and over a variety of ocean surface conditions. The blimp involved in the program is owned and operated by US-LTA of Eugene, Oregon. Ku-Band scatterometers in the gondola of the blimp will provide fully-coherent HH and VV polarized backscatter data which will be compared with flux measurements made with a fast humidity sensor and sonic anemometer in a platform suspended below the blimp. The platform will be flown between 5 and 10 meters above the water surface and will be 70 meters, or approximately 5.5 blimp diameters, below the gondola. One scatterometer will be rotating while a second, fixed system will provide long term information in a given direction. The blimp is capable of hovering in a nearly-fixed location for periods of time up to an hour before climbing to facilitate changing pilots. It should be able to remain over the ocean for up to 10 hours at a time. Procedures for implementing these measurements were successfully tested from the blimp in June, 1992 and the first set of data will collected in September, 1992.

C. Non-U.S. Efforts

Yves Quilfen provided the following description of the IFREMER contribution to the calibration/validatoin of the NSCAT geophysical model function (GMF):

The laboratory of Oceanography from Space (LOS) has been involved since the launch of ERS-1 in the calibration/validation of an emperical C-band backscattering model that is used to compute the off-line winds distributed by Ifremer (*Quilfen and Bentamy,* 1994). It has also developed a physical model working at C-band as well as at Ku-band (Elfouhaily, 1996) that compares well with the CMOD-IFREMER and with the SASS-II models. As Principal Investigator on NSCAT, the LOS has planned to use this expertise in the case of the NSCAT scatterometer to study the relationship between the baskscatering coefficient at Ku-band and the surface parameters. A strong interest is to compare the sea-surface response at C-band and Ku-band and to assess the compatibility of the masurements performed for these two frequencies by two different scatterometers.

The current SASS-II GMF will be evaluate in terms of consistency with the measurements in normalized radar cross section (NRCS) space. If it sis show that a new version of the model should be defined, it is planned to study the behavior of the mean NRCS and its azimuthal dependency by using different sources of data. The ERS-2/NSCAT collocated data-set that is planned to be made available from IFREMER will be the baseis of these studies although the work will also be performed by using ECMWF analyses. One advantage of the ERS data is that it is a global data set covering all the surface donditions and that the distribution of its errors is rather well known. The various buoy networks will be used to refine the model function wind speed dependency and as validation tools. An analysis of the influence on the NRCS of other surface parameters will be performed at a later date. A parallel activity will concern the ongoing work on the physical model that will be compared with the emperical one to understand the physical mechanisms underlying the backscattering response.

A first evaluation of the SASS-II model and an analysis of the sigma-0 using NSCAT/ERS-2/ECMWF collocated data will be presented at the January 1997 NSCAT cal/val workshop. A preliminary model function will be generated during the three months following the delivery of calibrated sigma-0 data.

D. References

Blanc, T.V., W.J. Plant, and W.C. Keller, "The Naval Research Laboratory's Air-Sea Interaction Blimp Experiment", *Bul. Am. Meteor. Soc.,* 70, 354-365, 1989.

Elfouhaily, T., "Physical modeling of Electromagnetic Backscatter from the Oceanic Surface and Effects of Geophysical Processes in the Boundary Layer," PhD. thesis, to be published, 1996.

Li, F., G. Neumann, S. Shaffer, and S. L. Durden, "Studies of the Location of Azimuth Modulation Minima for Ku Band Ocean Radar Backscatter," *J. Geophys. Res.*, Vol. 93, No. C7, pp. 8229-8238, July 1988.

Quilfen, Y., and A. Bentamy, "Calibration/Validation of ERS-1 Scatterometer Precision Products," Proc. Int. Geosc. Rem. Sens. Sym., Pasadena, California, pp. 89-93, 1994.

Weissman, D. E., "Dependence of the Microwave Radar Cross Section on Ocean Surface Variables: Comparison of Measurements and Theory Using Data From the Frontal Air-Sea Interaction Experiment," *J. Geophys. Res.*, Vol. 95, No. C3, pp 3387-3398, Mar 15, 1990.

Weissman, D. E., K.L. Davidson, R.A. Brown, C.A. Friehe and F. Li, "The Relationships Between Microwave Radar Cross Section and Both Wind Speed and Stress: Model Function Studies Using Frontal Air-Sea Interation Experiment Data," *J. Geophys. Res.*, Vol. 99, No. C5, 1994.

IX. Summary and Recommendations

A. Summary analysis

While scatterometry is a proven technique, there remain questions regarding the geophysical model function relating the radar backscatter to the wind vector. Empirical approaches have resulted in excellent operational model functions. Theoretical approaches have not faired as well. This is not surprising since the variation of backscatter with wind speed and direction is caused by the variation of the properties of the wind generate waves and swell on the ocean surface. Thus the relationship between the wind and the waves that are generated by the wind is the fundamental problem for deriving theory-based geophysical model functions.

We conclude that existing model functions (notably the Wentz or SASS-II) model function provide good first order accuracy but that further research is warranted to fully understand the model function. These are discussed below. We have arrived at a number of recommendations which are described below.

B. Key questions for future research

As a subcommittee we feel that the single most important area for future research in Ku-band model functions is: What is the long wave sensitivity of the model function? This question is crucial since NSCAT-derived winds will be inputs to numerical wave prediction models.

C. Recommendations for pre-NSCAT launch research

As a subcommittee we feel that the key areas for pre-launch research (in priority order) are:

1. Re-analyze data from the SEASAT time period using modern numerical weather prediction models (e.g., ECMWF) to generate surface analyses to:

   A. Develop a new empirical model function, using the techniques of *Freilich and Dunbar* (1993) and this re-analyzed data.

   B. Check the WAM wave model and investigate the long-wave dependence of the radar backscatter using a Freilich and Dunbar-type approach.

2. Develop criteria for model selection.

3. Conduct field experiments such as HI-RES using aircraft and tower-mounted scatterometer systems.

D. Required NSCAT sigma-0 accuracy to support post-launch model function refinement efforts.

The committee was unable to develop a consensus on a method for deriving detailed requirements on sigma-0 measurement accuracy specifically for model function refinement activities. In general, their concern is on the accuracy of the retrieved winds. However, a general consensus was arrived at that biases and errors in the measured sigma-0 due to instrument calibration and processing should be minimized and that they should remain stable over a several month time period. Variations on time scales less than two weeks must be less than ±0.1 dB. It may be possible to detect and correct for bias changes over time scales exceeding 1 or 2 months (M. Freilich, personal communication).

E. Recommendations for post-NSCAT launch geophysical validation

One area for NSCAT post-launch validation is to use ocean wave models. Ocean models used for analysis and prediction of surface waves (including surf), current (wind-driven), and water level (surge) are force primarily by the time-space evolution of surface winds. It has long been recognized that uncertainties in surface marine wind fields specified from typical historical and climatological meteorological data are the primary source of error in ocean model generated analyses (e.g., Cardone et al. 1990). This deficiency has been highlighted with the hindcasts in the SWADE IOP-1 event of October 1990 (*Graber et al*, 1991 and *Cardone et al.* 1994). Ocean wave models are very sensitive to errors in the atmospheric forcing and hence can be used as indicators of the fidelity of the wind field. This approach was first used for SEASAT scatterometer winds by *Bauer et al.* (1992). It is therefore suggested that a timely assessment of the quality and fidelity of NSCAT wind products can be obtained from global wave "nowcast" studies or from regional hindcast studies.

F. References

Bauer, E., S. Hasselman, K. Hasselmann, and H.C. Graber, "Validation and Assimilation of SEASAT Altimeter Wave Heights Using the WAM Wave Model," J. Geophys. Res., Vol. 97, No. 12,671-12,682, 1992.

Cardone, V.J., J.A. Greenwood, and M.A. Cane, "Trends in Historical Marine Wind Data," *Journal of Climate*, Vol. 32, pp. 873-880.

Graber, H.C., M.J. Caruso, and R.E. Jensen, "Surface Wave Simulations During the October Storm in SWADE," *Proc. MTS '91 Conf.*, Marine Technolgy Society, New Orleans, LA, pp. 159-164, 1991.

X. Bibliography of Papers Related to Geophysical Model Functions in Wind Scatterometry

The following bibliography has been divided into sections of related topics in the area of geophysical model functions. The primary emphasis is on Ku-band model functions with only a representative set of papers on C-band model functions. The assignment of a particular paper to a given division is somewhat arbitrary. In preparing this bibliography we have tried to be thorough, but the list is by no means complete.

Air/Sea Interaction

Blake, R.A., "The Dependence of Wind Stress on Wave Height and Wind Speed," *J. Geophys. Res.*, Vol. 96, No. C11, pp. 20,531-20,545, 1991.

Colton, M.C., "The Dependence of Radar Backscatter on the Energetics of the Air-Sea Interface," Ph.D. Dissertation, Naval Postgraduate School, Monterey, CA, Dec. 1989.

Donelan, M.A., "The Dependendence of the Aerodynamic Drag Coefficient on Wave Parameters, in *Proceedings of the First International Converence on Meteorology and Air Sea Interaction of the Coastal Zone,* pp. 381-387, American Meteorological Society, Boston, MAss., 1982.

Donelan, M.A., "Air-sea interaction", in *The Sea*, 9, Ocean Engineering Science, eds. B. LeMehaute and D. Hanes, John Wiley, New York, 239-292, 1990.

Friehe, C.A., W.J. Shaw, D.P. Rogers, K.L. Davidson, W.G. Large, S.A. Stage, G.H. Crescenti, S.J.S. Khalsa, G.K. Greenhut, and F. Li, "Air-Sea Fluxes and Surface Layer Turbulence Around a Sea Surface Temperature Front," *J. Geophys. Res.*, Vol. 96, No. C5, pp 8593-8609, May 15, 1991.

Jones, W.L., and L.C. Schroeder, "Radar Backscatter from the Ocean: Dependence on Surface Friction Velocity," Boundary Layer Meteorology, Vol. 13, pp.133-149, 1978.

Katsaros, K.B., and R.A. Brown, "Legacy of the Seasat Mission for Studies of the Atmosphere and Air-Sea- Ice Interactions," *Bull. Amer. Met. Soc.*, 72, 967-981, 1991.

Lleonart, G.T., and D.R. Blackman, "The Spectral Characteristics of Wind-Generated Capillary Waves," *J. Fluid Mech.,* vol. 97, pp.455-479, 1980.

Mitsuyasu, H., and Honda, "Wind-Induced Growth of Water Waves," J. Fluid Mec., Vol. 123, pp. 425-442, 1982.

Mitsuyasu, H., and Kusaba, "A Note on the Momentum Transfer from Wind to Waves," J. Geophys. Res., Vol. 90, No. C2, pp. 3343-3345, 1985.

Geophysical Model Functions

Bracalente, E., D. Boggs, W. Grantham, and J. Sweet, "The SASS1 Scattering Coefficient (sigma-0) Algorithm," *IEEE J. Oceanic Engineering*, Vol. OE-5, No. 2, pp. 145-154, April 1980.

Britt, C.L. and L.C. Schroeder, "SASS-1 Model Function Evaluation and Upgrade," *Euro. Space Agency Spec. Publi.*, ESA SP-215, 1984.

Cardone, V. J., J. D. Young, W. J. Pierson, R. K. Moore, J. A. Greenwood, C. Greenwood, A. K. Fung, R. E. Salfi, H. L. Chan, M. Afarani and M. Komen, "The Measurement of the Winds Near the Ocean Surface with a Radiometer-Scatterometer on SKYLAB," Final Report of EPN 550 Contr. No. NAS-9-13642, NASA Lyndon B. Johnson Space Center, Houston, Texas, 1975.

Colton, M.C., W.J. Plant, W.C. Keller, and G.L. Geernaert, "Tower-based measurements of normalized radar cross section from Lake Ontario: Evidence of wind stress dependence," J. Geophys. Res., vol. 100, no. C5, pp 8791-8813, 1995.

Chen, K.M., A. Fung and D.E. Weissman, "A Backscattering Model for the Ocean Surface", *IEEE Trans. on Geoscience & Remote Sensing*, Vol. 30, No. 4, pp 811-817, July 1992.

Daley, J.C., "Wind Dependence of Radar Sea Return," *J. Geophys. Res.*, Vol. 78, pp. 7823-7833, 1973.

Donelan, M. A., and W.J. Pierson, Jr., "Radar Scattering and Equilbrium Ranges in Wind-Generated Waves with Application to Scatterometry," *J. Geophys. Res.*, Vol. 92, pp. 4971-5029, 1987.

Durden, S.L., and J.F. Vesecky, "A Physical Radar Cross Section Model for a Wind Driven Sea with Swell", *IEEE J. Ocean. Engg*, Vol. OE-10, pp 445-451, October, 1985.

Feindt, F., V. Wismann, W. Alpers, and W.C. Keller, "Airborne Measurements of the Ocean Radar Cross Section at 5.3 GHz asa Function of Wind Speed," *Radio Sci.*, Vol 21. pp. 845-856, 1986.

Freilich, M.H., and R.S. Dunbar, "Derivation of Satellite Wind Model Functions Using Operational Surface Wind Analyses: An Altimeter Example," *J. Geophys. Res.*, Vol. 98, No. C8, pp 14633-14649, 1993.

Freilich, M.H., and R.S. Dunbar, "A Preliminary C-band Scatterometer Model Function for the ERS-1 AMI Instrument," *Proc. First ERS-1 Symposium*, ESA SP-359, pp 79-84, 1993.

Fung, A.K., and K.K. Lee, "A Semi-Empirical Sea Spectrum Model for Scattering Coefficient Estimation", *IEEE Journal of Oceanic Engg*, Vol. OE-7, No. 4, 1982.

Fung, A.K., and G.W. Pan, "A Scattering Model for Perfectly Conducting Random Surfaces: I. Model Development", *Int. J. Remote Sensing*, Vol. 8, No. 11, pp 1579-1593, 1987.

Geernaert, G.L. "Variation of the Angle Between the Surface Layer Wind Vector and the Wind Stress Vector and its Dependence on Thermal Stratification and Advection," *J. Geophys. Res., 9*, 8215-8220., 1988.

Glazman, R.E., "Statistical Problems of Wind-Generated Gravity Waves Arising in Microwave Remote Sensing of Surface Winds," *IEEE Trans. Geo. and Rem. Sens.*, Vol. 29, No. 1, pp 135-142, Jan 1991.

Guinard, N.W., J.T. Ransone, Jr., and J.C. Daley, "Variation of the NRCS of the Sea with Increasing Roughness," *J. Geophys. Res*., Vol 76, p. 1525, 1971.

Hawkins, J.D., and P. G. Black, "SEASAT Scatterometer Detection of Gale-Force Winds Near Tropical Cyclones," *J. Geophys. Res.*, Vol. 88, No. C3, pp. 1674-1682, Feb. 1983.

Hoffman, R.N. and J-F Louis, "The Influence of Atmospheric Stratification on Scatterometer Winds," *J. Geophys. Res.*, Vol. 95, No. C6, pp 9723-9730, June 15, 1990.

Holliday, D., "A Radar Ocean Imaging Model for Small to Moderate Incidence Angles," *Int. J. Remote Sensing*, Vol. 7, pp. 1809-1834, 1986.

Janssen, P., and P.M. Woiceshyn, "Wave Age and the Scatterometer Retrieval Algorithm," pp. 141-143, in Attema, E., *ERS-1 Geophysical Validation: Workshop Proceedings*, European Space Agency ESA-WPT-36, Paris, France, Workshop at Penhors, Bretagne, France, April 27-30, 1992.

Jessup, A., W.C. Keller and K. Melville, "Measureemnts of Sea Spikes in Microwave Backscatter at Moderate Incidence," J. Geophys. Res., Vol. 95, No. C6, pp. 9679-9688, 1990.

Jones, W.L., L.C. Schroeder, and J. L. Mitchell, "Aircraft Measurements of the Microwave Scattering Signature of the Ocean,'" *IEEE Trans. Antennas and Propagation*, Vol. AP-25, No. 1, Jan. 1977.

Jones, W. L., F. J. Wentz, and L. C. Schroeder, "Algorithm for Inferring Wind Stress from SeaSat-A," *J. Spacecraft and Rockets*, Vol. 15, No. 6, pp. 368-374, Nov-Dec. 1978.

Keller, W.C., V. Wismann, and W. Alpers, "Tower-Based Measurements of the Ocean C Band Radar Backscatting Cross Section," *J. Geophys. Res.*, Vol. 94, No. C1, pp 924-930, Jan 15, 1989.

Keller, W.C., W. Plant, and D. Wismann, "The Dependence of X-band Microwave Sea Return on Atmospheric Stability," *J. Geophys. Res.*, Vol 90, No. C1, pp. 1019-1029, 1985.

Keller, W. C., and W. J. Plant, "Cross Sections and Modulation Transfer Functions at L and Ku Bands Measured During the Tower Ocean Wave and Radar Dependence Experiment," *J. Geophys. Res.*, Vol. 95, No. C9, pp 16277-16289, Sept 15, 1990.

Li, F., W. Large, W. Shaw, E.J. Walsh, and K. Davidson, "Ocean Radar Backscatter Relationship with Near Surface Winds: A Case Study During FASINEX, *J. Phys. Oceanogr*., 12, 342-353, 1989.

Li, F., G. Neumann, S. Shaffer, and S. L. Durden, "Studies of the Location of Azimuth Modulation Minima for Ku Band Ocean Radar Backscatter," *J. Geophys. Res.*, Vol. 93, No. C7, pp. 8229-8238, July 1988.

Li, F., G. Neumann, and R. H. Weller, "Observations of Ocean Ku-Band Radar Cross Section at Low Wind Speed During FASINEX," *Proc. Proceedings of the International Geoscience and Remote Sensing Symposium*, 1990.

Liu, Y., and W.J. Pierson, "Comparisons of Scatterometer Models for the AMI on ERS-1: The Possibility of Systematic Azimuth Angle Biases of Wind Speed and Direction," I*EEE Trans. Geosci. Remote Sens.*, Vol. 32, No. 3, pp. 626-635, May 1994.

Long, A.E., "Towards a C-band Radar Sea Echo Model for the ERS1 Scatterometer," *Proceedings of the 3rd Internal Colloquium on Spectral Signatures*, ESA/SP-247, pp 29-34, 1985.

Long, A.E., "Summary of CMOD2, Wismann, CMOD2_W and CMOD2_1 Models," ESRIN 28/02/91, ESTEC/WMA/AEL/9101, 1991.

Long, A.E., "ERS1: C-Band Sea-Echo Models," ESRIN 8/04/91, ESTEC/WMA/AEL/9104, 1991.

Long, D.G., R. Reed, and D.V. Arnold, "Statistics of Radar Backscatter from Wind Waves," *Proc. Int. Geosc. Rem. Sens. Sym.*, Lincoln, Nebraska, 27-31 May, pp 1475-1477, 1996.

Long, D.G., R.S. Collyer, R. Reed, and D.V. Arnold, "Dependence of the Normalized Radar Cross Section of Water Waves on Bragg Wavelength--Wind Speed Sensitivity," *IEEE Trans. Geosc. and Remote Sens.*, Vol. 34, No. 3, pp 656-666, 1996.

Long, S. R., Larry F. Bliven, Q. Zheng, X-H Yan, and N. E. Huang, "On the Ocean Surface Microscale Features and Remote Sensing of the Ocean Surface Wind," Unpublished manuscript, Laboratory for Hydrosperic Processes, NASA Goddard Spaceflight Center, Greenbelt, MD, 9 Sept, 1991.

Masuko, H., K. Okamoto, M. Shimada and S. Niwa, "Measurement of Microwave Backscattering Signatures of the Ocean Surface Using X-Band and Ka-Band Airborne Scatterometers", *J. Geophys. Res.*, Vol. 91, No. C11, pp 13,065-13,083, November 15, 1986.

Mitsuyasu, H., T. Kusaba, K. Marubayashi, and M. Ishibashi, "The Microwave Backscattering from Wind Waves," *Proceedings of PORSEC*, Okinawa, 1992.

Plant, W.J., and W.C. Keller, "Evidence of Bragg Scattering in Microwave Doppler Spectra of Sea Return," *J. Geophys. Res.*, Vol. 95, No. C9, pp 16299-16310, Sept 15, 1990.

Plant, W.J., "A Two-Scale Model of Short Wind-Generated Waves and Scatterometry," *J. Geophys. Res.*, Vol. 91, pp. 10735-10749, 1986.

Pierson, W.J., Jr., "Dependence of Radar Backscatter on Environmental Parameters," from G. L. Geernaert and W.J. Plant (eds), *Surface Waves and Fluxes*, Vol II, pp 173-220, Kluwer Academic Publishers, Netherlands, 1990.

Pierson, W.J., Jr., "Probabilities and Statistics for Backscatter Estimates Obtained by a Scatterometer," *J. Geophys. Res.*, Vol. 94, No. C7, pp 9743-9759, July 15, 1989.

Pierson, W.J., Jr., "A Note on the Modulation of Radar Backscatter as a Function of Wind Direction," Unpublished Manuscript, June 1992.

Schroeder, L., D.H. Boggs, G. Dome, I.M. Halberstam, W.L. Jones, W.J. Pierson, and F.J. Wentz, "The Relationship Between the Wind Vector and the Normalized Radar Cross Section Used to Derive Seasat-A Satellite Scatterometer Winds," *J. Geophys. Res.*, Vol. 87, No. C5, pp. 3318-3336, 1982.

Schroeder, L. C., W.L. Jones, P.R. Schaffner and J.L. Mitchell, "Flight measurements and analysis of AAFE RADSCAT wind speed signature of the ocean", NASA Technical Memorandum 85646, January 1984.

Schroeder, L., P.R. Schaffner, J.L. Mitchell, and W.L. Jones, "AAFE RADSCAT 13.9-GHz Measurements and Analysis: Wind-Speed Signature of the Ocean," *IEEE J. Oceanic Engineering*, Vol. OE-10, No. 4, pp. 346-357, Oct. 1985.

Sylvester, W.B., W.J. Pierson, S.R. Breitstein, "Techniques for Evaluating the Performance of Models of Radar Backscatter From the Ocean Surface: Suggestions for Their Improvement," *Proc. Proceedings of the International Geoscience and Remote Sensing Symposium*, 1989.

Sylvester, W.B., W.J. Pierson, S.R. Breitstein, "Further Results on Techniques for Evaluating the Performance of Models of Radar Backscatter From the Ocean Surface: Suggestions for Their Improvement," Paper preprint., 1991.

Unal, C.M.H., P. Snoeij, and P.J.F. Swart, "The Polarization-Dependent Relation Between Radar Backscatter from the Ocean Surface and Surface Wind Vector at Frequencies Between 1 and 18 GHz," *IEEE Trans. Geo. and Rem. Sens.*, Vol. 29, No. 4, pp 621-626, July 1991.

Weissman, D.E., "The Response of Microwave Cross Sections of the Sea to Wind Fluctuations," in review *J. Geophys. Res.*, 1994.

Weissman, D.E., "Dependence of the Microwave Radar Cross Section on Ocean Surface Variables: Comparison of Measurements and Theory Using Data From the Frontal Air-Sea Interaction Experiment," *J. Geophys. Res.*, Vol. 95, No. C3, pp 3387-3398, Mar 15, 1990.

Weissman, D.E., and W.J. Plant, "Calculations of the Microwave Radar Cross Section Dependence on Wave Height and Slope Skewness," *Oceans'90 Proceedings*, Washington, D. C., 24-26 Sept., 1990.

Weissman, D.E., W.J. Plant, R.A. Brown, K.L. Davidson, W.J. Shaw, "Relating the Microwave Radar Cross Section to the Sea Surface Stress: Physics and Algorithms," *Proceedings of the International Geoscience and Remote Sensing Symposium*, Espoo, Finland, 3-7 June, 1991.

Weissman, D.E., K.L. Davidson, W.J. Plant, R. A. Brown, "Relating the Microwave Radar Cross Section to the Sea Surface Stress: Developing a New Model Function," *Oceans'91 Proceedings*, Honolulu, Hawaii, Oct. 1-3, 1991.

Weissman, D.E., K.L. Davidson, R.A. Brown, C.A. Friehe and F. Li, "The Relationships Between the Microwave Radar Cross Section and Both Wind Speed and Stress: Model Function Studies Using Frontal Air-Sea Interation Experiment Data," *J. Geophys. Res.*, Vol. 99, No. C5, 1994.

Weissman, D.E., F.K. Li, S. Lou, S.V. Nghiem, G. Neumann, R.E. McIntosh, S.C. Carson, J.R. Carswell, H.C. Graber, and R.E. Jensen, "Measurements of Ocean Surface Stress Using Aircraft Scatterometers," in review, *J. Atmos. Ocean. Tech..*, Jan. 1996.

Wentz, F. J., S. Peteherych, and L.A. Thomas, "A Model Function for Ocean Radar Cross-sections at 14.6 GHz," *J. Geophys. Res.*, Vol. 89, pp 3689-3704, May 20, 1984.

Wentz, F.J., S. Peteherych, and L.A. Thomas, "New Algorithms of the Microwave Measurements of Ocean Winds with Application to SEASAT and SSM/I," *J. Geophys. Res.*, Vol. 91, pp 2289-2307, 1986.

West, J.C., P. A Hwang, R.K. Moore, J.C. Holtzman, and O.H. Shemdin, "The Modulation of a Radar Signal From the Ocean Surface Due to Slope and Hydrodynamic Effects," *J. Geophys. Res.*, Vol. 95, No. C9, pp 16291-16297, Sept. 15, 1990.

Wright, J. W., "A New Model for Sea Clutter", *IEEE Trans. Antennas and Prop.*, AP-16, p. 217, 1968.

Woiceshyn, P.M., and P. Janssen, "Sensitivity Study--Scatterometer Retrievals with Wave Age Parameters," pp. 133-139, in Attema, E., *ERS-1 Geophysical Validation: Workshop Proceedings*, European Space Agency ESA-WPT-36, Paris, France, Workshop at Penhors, Bretagne, France, April 27-30, 1992.

Woiceshyn, P.M., M.G. Wurtele, D. H. Boggs, L.F. McGoldrick, and S. Peteherych, "The Necessity for a New Parameterization of an Empirical Model for Wind/Ocean Scatterometry," *J. Geophys. Res.*, Vol. 91, No. C2, pp 2273-2288, Feb. 1986.

Wu, J. "Dependence of Microwave Sea Returns on Wind-Friction Velocity Under Varied Atmospheric Stability Conditions," *IEEE J. Oceanic Engineering*, Vol 14, No. 3, pp 254-258, July 1989.

Zheng, Q., Z-H Yan, N.E. Huang, V. Klemas, and J. Pan, "The Effects of Water Temperature on Radar Scattering from the Ocean Surface," in review, *Global Atmosphere and Ocean Science*, May 1995.

Geophysical Model Function Validation

Barrick, D.E., J.C. Wilkerson, P. Woiceshyn, G.H. Born and D. Lame, "Seasat Gulf of Alaska Workshop II Report," NASA Jet Propulsion Laboratory Report 622-107. Pasadena, CA 91103, 1980.

Bartel, K. "Validation of Seasat Scatterometer Wind Vectors in the Norwegian Sea," *J. Geophys. Res.*, Edinburgh, Scotland, 13-16 Sept, 1988.

Blanc, T.V., W.J. Plant, and W.C. Keller, "The Naval Research Laboratory's Air-Sea Interaction Blimp Experiment", *Bul. Am. Meteor. Soc.*, 70, 354-365, 1989.

Born, G. et al., "Seasat Gulf of Alaska Workshop Report." Vol. 1, 622-010. NASA Jet Propulsion Laboratory Report 622-107. Pasadena, CA 91103, 1979.

Boutin, J., and Etcheto, "Consistency of GEOSAT, SSM/I, and ERS-1 Global Surface Wind Speeds," J. Atmos. Ocean Tech., Vol. 13, No. 1, pp. 183-197, 1996.

Businger, J., R.H. Stewart, T. Guymer, D.B. Lame and G.H. Born, "Seasat JASIN Workshop Report," Rep. 80-62, Jet Propulsion Laboratory, Pasadena, CA 91103, 1980.

Davison, J., and D.E. Harrison, "Comparison of Seasat Scatterometer Winds With Tropical Pacific Observations," *J. Geophys. Res.*, Vol. 95, No. C3, pp 3404-3410, Mar 15, 1990.

Dobson, E.B., F.M. Monaldo, J. Goldhirsh, and J. Wilkerson, "Validation of Geosat Altimeter-Derived Wind Speeds and Significant Wave Heights Using Buoy Data," J. *Geophys. Res.,* Vol 10, pp. 719-731, 1987.

Ebuchi, N., "Directional Distribution of Wind Vectors Observed by ERS-1/AMI Scatterometer," *Proc. IGARSS'93*, 1993.

Freilich, M.H.,"Satellite Scatterometer Comparisons with Surface Measurements: Techniques and SEASAT Results," *Proceedings of a Workshop on ERS-1 Wind and Wave Calibration*, 2-6 June 1986, pp. 57-62, (ESA SP-262, Sept. 1986).

Geernaert, G.L., S.E. Larsen, and F. Hansen, "Measurements of the Wind Stress, Heat Flux and Turbulent Intensity During Storm Conditions Over the North Sea," *J. Geophys. Res., 92*, C11, 13,927-13939, 1987.

Geernaert, G.L., K.L. Davidson, S. E. Larsen, and T. Mikkelsen, "Wind Stress Measurements During the Tower Ocean Wave and Radar Dependence Experiment," *J. Geophys. Res. 93*, C11, 13,913-13,923, 1988.

Guymer, T.H., J.A. Businger, W.L. Jones, and R.H. Stewart, "Anomalous Wind Estimates From the Seasat Scatterometer," *Nature*, Vo;. 294, pp. 735-737, Dec. 1981.

Johnson, P.E., D.G. Long, and T.E. Oliphant, "Geophysical Modeling Error in Wind Scatterometry," *Proc. Int. Geosc. Rem. Sens. Sym.*, Lincoln, Nebraska, 27-31 May, pp 1721-1723, 1996.

Jones, W.L., L.C. Schroeder, D. H. Boggs, E.M. Bracalente, R.A. Brown, G.J. Dome, W.J. Pierson, and F.J. Wentz, "The SEASAT-A Satellite Scatterometer: The Geophysical Evaluation of Remotely Sensed Wind Vectors Over the Ocean," *J. Geophys. Res.*, Vol. 87, No. C5, pp. 3297-3317, April 1982.

Liu, W.T., "The Effects of the Variations in Sea Surface Temperature and Atmospheric Stability in the Estimation of Average Wind Speed by Seasat-SASS", *J. Phys Oceanogr.*, vol. 14, pp. 392-401, 1984.

Liu, W.T., and W.G. Large, "Determination of Surface Stress by Seasat-SASS: A Case Study with JASIN Data," J. Phys. Ocean., Vo;. 11, No. 12, pp. 1603-1611, 1981.

de Loor, G.P., "Analysis of the ESA Windscatterometer Campaign Data," *Proceedings of the 5th International Coloquium-Physical Measurements and Signatures in Remote Sensing*, Courchevel, France, 14-18 January, 1991 (ESA SP-319, May 1991).

Worthington, A.M., *A Study of Splashes* The McMillan Co., New York, NY. reprint of 1908 edition, original work reported in *Proc. Roy. Soc. (London), 34*, pp. 213, 1963.

Wentz, F.J., "Intercomparison of ERS-1 Winds with SSM/I Winds", *1992 ADEOS/NSCAT Science Team Meeting Report*, pp 309-320, 1992b.

Ocean Scattering Theory

Agnon, Y., and M. Stiassnie, "Remote Sensing of the Roughness of a Fractal Sea Surface," *J. Geophys. Res.*, Vol. 96, No. C7, pp. 12773-12779, 1991.

Bahar, E., "Scattering Cross Sections for Random Rough Surfaces: Full Wave Analysis," *Radio Science*, Vol. 16, pp. 1327-1335, 1981.

Bahar, E., "Scattering Cross Sections for Composite Rough Surfaces: Full Wave Analysis," *Radio Science*, Vol. 16, pp. 331-341, 1981.

Banner, M.L., and C.L. Vincent, "On the Microwave Reflectivity of Small-Scale Breaking Water Waves," *Proc. R. Soc.*, London, Ser. *A, 399*, pp. 93-109, 1985.

Bass, F., I.M. Fuks, A.J. Kalmykov, I.E. Ostrovsky, and A.D. Rosenberg, "Very High Frequency Radiowave Scattering by a Disturbed Sea Surface, Parts I and II", *IEEE Trans. Antennas Propagat.*, AP-16, pp. 554-559 and 560-568, 1968.

Barrick, D.E., and W.H. Peake, "A Review of Scattering from Surfaces with Different Roughness Scales," *Radio Sci.* 3, pp 865-868, 1968.

Bliven, L.F., and J-P Giovanangeli, "Microwave Scattering From Wind- and Rain-Roughened Seas," Preprint, 1990.

Carswell, J.R., S.C. Carson, R.E. McIntosh, F.K. Li, G. Neumann, D.J. Mclaughlin, J.C. Wilkerson, P.G. Black and S.V. Nghiem, "Airborne Scatterometers: Investigating Ocean Backscatt Under Low- and High-Wind Conditions," *Proc. IEEE*, Vol. 82, No. 12, Dec. 1994.

Chen, J., T.K.Y. Lo, H. Leung, and J. Litva, "The Use of Fractals for Modeling EM Waves Scattering from Rough Sea Surface," *IEEE Trans. Geosci. Remote Sens.*, Vol. 34, No. 4, pp. 966-972, 1996.

Chen, K.S., A.K. Fung, and F. Amar, "An Empirical Bispectrum Model for Sea Surface Scattering," *IEEE Trans. Geosci. Remote Sens.*, Vol. 31, No. 4, pp. 830-835, 1993.

Durden, S. L., and J.F. Vesecky, "On the Ability of Rough Surface Scattering Approximations to Predict Hydrodynamic Modulation of the Ocean Cross Section: A Numerical Study," J. Geophys Res., Vol 94, pp 12703-12708, 1989.

Fung, A.K., and K.S. Chen, "Dependence of the Surface Backscattering Coefficients on Roughness, Frequency, and Polarization States," *Int. J. Remote Sensing*, Vol. 13, No. 9, pp. 1663-1680

Fung, A. K., M. R. Shah, and S. Tjuatja, "Numerical Simulation of Scattering from Three Dimensional Randomly Rough Surfaces," *IEEE Trans. Geosci. and Remote Sens.*, Vol. 32, No. 5, pp. 986-994, Sept. 1982.

Fung, A.K., and K.S. Chen, "A Kirchhoff Model for Skewed Surfaces," *J. Electrom. Waves and Appl.*, Vol. 5, No. 2, pp. 205-216, 1991.

Fung, A.K., and K.K. Lee, "A Semi-Empirical Sea-Spectrum Model for Scattering Coefficient Estimation," *IEEE J. Ocean. Eng.*, Vol. OE-7, No. 4, pp. 166-176, 1982.

Gotwols, B.L., and D.R. Thompson, Ocean microwave backscatter distributions, *J. Geophys. Res.*, Vol. C5, No. 99, pp. 9741-9750, May 1994.

Greenwood, A.D., D.V. Arnold, P.E. Johnson, R. Reed, and D.G. Long, Azimuth Modulation of Radar Backscatter at Near-Normal Incidence Using a Two-Dimensional Scattering Model," submitted to *Radio Science*, 1995.

Hara, T., and W.J. Plant, "Hydrodynamic modulation of short wind-wave spectra by long waves and its measurement using microwave backscatter," *J. Geophys. Res.*, Vol. 99, No. C5, pp. 9767--9784, May 1994.

Hauser, D., G. Caudal, and L.K. Shay, "Behavoir of the Ocean Radar Cross-Section at Low Incidence, Observed in the Vicinity of the Gulf Stream," *IEEE Trans. Geosci. Remote Sens.*, Vol. 33, No. 1, pp. 162-171, Jan 1995.

Holliday, D., "Resolution of a Controversy Surrounding the Kirchhoff Approach and the Small Perturvation Method in Rough Surface Scattering Theory," *IEEE Trans. Ant. and Prop.*, Vol AP-35, pp. 120-122, 1987.

Ishimaru, A., *Wave Propagation and Scattering in Random Media, V. 1 and 2*, Academic Press, New York, 1978.

Ishimaru, A., *Electromagnetic Wave Propagation, Radiation, and Scattering*, Prentice Hall, 1991.

Jessup, A.T., W.C. Keller, and W.K. Melville, "Measurements of sea spikes in microwave backscatter at moderate incidence," *IEEE Trans. Geosci. Remote Sens.*, Vol. 95, No. C6, pp. 9679--9688, June 1990.

Keller, W.C., W.J. Plant, R.A. Petitt, and E.A Terray, "Microwave backscatter from the sea: Modulation of recieved power and doppler bandwidth by long waves," *J. Geophys. Res.*, Vol. 99, No. C5, pp. 9751-9766, May 1994.

Komen, G. J. and W. A. Oost, eds., *Radar Scatting from Modulated Wind Waves*, Kluwer Academic Publishers, Dordrecht, The Netherlands, 1988.

Lee, P.H.Y., J.D. Barter, K.L. Beach, C.L. Hindman, B.M. Lake, H. Rungaldier, J.C. Shelton, A.B. Williams, R. Yee, and H.C. Yuen, "X Band Microwave Backscattering from Ocean Waves," *J. Geophys. Res.*, Vol. 100, No. C2, pp 2591-2611, 1995.

Liu, Y., and W.J. Pierson, "Comparisons of Scatterometer Models for the AMI on ERS-1: The Possibility of Systematic Azimuth Angle Biases of Wind Speed and Direction," *IEEE Trans. Geosci. Remote Sens.*, Vol. 32, No. 3, pp. 626-635, May 1994.

Longuet-Higgins, M.S., "The Effect of Nonlinearities on Statistical Distributions in the Theory of Sea Waves," *J. Fluid Mechanics*, Vol. 17, Part 3, pp. 459-480, 1963.

Lyzenga, D.R., A. L. Maffett and R. A. Shuchman, "The contribution of wedge scattering to the radar cross section of the ocean surface," *IEEE Trans. Geosci. Remote Sens., GE-21*, 4, 502-505, 1983.

Lyzenga, D.R., "Interaction of Short Surface and Electromagnetic Waves with Ocean Fronts," *J. Geophys. Res.*, Vol. 96, No. C6, pp. 10765-10772, 1991.

Plant, W.J., E.A Terray, and R.A. Petitm Jr., "The dependence of microwave backscatter from the sea on illuminated area: Correlation times and lengths," J. Geophys. Res., Vol. 99, No. C5, pp. 9705-9723, May 1994.

Plant, W.J., and W.C. Keller, "Evidence of bragg scattering in microwave doppler spectra of sea return," *J. Geophys. Res.*, Vol. 95, No. C9, pp. 16299-16310, September 1990.

Plant, W.J., and W.C. Keller, "Parameteric dependance of ocean wave-radar modulation transfer functions," *IEEE Trans. Geosci. Remote Sens.*, Vol. 88, No. C14, pp. 9747-9756, Nov 1983.

Ross, D., and W.L. Jones, "On the Relationship of Radar Backscatter to Wind Speed and Fetch," *Boundary Layer Meteorology*, Vol. 13, pp. 151-163, 1978.

Trizna, D.B., "Statistics of low grazing angle radar sea scatter for moderate and fully developed ocean waves," *IEEE Trans. Antennas and Propagation*, Vol. 39, No. 12, pp. 1681--1690, December 1991.

Trunk,G.V., "Radar properties of non-Rayleigh sea clutter," *IEEE Trans. Aerospace and Electronic Systems*, Vol. AES-8, No. 2, pp. 196-204, March 1972.

Valenzuela, G. R., "Theory for the interaction of electromagnetic and oceanic waves-A review," *Boundary Layer Meteorol., 13*, 61-85, 1978.

Wentz, F.J., "A Two-Scale Scattering Model for Foam-Free Sea Microwave Brightness Temperature," J. Geophys. Res., Vol 80, No. 24, pp. 3441-3446, 1975.

Wentz, F.J., "A Two-Scale Scattering Model with Application to the JONSWAP'75 Aircraft Microwave Scatterometer Experiment," NASA Contractor Report 2919, Dec. 1977.

Wetzel, L., "On Microwave Scattering by Breaking Waves," in O. M. Phillips and K. Hasselmann, *Wave Dynamics and Radio Probing of the Ocean Surface.* pp. 273-284, 1986.

Wetzel, L.B., "On the Theory of Electromagnetic Scattering From a Raindrop Splash," NRL Memorandum Report 6103, Naval Research Lab., Wash. DC., 42 pp., 1987.

Wright, J.W., Backscattering from Capillary Waves with Application to Sea Slutter. *IEEE Trans. Antennas Propag.,* AP-14, 749-754, 1966.

Rain Effects

Atlas, D., "Footprints of Storms at Sea: A View from Spaceborne Synthetic Aperture Radar," *J. Geophys. Res.*, Vol. 99, No. C4, pp 7961-7970, 1994.

Bliven, L.F., H. Branger, P. Sobieski, and J-P Giovanangeli, "An Analysis of Scatterometer Returns from a Water Surface Agitated by Artificial Rain: Evidence that Ring-Waves are the Main Feature," in press, 1993.

Bliven, L.F., J.P. Giovanangeli, and G. Norcross, "A Study of Rain Effects on Radar Scattering From Water Waves," Preprint volume. Seventh conference on Ocean-Atmosphere Interaction Jan. 13 to Feb. 5, 1988 Anaheim, Calif. *Amer. Meteor. Soc., 1988.*

Bliven, L.F., and J.P. Giovanangeli, "An Experimental Study of Microwave Scattering from Rain- and Wind-Roughened Seas," Int. J. Remote Sensing, Vol. 14, No. 5, pp. 855-869, *1993.*

Bliven, L.F., and G. Norcross, "Effects of Rainfall on Scatterometer Derived Wind Speeds," *Proceedings of the International Geoscience and Remote Sensing Symposium,* Edinburg, Scotland 13 to 16 Sept. 1988, ESA SP 284 (IEEE 88 CH 2497.6), 1988.

Moore, R.K., A.H.Chaudhry, and I.J. Birrer, "Errors in Scatterometer-Radiometer Wind Measurement Due to Rain," *IEEE J. Oceanic Engineering,* Vol. OE-8, No. 1, pp 37-48, Jan 1983.

Spencer, M., and M. Shimada, "Effect of Rain on Ku-Band Scatterometer Wind Measurements," *Proceedings of the International Geoscience and Remote Sensing Symposium,* 1991.

Scatterometer Theory and Wind Retreival

Brown, R.A. "On a Satellite Scatterometer as an Anemometer," *J. Geophys. Res.*, Vol. 88, No. C3, pp. 1663-1673, Feb. 1983.

Chi, C-Y and F.K. Li, "A Comparative Study of Several Wind Estimation Algorithms for Spaceborne Scatterometers," *IEEE Trans. Geosci. and Rem. Sens.*, Vol. GE-26, No. 2, pp. 115-121, March 1988.

Chi, C-Y, D.G. Long, and F.K. Li, "Roundoff Noise Analysis for Digital Signal Power Processors Using Welch's Spectrum Estimation," *IEEE Trans. Acoustics, Speech, and Signal Processing,* Vol. ASSP-35, No. 6, pp. 784-795, 1987.

Chi, C-Y, D.G. Long, and F.K. Li, "Radar Backscatter Measurement Accuracies Using Digital Doppler Processors in Spaceborne Scatterometers," *IEEE Trans. Geosci. and Rem. Sens.*, Vol. GE-24, No. 3, pp. 246-437, 1988.

Dunbar, S., S.V. Hsiao, and B.H. Lambrigtsen, "Science Algorithm Specification for the NASA Scatterometer Project," Vols. 1 & 2, D-5610, NASA Jet Propulsion Laboratory Report 622-107. Pasadena, CA 91103, 1988.

Fischer, R.E., "Standard Deviation of Scatterometer Measurements from Space," *IEEE Trans. on Geoscience Electronics*, Vol. GE-10, No. 2, pp. 106-113, 1972.

Huang, N.E., "Laboratory Calibration of Scatterometer," Unpublished manuscript, Laboratory for Hydrosperic Processes, NASA Goddard Spaceflight Center, Greenbelt, MD, 1992.

Leotta, D., and D.G. Long, "Probability Distribution of Wind Retrieval Error Versus True Wind Vector and Swath Location for the NASA Scatterometer," *Proceedings of the International Geoscience and Remote Sensing Symposium*, pp. 1466-1469, Vancover, B.C., July 1989.

Long, D.G., and M.W. Spencer "Radar Backscatter Measurement Accuracy for a Spaceborne Pencil-Beam Wind Scatteromter with Transmit Modulation," to appear, *IEEE Trans. on Geosc. and Rem. Sens.*, 1996.

Long, D.G., and G.B. Skouson, "Calibration of Spaceborne Scatterometers Using Tropical Rainforests," *IEEE Trans. Geosc. and Remote Sens.*, Vol. 34, No. 2, pp 413-424, 1996.

Long, D.G., P. Hardin, and P. Whiting, "Resolution Enhancement of Spaceborne Scatterometer Data," *IEEE Trans. Geosci. Remote Sens.*, Vol. 31, No. 3, pp. 700-715, May 1993.

Long, D.G., "Wind Field Model-Based Estimation of SEASAT Scatterometer Winds," *J. Geophys. Res.*, Vol. 98, No. C8, pp.14651-14668, 1993.

Long, D.G., and J.M. Mendel, "Identifiability in Wind Estimation from Wind Scatterometer Measurements," *IEEE Trans. on Geosc. and Rem. Sens.*,.Vol. 29, No. 2, pp. 268-276, 1991.

Long, D.G., and J.M. Mendel, "Model-Based Estimation of Wind Fields over the Ocean From Scatterometer Measurements Part I: The Wind Field Model," *IEEE Trans. on Geosc. and Rem. Sens.*, Vol. 28. No. 2, pp. 349-360, May 1990.

Long, D.G., and J.M. Mendel, "Model-Based Estimation of Wind Fields over the Ocean From Scatterometer Measurements Part II: Estimation of the Model Parameters," *IEEE Trans. on Geosc. and Rem. Sens.*, Vol. 28. No. 2, pp. 361-373, May 1990.

Long, D.G., C-Y Chi, and F.K. Li, "The Design of an Onboard Digital Doppler Processor for a Spaceborne Scatterometer," *IEEE Trans. Geosci. and Rem. Sens.*, Vol. GE-26, No. 6, pp. 869-878, Nov. 1988.

Naderi, F.M., M.H. Freilich, and D.G. Long, "Spaceborne Radar Measurement of Wind Velocity Over the Ocean--An Overview of the NSCAT Scatterometer System", *Proceedings of the IEEE*, pp. 850-866, Vol. 79, No. 6, June 1991.

Oliphant, T.E., and D.G. Long, "Cramer-Rao Bound for Wind Estimation from Scatterometer Measurements," *Proc. Int. Geosc. Rem. Sens. Sym.*, Lincoln, Nebraska, 27-31 May, pp 1724-1726, 1996.

Oliphant, T.E., and D.G. Long, "Development of a Statistical Method for Eliminating Improbable Wind Aliases in Scatterometer Wind Retrieval," *Proc. Int. Geosc. Rem. Sens. Sym.*, Lincoln, Nebraska, 27-31 May, pp 1715-1717, 1996.

Pierson, W. J., W. B. Sylvester, and M.A. Donelan, "Aspects of the Determination of Wind by Means of Scatterometry and of the Utilization of Vector Winds data for Meteorological Forecasts," J. *Geophys. Res*., Vol. 91, No. C2, pp. 2263-2272, 1986.

Shaffer, S.J., R.S. Dunbar, S.V. Hsiao, and D.G. Long, "A Median-Filter-Based Ambiguity Removal Algorithm for NSCAT," *IEEE Trans.Geosci. Remote Sens.*, Vol. 29, No. 1, pp. 167-174, Jan. 1991.

Spencer, M.W., and D.G. Long, "Tradeoffs in the Design of a Spaceborne Scanning Pencil-Beam Scatterometer," to appear, *IEEE Trans. on Geosc. and Rem. Sens.*, 1996.

Ulaby, F.T., R. K. Moore, and A. K. Fung, *Microwave Remote Sensing -- Active and Passive*, Vols. 1 and 2, Addison-Wesley Publishing Co., Reading, Mass., 1981.

Ulaby, F.T., R. K. Moore, and A. K. Fung, *Microwave Remote Sensing --Active and Passive*, Vol. 3, Artech House, Inc., Dedham, MA, 1986.

Wentz, F.J., "A Simplified Wind Vector Algorithm for Satellite Scatterometers," *J. Geophys. Res.*, Vol. 8, No. 5, pp 697-704, 1991.

Yourg, J.D., and R.K. Moore, "Active Microwave Measurements from Space of Sea-Surface Winds," IEEE *J. Oceanic Eng*., Vol. OE2, No. 4, pp. 309-317, 1977.

Wind and Wave Modeling, Spectra, and Characteristics

Allen, K. R., and R. I. Joseph, "A Canonical Statistical Theory of Surface Wind Waves," J. Fluid Mech., Vol 204, pp. 185-228, 1989.

Apel, J.R., "An Improved Model of the Ocean Surface Wave Vector Spectrum and its Effects on Radar Backscatter," *J. Geophys. Res.*, Vol. 99, 1994.

Banner, M.L., I.S.F. Jones, and J.C. Trinder, "Wavenumber Spectra of Short Gravity Waves," *J.Fluid Mech.*, 198,321-344, 1989.

Banner, M. J., "Equilibrium Spectra of Wind Waves," *J. Phys. Oceanog.*, Vol. 20, pp. 966-984, 1990.

Beal, R.C., *Directional ocean wave spectra*. John Hopkins University Press, 1991.

Barrick, D.E., and B. L. Weber, "On the nonlinear theory for gravity waves on the ocean's surface. Part II: Interpretation and applications," *J. Phys. Oceanogr.*, Vol. 7, pp. 11-21, 1977.

Bliven, L.F, N.E. Huang, and S.R. Long, "Experimental Study of the Influence of Wind on Benjamin-Feir Sideband Instability," *J. of Eng. Mechanics*, Vol. 162, pp. 237-260, Mar. 1986.

Cox, C., and W. Munk, "Statistics of the Sea Surface Derived From Sun Glitter", *J. Mar. Res.*, Vol. 13, 198-227, 1954.

Cox, C., "Measurements of Slopes of High Frequency Waves", J.Mar.Res. 16, 199-22 5, 1958.

Ding, L., and D.M. Farmer, "Observations of breaking surface wave statistics," *J. Phys. Oceanography*, Vol. 24, pp. 1368-1387, June 1994.

Donelan, M.A., J. Hamilton, and W.H. Hui, "Directional Spectra of Wind-Generated Waves", *Phil. Trans. R. Soc. Lond. A*, Vol. 315, pp. 509-562, 1985.

Donelan, M., F. Dobson, S. Smithi, and R. Anderson, "Dependence of Sea Surface Roughness on Wave Development," *J. Geophys. Res.*, Vol. 23, pp. 2143-2149, 1993.

Fraiser, S.J., Y. Liu, D. Moller, R.E. McIntosh, and C. Long, "Directional Ocean Wave Measurements in a Coastal Setting Using a Focused Array Imaging Radar," IEEE Trans. Geosci. Remote Sens., Vol. 33, No. 2, pp 428-440, Mar. 1995.

Freilich, M.H., and D.B. Chelton, "Wavenumber Spectra of Pacific Winds Measured by the Seasat Scatterometer," *J. Phys. Oceanogr.*, Vol. 16, No. 4, pp. 741-757, April 1986.

Fung, A.K., and K.K. Lee, "A Semi-Empirical Sea Spectrum Model for Scattering Coefficient Estimation", *IEEE Journal of Oceanic Engg*, Vol. OE-7, No. 4, 1982.

Halpern, D., A. Hollingsworth, and F.J. Wentz, "ECMWF and SSMI Global Surface Wind Speeds," *J. Atmospheric and Oceanic Technology*, 1994.

Huang, N.E., and C.-C. Tung, "The influence of the directional energy distribution on the nonlinear dispersion relation in a random gravity wave field," *J. Phys. Oceanogr.*, Vol. 7, pp. 403-414, 1977.

Huang, N.E., S.R. Long, L.F. Bliven,and C-C Tung, "The Non-Gaussian Joint Probability Density Function of Slope and Elevation for a Nonlinear Gravity Wave Field," *J. Geophys. Res.*, 89, C2, 1961-1972, March 1984.

Huang, N.E., L.F. Bliven, S.R. Long, and C-C Tung, "An Analytical Model for Oceanic Whitecap Coverage," *J. Phys. Oceanogr.*, Vol. 16, No. 10, pp. 1597-1604, Oct. 1986

Huang, N.E., S.R. Long, and L. F. Bliven, "An Experimental Study of the Statistical Properties of Wind-Generated Gravity Waves," *Wave Dynamics and Radio Probing of the Ocean Surface*, O. M. Phillips and K. Hasselmann, eds., Plenum Plublishing Co., 1986.

Huang, N.E., C-C Tung, and S.R. Long, "The Probability Structure of the Ocean Surface," *The Sea: Ocean Engineering Science,* pp. 335-366, Vol. 9, John Wiley and Sons, Inc., 1990.

Huang, N.E., C-C Tung, and S.R. Long, "Wave Spectra," *The Sea: Ocean Engineering Science,* pp. 197-237, Vol. 9, John Wiley and Sons, Inc., 1990.

Hughes, B.A., H.L. Grant, and R.W. Chappel, "A Fast Response Surface-Wave Slope Meter and Measured Wind-Wave Moments", *Deep Sea Res.*, 24, 1211-1223, 1977.

Hwang, P., "Surface Slope Measurements with a Wave Follower in TOWARD 84/86," Rept. No. ORE 86-3, *Ocean Research and Engineering*, Oct. 1986.

Jähne, B., and K.S. Riemer, "Two-Dimensional Wave-Number Spectra of Small-Scale Water Surface Waves", *J. Geophys. Res.*, 95, C7, 11531-11,546, 1990.

Keller, W., and B.L. Gotwols, "Two-Dimensional Optical Measurement of Wave Slope", *Appl. Opt.*,22, 3476-3478, 1983.

Kitaigorodskii, S.A., "On the Theory of the Equilibrium Range in the Spectrum of Wind-Generated Gravity Waves", *J.Phys.Oceanogr.*, 13, 816-827, 1983.

Kinsman, B., *Wind Waves*, Englewood Cliffs, New Jersey: Prentice-Hall, Inc., 1965.

Long, D.G., and D. Luke, "The Wavenumber Spectra of Scatterometer-derived Winds," *Proceedings of the International Geoscience and Remote Sensing Symposium,* pp. 1005-1007, Houston, Texas, May 26-29, 1992.

Mitsuyasu, H., and Honda, "Wind-Induced Growth of Water Waves," J. Fluid Mec., Vol. 123, pp. 425-442, 1982.

Mitsuyasu, H., and Kusaba, "A Note on the Momentum Transfer from Wind to Waves," J. Geophys. Res., Vol. 90, No. C2, pp. 3343-3345, 1985.

Phillips, O.M. and K. Hasselmann, *Wave Dynamics and Radio Probing of the Ocean Surface,* Plenum Press, New York: New York, 1986.

Phillips, O.M., "Spectral and Statistical Properties of the Equilibrium Range in Wind-Generated Gravity Waves", *J. Fluid Mech.*, 156, 505-531, 1985.

Pierson, W.J., and R.A. Stacy, "The Elevation, Slope, and Curvature Spectra of a Wind Roughened Sea Surface," *NASA Contr. Rep. 2247*, 122 pp., National Technical Information Service, Springfield VA, 1973.

Pierson, W.J., Jr., and L. Moskowitz, "A Proposed Spectral Form for Fully Developed Wind Seas Based on the Similarity Theory of S.A. Kitaigorodskii", *J. Geophys. Res.*, Vol. 69, No. 24, pp. 5181-5190, 1964.

Pierson, W.J., Jr, "Oscillatory Third Order Perturbation Soutions for Sums of Interacting Long-Crested Stokes Waves in Deep Water," *J. Ship Reseach*, pp. 354-383, June 1993.

Plant, W.J., and J.W. Keller, "Phase speeds of upwind and downwind traveling short gravity waves," *J. Geophys. Res.*, Vol. 85, No. C6, pp. 3304-3310, June 1980.

Shemdin, O.H., H.M. Tran, and S.C. Wu, "Directional Measurements of Short Ocean Waves with Stereophotography", *J. Geophys.Res.*, 93, 13891-13901, 1988.

Snyder, R.L., and R.M. Kennedy, "On the formation of whitecaps by a threshold mechanism," *J. Phys. Oceanography,* Vol. 13, pp. 1482--1518, Aug 1983.

Stilwell, D., "Directional Energy Spectra of the Sea from Photographs", *J. Geophys.Res.*, 74, 1974-1986, 1969.

Tung, C.C., M. ASCE, and N.E. Huang, "Spectrum of Breaking Waves in Deep Water," *J. of Eng. Mechanics*, Vol. 113, No. 3, pp. 293-302, Mar. 1987.

Tung, C.C., and N.E. Huang, "The Effect of Wave Breaking on the Wave Energy Spectrum," *J. Phys. Oceanogr.*, Vol. 17, No. 8, pp. 1156-1162, Aug. 1987

Weber, B.L., and D.E. Barrick, "On the nonlinear theory for gravity waves on the ocean's surface. Part I: Derivations," *J. Phys. Oceanogr.*, Vol. 7, pp. 3-10, 1977.

Wentz, F.J., "Measurement of Oceanic Wind Vector Using Satellite Microwave Radiometers," *IEEE Trans. Geoscience and Remote Sensing*, Vol 30. No. 5, pp. 960-972, 1992.

Wu, J., "Mean Square Slope of the Wind-Disturbed Water Surface, Their Magnitude, Directionality and Composition," *Radio Science*, Vol. 25, No. 1, pp 37-48, Jan-Feb 1990.

Wave Tank Studies

Bliven, L.F., J.P. Giovanangeli, R.H. Wanninkhof, and B. Chapron, "A Laboratory Study of Friction - Velocity Estimtes from Scatterometry: Low and High Regimes," Int. J. Remote Sensing, Vol. 14, No. 9, pp. 1775-1785, *1993.*

Ebuchi, N., H. Kawamura, and Y. Toba, "Physical Processes of Microwave Backscattering from Laboratory Wind-Wave Surfaces," J. Oceanogr., Vol. 48, pp. 139-154, 1992.

Ebuchi, N., H. Kawamura, and Y. Toba, "Physical Processes of Microwave Backscattering from Laboratory Wind-Wave Surfaces," in press, *J. Geophys. Res.*, 1993.

Giovanangeli, J-P, L.F. Bliven, and O. Le Calve, "A Wind-Wave Tank Study of the Azimuthal Response of a Ka-Band Scatterometer," *IEEE Trans. Geo. and Rem. Sens.*, Vol. 29, No. 1, pp 143-148, Jan 1991.

Kahma, K.K., and M.A. Donelan, "A Laboratory Study of the Minimum Wind Speed for Wind Wave Generation," J. *Fluid Mech.*, vol. 192, pp 339-364, 1988

Keller, M.R., W.C. Keller and W.J. Plant, "A Wave Tank Study of the Dependence of the X-band Cross Sections on Wind Speed and Water Temperature", *J. Geophys. Res.*, Vol. 97, No. C4, pp 5771-5792, 1992.

Van Halsema, D., et al., "Dual-polarized Scatterometer Measurements of Wind and Mechanically Generated Waves in a Very Large Wind/Wave Flume, the VIERS-1 Project," *Proceedings of the 5th International Coloquium-Physical Measurements and Signatures in Remote Sensing*, Courchevel, France, 14-18 January, 1991 (ESA SP-319, May 1991).

Lai, R.J., S.R. Long, and N.E. Huang, "Laboratory Studies of Wave-Current Interaction: Kinematics of the Strong Interaction," *J. Geophys. Res.*, 94, C11, 16,201-16,214, 15 Nov. 1989.

APPENDIX

A. Scatterometer System Design and Kp

A wind scatterometer is a radar designed to measure the sigma-0 of the ocean's surface at least two different azimuth angles in order to infer the near-surface wind. The scatterometer does not directly measure sigma-0. Instead, it measures radar echo power, Pr, from which sigma-0 is calculated using the radar equation. To determine the radar echo power, two separate measurements are made: one of the echo power plus noise, Ps+n, and one of the noise-only power, Pn. This noise arises in the radar receiver and the radiometric temperature of the target and antenna system. The echo power plus noise and noise-only power measurements are subtracted to obtain the measurement of Pr, i.e., Pr' = Ps+n' - Pn' where the primes are used to denote sample values of Pr, Ps+n, and Pn.

Because finite integration times and bandwidths are used in computing the measurements of the noise-only and echo power plus noise power, these measurements are random variables whose means correspond to the true values of Ps+n and Pn. It can be shown that the measurements (Ps+n' or Pn') are integrals (SASS) or sums of integrals (NSCAT) of sample functions of independent Raleigh distributed random processes. By the central limit theorem, Ps+n' and Pn' have Gaussian distributions (*Fisher*, 1972; *Chi et al.* 1986). The resulting "measurement" of Pr also has a Gaussian distribution. Note that if the measurements are unbiased Mean[Pr']=Pr. Pr is related to σ^o via the radar equation:

$$\mathrm{Pr} = \frac{P_T L G^2 \lambda^2 A}{(4\pi)^3 R^4}\sigma^o = X\sigma^o. \qquad \text{(A.1)}$$

Thus, σ^o also has Gaussian distribution with mean σ^o. It can be shown that the variance of the σ^o measurement, denoted by σ^o', can be expressed as a quadratic function of the true value of σ^o,

$$\mathrm{Var}[\sigma^o{}'] = \alpha\ \sigma^{o2} + \beta\ \sigma^o + \gamma \qquad \text{(A.2)}$$

where the coefficients α, β, and γ are dependent on the radar system design and the measurement signal to noise ratio (*Chi et al.* 1986; *Long et al.*, 1988). Thus, the variability of the measurements of σ^o are a quadratic function of the actual σ^o of the ocean's surface. The normalized standard deviation of σ^o, denoted by Kp, is

$$\mathrm{Kp}[\sigma^o] = \frac{\sqrt{\mathrm{Var}[\sigma^o]}}{\sigma^o}.$$

This σ^o variability introduced as the result of radar receiver noise is termed "communication Kp." Additional variability is introduced in σ^o as a result of uncertainties (e.g., calibration errors) in the knowledge of X in Eq. (A.1) when σ^o is "retrieved "from the power measurements. This variability is termed "retrieval Kp." As discussed in the main text, this retrieval error is modeled as a Gaussian random variable. It may then be combined into the α, β, and γ of Eq. (A.2) (*Long*, 1992).

In effect the measurement σ^o measurement model can be expressed as,

$$\sigma^o{}' = \sigma^o(1+\mathrm{Kp}[\sigma^o{}']\nu)$$

where ν is a normally distributed random variable (*Long and Mendel*, 1991).

Note that while σ^o is strictly positive, the measurement $\sigma^{o\prime}$ can be negative with a non-zero probability. The conditional probability distribution of $\sigma^{o\prime}$ can be expressed as,

$$p(\sigma^{o\prime}|\sigma^o) = \frac{1}{\sqrt{2\pi(\alpha\sigma^{o2} + \beta\sigma^o + \gamma)}} Exp\left[-\frac{1}{2}\left(\sigma^{o\prime} - \sigma^o\right)^2 \Big/ \left(\alpha\sigma^{o2} + \beta\sigma^o + \gamma\right)\right].$$

Note that the true value of σ_0, must be known to determine the variance of $\sigma^{o\prime}$.

To formulate the maximum likelihood (ML) estimate of the wind we *assume* that σ^o is related to the wind vector via the model function. Let σ^o_M denote the value of σ^o computed from the true wind vector $\mathbf{U}$ using the model function with the measurement geometry (i.e., the relative azimuth angle, incidence angle, and polarization). The key assumption is that $\sigma^o = \sigma^o_M$ so that the conditional probability distribution can be expressed as,

$$p(\sigma^{o\prime}|\sigma^o_M) = \frac{1}{\sqrt{2\pi(\alpha\sigma^{o2}_M + \beta\sigma^o_M + \gamma)}} Exp\left[-\frac{1}{2}\left(\sigma^{o\prime} - \sigma^o_M\right)^2 \Big/ \left(\alpha\sigma^{o2}_M + \beta\sigma^o_M + \gamma\right)\right]$$

which we can denote as, $p(\sigma^o|\mathbf{U}) = p(\sigma^{o\prime}|\sigma^o_M)$. Note that variance may be incorrectly computed if there is error in the geophysical model function so that $\sigma^o \neq \sigma^o_M$.

Since the measurements are statistically independent (because the noise is), the joint conditional probability distribution of the σ^o measurements used to retrieve the wind can be expressed as,

$$p(\sigma^o_1{}', \sigma^o_2{}', \ldots, \sigma^o_N{}'|\mathbf{U}) = \prod_{i=1}^{N} p(\sigma^o_i|\mathbf{U}).$$

The log-likelihood function is computed by taking the log of this expression and discarding any constants. For convenience we usually form an objective function as the negative of the log-likelihood function. The ML estimate of the wind vector $\mathbf{U}=(|U|,\chi)$ found by determining the $\mathbf{U}$ which minimizes the objective function,

$$J_{MLE}(\mathbf{U}) = \sum_{k=1}^{N}\left[\left|\frac{(z_k - \sigma^o_{Mk})}{\delta_k}\right|^2 + \ln\delta_k\right]$$

where we have set $z_k = \sigma^{o\prime}$ and

$$\delta_k{}^2 = \alpha_k\,\sigma^{o2}_{M}{}_k + \beta_k\,\sigma^o_{M}{}_k + \gamma_k.$$

Although the log of the standard deviation of the backscatter sample enters into the ML theory, *Pierson* (1989, 1990) has suggested that it may not be necessary. Pierson's modified ML estimator can be expressed as, [compare with Eq. (1.2)]

$$J_{PMLE}(\mathbf{U}) = \sum_{k=1}^{N}\frac{(z_k - \sigma^o_{MK})^2}{\delta_k{}^2}$$

In this form, it is possible to contrast it with the Sum of Squares (SOS) algorithm used for the recovery of the winds for Seasat. The SOS algorithm is

$$J_{sos}(\mathbf{U}) = \sum_{k=1}^{N} \frac{(z_k - \sigma_{Mk}^{o})^2}{\delta_k^{\,2} + M_{FE}} \qquad \text{(A.3)}$$

The SOS algorithm arose in part from the assumed power law in the SASS-1 G-H table which for every aspect and incidence angle had the form (hence the G-H tables)

$$10\log_{10}\sigma_M^0 = G(\chi,\theta) + H(\chi,\theta)\log_{10}|U|.$$

The denominator of Eq. (A.3) was kept constant, and its value was found from three incorrect assumptions: (1) that the backscatter in dB was a normally distributed variable, (2) that the variance (or standard deviation) could be calculated from K_p, and (3) that the sample value could be used for the denominator. The first assumption was incorrect, and the second resulted in the inability to apply the SOS algorithm if K_p was greater than one. The third does not follow from the theory. The denominator is a function of the model function and not the sample values.

An additional empirical constant, M_{FE}, was added to the denominator of the terms in the SOS to describe the "geophysical modeling error"; however, it is doubtful that a single constant can describe the errors in the model (Johnson et al., 1996).

Additional comments regarding the geophysical model function error and predictions for NSCAT performance may be found in *Pierson and Sylvester* (1996)

i. References

Chi, C-Y, D. G. Long, and F.K. Li, "Radar Backscatter Measurement Accuracies Using Digital Doppler Processors in Spaceborne Scatterometers," *IEEE Trans. Geosci. and Rem. Sens.*, Vol. GE-24, No. 3, pp. 246-437, 1988.

Fischer, R. E., "Standard Deviation of Scatterometer Measurements from Space," *IEEE Trans. on Geoscience Electronics*, Vol. GE-10, No. 2, pp. 106-113, 1972.

Johnson, P.E., D.G. Long, and T.E. Oliphant, "Geophysical Modeling Error in Wind Scatterometry," *Proc. Int. Geosc. Rem. Sens. Sym.*, Lincoln, Nebraska, 27-31 May, pp 1721-1723, 1996.

Long, D. G., "The Scatterometer Measurement Model With Correlated Noise and Bias," Report prepared for the Jet Propulsion Laboratory, Pasadena, CA, 10 Sept. 1991.

Long, D. G., and J. M. Mendel, "Identifiability in Wind Estimation from Wind Scatterometer Measurements," *IEEE Trans. on Geosc. and Rem. Sens.*,.Vol. 29, No. 2, pp. 268-276, 1991.

Long, D.G., C-Y Chi, and F.K. Li, "The Design of an Onboard Digital Doppler Processor for a Spaceborne Scatterometer," *IEEE Trans. Geosci. and Rem. Sens.*, Vol. GE-26, No. 6, pp. 869-878, Nov. 1988.

Pierson, W.J., Jr., and W.B. Sylvester, "Predicted Results from NSCAT on ADEOS Using the SASS-II Model Function," unpublished report presented at the ADEOS/NSCAT Science Working Team Meeting, Pasadena, California, 4-6 June, 1996

B. The NSCAT model function

For reference, this section describes the baseline implementation of the geophysical model function and the wind retrieval algorithm implemented for the NSCAT ground processing system.

i. NSCAT tabular model function form

Over the years there has been much controversy concerning the functional form of the model function. Because wind retrieval algorithms have traditionally had the functional form of the model function "hard-coded" into them, changing the functional form of the model function has had significant impact on the computer code employed to retrieve winds. Since model function refinement activities planned for NSCAT might lead to changes in the model function form, a tabular approach was adopted for the NSCAT algorithm development activities, thus effectively decoupling the wind retrieval *algorithm* from the detailed form of the *model function.*

The tabular approach does not require an explicit analytical function form for the model function. Instead, the model function is tabulated on a uniform grid in the dependent parameter space. This procedure permits a great latitude in formulating models.

As currently defined in the NSCAT algorithm specifications (*Dunbar, Hsaio and Lambrigtsen,* 1988), the geophysical model function is tabulated on a four-dimensional parameter grid of wind speed, relative azimuth angle, incidence angle, and polarization. If necessary, additional independent parameters, e.g., sea-surface temperature (SST), can be easily be included.

Though not critical to the current implementation, the baseline design quantizes wind speed into 1 m/s bins while the azimuth and incidence angles are quantized to 5° bins. There are two polarizations, H and V. The model function table is created by evaluating the selected geophysical model at the center of each bin and storing the resulting sigma-0 in linear space in the table. Linear interpolation is used to compute sigma-0 for parameter values between bins when evaluating the model function during wind retrieval.

ii. NSCAT wind retrieval

As currently defined in the NSCAT algorithm specifications (*Dunbar, Hsaio and Lambrigtsen,* 1988), the NSCAT wind retrieval algorithm will be based on maximum-likelihood principles.

Typically, a total of 16 sigma-0 measurements (each having approximately 25 km resolution) will be available for each 50 x 50 km wind vector cell on the ocean surface, four each from the four antenna beams covering a given side of the swath. An objective function, based on maximum likelihood (ML) principles (*Chi and Li,* 1988; *Pierson,* 1990; *Long and Mendel,* 1991), is minimized to estimate the wind vector:

$$J_{MLE}(|U|,\varphi) = \sum_{i=1}^{N} \left\{ \left| \frac{(z_i - \sigma_i^o)}{\delta_i} \right|^2 + \ln \delta_i \right\} \qquad \text{(B.1)}$$

where z_i are the measured (sample) sigma-0 values and σ_i^o are the sigma-0 values corresponding to the wind velocity at the appropriate polarization and azimuth/incidence angles from the model. The variance of σ_i^o is given by

$$\delta_i^2 = Var[\sigma_i^o] = \alpha\sigma_i^{o2} + \beta\sigma_i^o + \gamma = K_p^2\sigma_i^{o2} \qquad \text{(B.2)}$$

where α, β, and γ are parameters computed from the properties of the digital filter (*Long, Li and Chi*, 1988) and modified to include the σ^o retrieval error and the *assumed* model function error (*Long*, 1988). Note that the contribution to the square error sum of the individual measurements in the ML objective function is weighted by the inverse of the *expected* variance of the individual measurements. The expected variance is a function of the true sigma-0 value rather than of the measured value z_i. In implementation the true sigma-0 value is replaced by the model sigma-0 value, i.e., $\sigma_i^o = \sigma_{Mi}^o$. (Refer to the previous section.)

Equation (B.1) generally has several local minima (and possibly several global minima), corresponding to near-intersections of the sigma-0 versus azimuth angle curves (see *Naderi* et al., 1991; *Pierson*, 1990; *Long and Mendel*, 1991). The relative values of the objective function at each minimum are used to rank the likelihood of each solution. The set of possible wind vector solutions are known as "ambiguities" or "aliases", although the former is preferred. Typically, the ambiguities have similar wind speeds but differing wind direction. The occurrence of multiple solutions is the result of the approximately biharmonic nature of the model function with respect to wind direction. Selection of a single wind vector requires a second step termed "ambiguity removal" which is not considered here.

iii. References

Chi, C-Y and F.K. Li, "A Comparative Study of Several Wind Estimation Algorithms for Spaceborne Scatterometers," *IEEE Trans. Geosci. and Rem. Sens.*, Vol. GE-26, No. 2, pp. 115-121, March 1988.

Dunbar, S., S. V. Hsiao, and B. H. Lambrigtsen, "Science Algorithm Specification for the NASA Scatterometer Project," Vols. 1 & 2, D-5610, NASA Jet Propulsion Laboratory Report 622-107. Pasadena, CA 91103, 1988.

Long, D.G., "Documentation for the NSCAT Simulation Programs," Jet Propulsion Laboratory Internal Memo, 3343-88-177, Dec. 20, 1988.

Long, D. G., and J. M. Mendel, "Identifiability in Wind Estimation from Wind Scatterometer Measurements," *IEEE Trans. on Geosc. and Rem. Sens.*, Vol. 29, No. 2, pp. 268-276, 1991.

Long, D. G., C-Y Chi, and F. K. Li, "The Design of an Onboard Digital Doppler Processor for a Spaceborne Scatterometer," *IEEE Transactions on Geoscience and Remote Sensing*, Vol. 26, No. 6, pp. 869-878, Nov. 1988.

Naderi, F. M., M. H. Freilich, and D. G. Long, "Spaceborne Radar Measurement of Wind Velocity Over the Ocean--An Overview of the NSCAT Scatterometer System", *Proceedings of the IEEE*, pp. 850-866, Vol. 79, No. 6, June 1991.

Pierson, W. J., Jr., "Dependence of Radar Backscatter on Environmental Parameters," from G. L. Geernaert and W. J. Plant (eds), *Surface Waves and Fluxes*, Vol II, pp 173-220, Kluwer Academic Publishers, Netherlands, 1990.

C. Historical perspective on wind scatterometry

During the period of the manned trips to the moon, it was decided that the program would be shortened and that a number of Apollo spacecraft would not be used for their original purpose. Instead, NASA initiated a program to mount some instruments on these spacecraft, put them in Earth orbit, and study the Earth. A group of scientists and instrument designers met to discuss possible instruments and their applications for geography, geodesy, agriculture, oceanography, meteorology and other areas of geophysics. This series of meetings evolved to the Skylab program, whose complement of instruments included a radar altimeter and a combination passive microwave and active pencil beam radar called S-193. The Apollo spacecraft were to travel to and from Skylab.

The applications of a radar altimeter to geodesy were described by *Greenwood et al.* (1969a), and its applications to oceanography were described by *Greenwood et al* (1969b). *Moore and Pierson* (1971) described the applications of a radar radiometer. Subsequently R. K. Moore coined the word "scatterometer". Passive microwave measurements were supposed to allow for attenuation effects for the radar.

The first scatterometer measurements were made by S-193 on Skylab, which was one of a suite of instruments for the Earth Resource Experiment Program (EREP) (*Barrick and Swift*, 1980). At that time, the anisotropy of the backscatter as a function of wind direction was not known and there was only one measurement of the backscatter made for each area in the swath [see *Cardone, et al.* (1975)]

The AAFE (Advanced Application Flight Experiments) program at Langley made the first of many circle flights (*Schroeder, et al.* 1984), showing that the backscatter was a strong function of wind direction. It was concluded that the winds recovered by a scatterometer would be at least as accurate as the conventional reports from ships at sea.

The plans for the SEASAT-A Scatterometer (SASS) were to measure the backscatter for two different directions 90° apart so that the values could be averaged and a more reliable wind speed obtained. The idea that both wind speed and direction could be obtained from the SASS data appears to have been first described by *Pierson, Cardone and Greenwood* (1974), and the model function concept and wind recovery algorithms followed as an extension of these ideas.

During the operation of SASS, an extensive comparison of SASS measurements and wind measurements made by ships and buoys in the North Atlantic as part of the JASIN experiment lead to the development of the empirical SASS-1 model function (*Jones et al., 1982, Schroeder et al.,* 1982; *Bracalente et al.,* 1980). The dramatic success of SASS lead to the development of the NASA Scatterometer (NSCAT) which is planned for flight on the Japanese ADEOS spacecraft in 1996 (*Naderi, Freilich and Long*, 1991) as well as providing the impetus for the development of the European Remote Sensing Satellite (ERS) scatterometer series (ERS-1 and ERS-2). Follow-on missions for NSCAT and ERS are in the planning stages. The NSCAT follow-on mission is known as *SeaWinds* and is described in *Freilich* et al. (1994) and *Wu* et al. (1994)

i. References

Barrick, D.E., and C.T. Swift, "The Seasat Microwave Instruments in Historical Perspective," *IEEE J. Oceanic Engineering*, Vol. OE-5, No. 2, pp. 74-79, April 1980.

Freilich, M.H., D. G. Long, and M. W. Spencer, "SeaWinds: A Scanning Scatterometer for ADEOS II -- Science Overview," *Proceedings of the International Geoscience and Remote Sensing Symposium,* Pasadena, California, August 8-12, pp. 960-963, 1994.

Cardone, V. J., J. D. Young, W. J. Pierson, R. K. Moore, J. A. Greenwood, C. Greenwood, A. K. Fung, R. E. Salfi, H. L. Chan, M. Afarani and M. Komen, "The Measurement of the Winds Near the Ocean Surface with a Radiometer-Scatterometer on SKYLAB," Final Report of EPN 550 Contr. No. NAS-9-13642, NASA Lyndon B. Johnson Space Center, Houston, Texas, 1975.

Greenwood, J. A., A. Nathan, W. J. Pierson, G. Neumann, F. C. Jackson and T. Pease, "Radar altimetry from a spacecraft and its potential applications to geodesy," *Remote Sensing of Environment*, Vol. 1, pp. 59-70, 1969.

Greenwood, J. A., A. Nathan, W. J. Pierson, G. Neumann, F. C. Jackson and T. Pease, "Oceanographic applications of radar altimetry from spacecraft," *Remote Sensing of Environment,* Vol. 1, pp. 71-80.

Jones, W. L., L. C. Schroeder, D. H. Boggs, E. M. Bracalente, R. A. Brown, G. J. Dome, W. J. Pierson, and F. J. Wentz, "The SEASAT-A Satellite Scatterometer: The Geophysical Evaluation of Remotely Sensed Wind Vectors Over the Ocean," *J. Geophys. Res.*, Vol. 87, No. C5, pp. 3297-3317, April 1982.

Moore, R. K. and W. J. Pierson, "Worldwide oceanic wind and wave predictions using a satellite radar-radiometer," *Hydrodynamics,* Vol. 5, No. 2, pp. 52-60, 1971.

Naderi, F. M., M. H. Freilich, and D. G. Long, "Spaceborne Radar Measurement of Wind Velocity Over the Ocean--An Overview of the NSCAT Scatterometer System", *Proceedings of the IEEE*, pp. 850-866, Vol. 79, No. 6, June 1991.

Pierson, W. J., W. E. Marlatt, Z. H. Byrns and W. R. Johnson, "Oceans and atmosphere," in *SKYLAB EREP Investigations Summary*, NASA SP-399. National Aeronautics and Space Administration. U. S. Govt. Printing Office Stock No. 033-00-00741-8, pp. 189-256, 1978.

Pierson, W. J., V. J. Cardone and J. A. Greenwood, "The application of Seasat-A to meteorology," The University Institute of Oceanography (now CUNY Remote Sensing Laboratory). Prepared for the SPOC group of NOAA/NESS Contract 04-4158-11, 1974.

Pierson, W. J., Jr., "Dependence of Radar Backscatter on Environmental Parameters," from G. L. Geernaert and W. J. Plant (eds), *Surface Waves and Fluxes*, Vol II, pp 173-220, Kluwer Academic Publishers, Netherlands, 1990.

Schroeder, L., D.H. Boggs, G. Dome, I.M. Halberstam, W.L. Jones, W.J. Pierson, and F.J. Wentz, "The Relationship Between the Wind Vector and the Normalized Radar Cross Section Used to Derive Seasat-A Satellite Scatterometer Winds," *J. Geophys. Res.*, Vol. 87, No. C5, pp. 3318-3336, 1982.

Schroeder, L. C., W.L. Jones, P.R. Schaffner and J.L. Mitchell, "Flight measurements and analysis of AAFE RADSCAT wind speed signature of the ocean", NASA Technical Memorandum 85646, January 1984.

Wu, C., J. Graf, M.Freilich, D. G. Long, M. Spencer, W. Tsai, D. Lisman, and C. Winn, "The SeaWinds Scatterometer Instrument," *Proceedings of the International Geoscience and Remote Sensing Symposium,* Pasadena, California, August 8-12, pp. 1511-1515, 1994.

D. Locations of azimuth minima: recent results and examples

The normalized radar backscattering cross sections for V- and H-pol, σ^{o}_{VV} and σ^{o}_{HH}, vary with wind direction. Recent published data contain important results on the location of the minima in the variation of radar backscatter as a function of wind direction for Ku-band. These new results, especially those of *Li, et al*. (1988), reveal various inconsistencies in the empirical fits to the azimuthal variation of the backscatter. The one complete example in *Li, et al*. (1988) from FASINEX shows that the upwind-downwind backscatter differences are small for vertical polarization and large for horizontal polarization. Their Figs. 5, 6, and 7 show that the minima near crosswind were close to 92° and 268° for vertical polarization and averaged to about 97° and 263° for horizontal polarization and that the maxima at upwind and downwind were essentially 180° apart. *Li, et al.* (1988) also illustrate that the SASS-1 model function has minima at exactly 90° and 270° for both polarizations.

For a given wind speed incidence angle and polarization, the variation of the backscatter (with a complicated dependence on the sea state and perhaps water temperature) is some function of the wind direction. The variable, χ, will be used for wind direction. The most general representation, with no jump discontinuities for the purpose at hand, is a function that uses sines and cosines as the orthogonal basis as given by Eq. (D.1) below.

$$\sigma^{o}(\chi) = A_O + \sum_{n=1}^{N} A_n \cos n\chi + B_n \sin n\chi \qquad \text{(D.1)}$$

Assuming azimuth symmetry

$$\sigma^{o}(\chi) = \sigma^{o}(-\chi) \qquad \text{(D.2)}$$

so that the B_N in Eq. (D.1) are zero.

Attempts to fit Eq. (D.1) to backscatter data have set the values for A_n equal to zero for N greater than 2, 3, or 4 as illustrated in the literature (see previous discussion).

An alternative equation to be fitted would be Eq. (D.3) which would express the angular variation in bels.

$$\sigma^{o}(\chi)_B = a_0 + \sum_{n=1}^{N} a_n \cos n\chi \qquad \text{(D.3)}$$

In application, if a poor fit to azimuthally varying data is obtained for, say, either $N = 2$ or 3, then going to $N = 4$ or 5, thus increasing the number of terms in either Eq. (D.1) or (D.3), complicates the analysis, especially if absolute relative maxima are required at 0° and 180°. Added terms require corrections for all of the coefficients since they determine the maxima at 0° and 180°. Strange things can also happen to derivatives when N becomes large. The result may no longer be a monotonically decreasing function from χ=0° to $\chi = \chi_M$ (the minimum) and a monotonically increasing function from χ_M to a secondary maximum at χ=180°.

This section is courtesy of W. Pierson to extend the discussion presented in Section 5.D.

i. Large *N* Values

If $N = 3$, Eq. (D.1) is used to fit wind direction effects. There are four unknown constants to be determined from the data. There are several ways to do this, but whichever method is used there are only four features of the azimuthal variation that can be modeled by either Eq. (D.1) or Eq. (D.3). One of many ways to fit the data is to require that at $\chi=0°$, $\sigma^o(0) = \sigma^o_U$; at $\chi=180°$, $\sigma^o(180°) = \sigma^o_D$; at $\chi=90°$; $\sigma^o(90°) = \sigma^o_C$ and at, $\chi=\chi_M$, the minimum, $d\sigma^o(\chi)/d\chi = 0$. Thus,

$$A_0 + A_1 + A_2 + A_3 = \sigma^o_U \tag{D.4}$$

$$A_0 - A_1 + A_2 - A_3 = \sigma^o_D \tag{D.5}$$

$$A_0 - A_2 = \sigma^o_C \tag{D.6}$$

$$A_1 \sin\chi_M + 2 A_2 \sin 2\chi_M + 3 A_3 \sin 3\chi_M = 0 \tag{D.7}$$

Eq. (D.7) can be rewritten as Eq. (D.8).

$$A_1 - 3 A_3 + 4 A_2 \cos \chi_M + 12 A_3 \cos^2 \chi_M = 0 \tag{D.8}$$

If $\cos \chi_M = 0$, then $A_1 = 3 A_3$ and the minimum will be at 90°. If $A_3 = 0$, then

$$\cos \chi_M = - A_1/4 A_2 \tag{D.9}$$

as in *Li, et al*. (1988). Also the value at the minimum is fixed and equals Eq. (D.10) as in *Donelan and Pierson* (1987).

$$\sigma^o(\chi_M) = A_0 - A_2 - (A^2_1/8 A_2) \tag{D.10}$$

If the shape of $\sigma^o(\chi)$ is realistic, Eqs. (D.4) to (D.7) imply that a considerable range of values of χ_M other than these two special cases can be fitted. Eqs. (D.4) to (D.7) can be solved for the *A*'s as in Eqs. (D.11) to (D.14).

$$A_0 = (\sigma^o_U + \sigma^o_D)/4 + \sigma^o_C/2 \tag{D.11}$$

$$A_2 = (\sigma^o_U + \sigma^o_D)/4 - \sigma^o_C/2 \tag{D.12}$$

$$A_3 = \frac{(\sigma^o_U - \sigma^o_D)/2 + (\sigma^o_U + \sigma^o_D - 2\,\sigma^o_C)\cos\chi_M}{4 - 12\cos^2\chi_M} \tag{D.13}$$

$$A_1 = (\sigma^o_U - \sigma^o_D)/2 - A_3 \tag{D.14}$$

These equations also determine the value of $\sigma^o(\chi_M)$ indirectly.

All of the above equations could be repeated using a_0, a_1, a_2 and a_3, σ^o_{UB}, σ^o_{DB}, σ^o_{CB} in bels and χ_M. The solutions would not be the same. For example,

$$\sigma^o_B(\chi , a_0, a_1, a_2, a_3) \neq \log_{10} \sigma^o(\chi A_0, A_1, A_2, A_3) \quad \text{(D.15)}$$

except at $\chi_M = 0°$, $\chi_M = 180°$ and $\chi_M = 90°$.

As a second method, the requirement that $\sigma^o(\chi_M) = \sigma^o_M$ can be used to replace Eq. (D.6) and the result is Eq. (D.16).

$$A_0 + A_1 \cos \chi_M + A_2 \cos 2 \chi_M + A_3 \cos 3 \chi_M = \sigma^o_M \quad \text{(D.16)}$$

Eqs. (D.4), (D.5), (D.16) and (D.7) can then be solved for the values of A_0, A_1, A_2 and A_3. For abbreviation, let $C_1 = \cos \chi_M$, $C_2 = \cos 2\chi_M$, $S_1 = \sin \chi_M$ and so on.

Then

$$A_3 = F_1/F_2 \quad \text{(D.17)}$$

where

$$F_1=(2(S2)(1-(C1))(\sigma^o_U-\sigma^o_D)/2-2(S2)(\sigma^o_U-\sigma^o_M))/(1-(C2))-(S1)(\sigma^o_U-\sigma^o_D)/2 \quad \text{(D.18)}$$

and

$$F_2 = 3(S3) - (S1) - (2(S2)((C1) - (C3))/(1 - (C2))) \quad \text{(D.19)}$$

$$A_2 = (\sigma^o_U-\sigma^o_M-(1-(C1))(\sigma^o_U - \sigma^o_D)/2-((C1)-(C3)) A_3)/(1-(C2)) \quad \text{(D.20)}$$

$$A_1 = (\sigma^o_U - \sigma^o_D)/2 - A_3 \quad \text{(D.21)}$$

$$A_0 = \sigma^o_U - A_1 - A_2 - A_3 \quad \text{(D.22)}$$

The same equations can be reproduced by using σ^o_B, σ^o_{DB}, σ^o_{MB} and χ_M to obtain the values for a_0, a_1, a_2 and a_3 rather than A_0, A_1, A_2 and A_3 The slopes of the fitted curves at $\chi = 0°$ and 180° are zero for both methods of fitting the data, but the curvature needs to be negative. A test that

$$- A_1 \cos \chi - 4 A_2 \cos 2 \chi - 9 A_3 \cos 3 \chi < 0 \quad \text{(D.23)}$$

evaluated at $\chi = 0°$, and $\chi = 180°$ ensures this for both methods since for some conditions A_3 (or, a_3) can be negative.

Since the fits are good at either set of the three required points and at χ_M a linear combination of the natural and logarithmic fits can also be considered as in either Eq. (D.24) or (D.25) with subscripts N for natural and L for logarithmic. For values of D and E between zero and one, a Fourier series for either Eq. (D.24) or (D.25) would require many higher harmonics.

$$\sigma^o_N = D \sigma^o(\chi, A_0, A_1, A_2, A_3)+(1-D) 10\text{^}\sigma^o_B(\chi_M, a_0, a_1, a_2, a_3) \quad \text{(D.24)}$$

$$\sigma^o_L = E\,\sigma^o_B(\chi, a_0, a_1, a_2, a_3)+(1-E)\log_{10}(\sigma^o(\chi,A_0,A_1, A_2, A_3) \qquad (D.25)$$

Eqs. (D.24) and (D.25) for either version of the A''s and a's can be used to generate many different curves as a function of χ that all satisfy the chosen requirements. Since, say,

$$\sigma^o_{UB} = \log_{10}(A_0 + A_1 + A_2 + A_3) = a_0 + a_1 + a_2 + a_3 \qquad (D.26)$$

and there are more similar equations, the a's are complicated functions of the A''s so that there are only five parameters to be determined. The best way to determine them is not within the scope of this report.

ii. Examples

Wentz, et al. (1984) fitted backscatter in natural units to Eq. (D.1) with $N = 2$, which forced the minima as a function of χ to depend on the values of A_1 and A_2. The SASS -1 model was fitted in logarithmic form to Eq. (D.3) for $N > 3$ with the added constraint that $a_1 = 3\,a_3$ to force the minimum to be at 90°. So as to contrast these two methods of fitting the azimuthal variation, possible approximate values of the backscatter for vertical and horizontal polarization have been selected from Fig. 3 of *Li, et al*. (1988).

Table D.1, which used Eqs. (D.11) to (D.14) gives the values selected for backscatter at upwind, crosswind and downwind for vertical polarization in both natural and logarithmic form. If A_3 or a_3 is to be zero, the angle at which χ is a minimum is shown. The choice of χ_M is open, and the values of A_0, A_1, A_2, A_3, σ^o_M, a_0, a_1, a_2, a_3 and σ^o_{MB} for three different values of χ_M are tabulated.

Table D.2, again with Eqs. (D.11) and (D.14), gives similar values for horizontal polarization. The range of values for χ_M extends from 90° to 115°. Note that as χ_M increases the values of A_3 and a_3 can become negative. For the same backscatter values at upwind, downwind and crosswind, the range of possible values for χ_M can be considerable.

Table D.3 is based on Eqs. (D.17) and (D.22), and it uses χ_M and the antilog of σ^o_{MB} values from Table D.2 to obtain a natural fit to the curves. The values do not agree with those in Table D.2 as would be expected because the conditions are different.

For Table D.4, the value of χ_M is kept at 110° and σ^o_{MB} is varied to find the a's as well as its antilog to find the A's.

For Table D.5, σ^o_{MB} is kept at -2.7 dB, or its antilog, and χ_M is set to 100°, 105°, 115° and 120°. The values for 110° can be found in Table D.4.

TABLE D.1. Parameters for Sample Vertical Polarization Curves for Natural and Logarithmic Fits for σ^o_{UB} = -1.55, σ^o_{DB} = 1.60 and σ^o_{CB} = -2.30 (or Equivalently σ^o_U = 0.0282, σ^o_D = 0.0251 and σ^o_C = 0.00501) for Various Values of χ_M. For a_3 = 0°, χ_M is 91°. (Tabulated Values for A_1, A_2, etc. Have Been Multiplied by the Power of 10 Shown).

NATURAL					
χ_M	A_0(X 10^2)	A_1(X 10^3)	A_2(X 10^2)	A_3(X 10^4)	σ^o_M(X 10^3)
90°	1.58	1.15	1.08	3.83	5.01
92°	1.58	1.53	1.08	0	4.99
95°	1.58	2.10	1.08	-5.73	4.84
LOGARITHMIC					
χ_M	a_0	a_1	a_2	a_3	σ^o_{MB}
90°	-1.937	0.01875	0.3625	0.00625	-2.3
92°	-1.937	0.0314	0.3625	-0.0064	-2.301
95°	-1.937	0.05094	0.3625	-0.0259	-2.306

Table D.2. Parameters for Sample Horizontal Polarization Curves for Natural and Logarithmic Fits for σ^o_{UB} = -1.95, σ^o_{DB} = -2.35, σ^o_{CB} = -2.7 (or Equivalently σ^o_U = 0.0112, σ^o_D = 0.00447, σ^o_C = 0.002) and Minimum at χ_M.

NATURAL					
χ_M	A_0(x 10^3)	A_1(x 10^3)	A_2(x 10^3)	A_3(x 10^4)	σ^o_M(x 10^3)
90°	4.92	2.53	2.92	8.44	2.00
95°	4.92	2.77	2.92	6.03	1.95
100°	4.92	3.01	2.92	3.70	1.83
100.48°	4.92	3.03	2.92	3.47	1.82
105°	4.92	3.27	2.92	1.09	1.62
106.78°	4.92	3.38	2.92	0	1.51
110°	4.92	3.62	2.92	-2.40	1.23
115°	4.92	4.22	2.92	-8.40	0.441
LOGARITHMIC					
χ_M	a_0	a_1	a_2	a_3	σ^o_{MB}
90°	-2.425	0.1500	0.275	0.0500	-2.700
95°	-2.425	0.1734	0.275	0.0266	-2.704
100°	-2.425	0.1975	0.275	0.0025	-2.716
100.48°	-2.425	0.2000	0.275	0	-2.718
105°	-2.425	0.2265	0.275	-0.0265	-2.741
106.78°	-2.425	0.2392	0.275	-0.0392	-2.753
110°	-2.425	0.2679	0.275	-0.0679	-2.786
115°	-2.425	0.3426	0.275	-0.1427	-2.884

Table D.3. Parameters for Sample Horizontal Polarization Curves for Natural Fits with σ^o_{UB} = -1.95, σ^o_{DB} = -2.35 (or Equivalently σ^o_U = 0.0112 and σ^o_D = 0.004467) for Various Values of σ^o_M and χ_M.

σ^o_M(X 10^3)	χ_M	A_0(X 10^3)	A_1(X 10^3)	A_2(X 10^3)	A_3(X 10^4)
1.995	90°	4.92	2.53	2.92	8.44
1.977	95°	4.93	2.77	2.91	6.04
1.766	106.78°	5.03	3.33	2.81	0.44
1.306	115°	5.22	3.95	2.63	-5.73

Table D.4. Parameters for Sample Horizontal Polarization Curves for Fits to σ^o_{UB} = -1.95, σ^o_{DB} = -2.35 (or equivalently σ^o_U = 0.0112 and σ^o_D = 0.004467) For χ_M = 110° and Various Values of σ^o_M or σ^o_{MB}.

NATURAL				
σ^o_M(X 10^3)	A_0(X 10^3)	A_1(X 10^3)	A_2(X 10^3)	A_3(X 10^4)
1.995	5.24	3.45	2.607	-0.733
1.778	5.15	3.50	2.698	-1.209
1.585	5.07	3.54	2.778	-1.634
1.413	4.99	3.58	2.850	-2.01
1.259	4.93	3.61	2.19	-2.35
LOGARITHMIC				
σ^o_{MB}	a_0	a_1	a_2	a_3
-2.70	-2.389	0.249	0.239	-0.049
-2.75	-2.410	0.260	0.260	-0.060
-2.80	-2.43	0.271	0.281	-0.0709
-2.85	-2.453	0.282	0.302	-0.0819
-2.90	-2.472	0.293	0.322	-0.0929

Table D.5. Parameters for Sample Horizontal Polarization Curves For Fits to σ^o_{UB} = -1.95, σ^o_{DB} = -2.35 and σ^o_{MB} = -2.7 (or Equivalently σ^o_U = 0.0122, σ^o_D = 0.00467 and σ^o_M = 0.020) as χ_M is Varied.

NATURAL				
χ_M	A_0(X 10^3)	A_1(X 10^3)	A_2(X 10^4)	A_3(X 10^4)
100°	5.00	2.99	2.85	3.85
105°	5.09	3.21	2.75	1.65
115°	5.54	3.73	2.39	-3.57
120°	5.79	4.10	2.05	-7.23
LOGARITHMIC FIT				
χ_M	a_0	a_1	a_2	a_3
100°	-2.417	0.196	0.267	0.00399
105°	-2.406	0.220	0.256	-0.0205
115°	-2.362	0.285	0.212	-0.0849
120°	-2.3166	0.3333	0.1666	-0.1333

iii. Graphical Examples

In the following two figures (Parts A through D in Fig. D.1 and Parts A through D in Fig. D.2), the graphs show the versatility of four (plus 1) parameter fits for postulated azimuthal dependence of backscatter. All but one of the curves have their maxima at 0° and 180° for a given polarization. For Fig. D.1 the values at crosswind are fixed and the location of χ_M is varied. For Fig. d.2, horizontal polarization is used, the values at 0° and 180° are fixed and the values of σ^o_M, σ^o_{MB}, and χ_M are varied. The graphs are selected to show that a truncated Fourier series that only uses terms up to the third harmonic provide a large range of possible curves to fit experimental results. In particular, the value of χ_M can range from about 95° to 110° for horizontal polarization as, in part, a function of the upwind downwind difference according to *Li, et al*. (1988), their Fig. 8. The tables and figures show how these values can be fitted.

Fig. D.1, Parts A through F, provides graphs of some of the curves whose parameters are given in Table 1 and 2. Only the values from zero to 180° are shown because the functions are even through the origin. They can also be continued through reflection at 180° out to 360°.

Figs. D.1A curve 1, is the graph of σ^o calculated as a normal variable [Eq. (D.1)] but plotted as logarithms as found from Fig. D.1B, curve 1. Fig. D.1A, curve 3, is the graph of σ^o_B fitted as logarithms [Eq. (D.3)], which is converted to natural form as curve 3 in Fig. D.1B. All curves have a minimum at 90° for Figs. D.1A and D.1B.

Curve D.1A-2 is the average of the values for curves D.1A-1 and D.1A-3 and curve D.1B-2 is the average of curves D.1B-1 and D.1B-3. The logarithms of the values for curve D.1B-2 would not equal the values shown for curve D.1A-2. The constants *D* and *E*, can be used to fit one more point. At χ = 45° for example, a curve defined by Eq. (B.24) can be made to pass through any point between curves D.1A-1 and D.1A-3.

The changes in the shapes of these various curves is most interesting. Curve D.1B-1, fitted naturally, becomes a quite different shape plotted as logarithms that would not be described by the sum of three cosine harmonics in curve D.1A-1. The Seasat SASS azimuthal variation would give a curve similar to curve D.1A-3 for the first three harmonics, and it is quite possible that all of the rest of the fitting procedure, which was masked by the final form as a G-H table, tried to supply additional terms that would change curve 1A-3 to curve D.1A-1. It may be that azimuthally varying backscatter data ought to be fitted in terms of natural values and that four parameter fits, A_0, A_1, A_2,, A_3 (which implies a value for χ_M) will be sufficient. This possibility has yet to be demonstrated either empirically or theoretically, but the azimuthal variation of the SASS-1 model is clearly incorrect for horizontal polarization.

Curves D.1C-1 and D.1C-2 are for natural fits with minima at 90° and 95° plotted in logarithmic form.

Curves D.1D-1, D.1D-2 and D.1D-3 are for horizontal polarization fitted to natural values for χ_M at 90°, 100° and 110°.

Fig. D.1 shows that for the same choice of the values at 0°, 90° and 180° and various values of χ_M there are a large number of different curves that can satisfy the required conditions.

Fig. D.2A shows logarithmic fits with $\chi_M = 110°$ as σ^o_{MB} varies from -2.7 to -2.9 for five different curves.

Fig. D.2B, curves 1 and 2, are natural fits to minima at -2.7B and -2.9B plotted as logarithms and Fig. B.2B curves 3 and 4 are logarithmic fits plotted as logarithms. The regions between curves 1 and 3 and 2 and 4 can be fitted at one more value of χ by appropriate choices of E in Eqn. (D.25).

Fig. D.2C shows normal fits plotted logarithmically with the same value of σ^o_M but with χ equal to 100°, 105°, 115° and 120°.

Fig. D.2D curve 1 is a normal plot of a logarithmic fit. Curve 2 is a normal plot of a normal fit. Curve 3 is normal plot of a logarithmic fit, and curve 4 is a normal plot of a normal fit. Of all of the curves in these figures, curve 1 of Fig. D.2D is the only one that cannot be used since it has a maximum near 30° and not at 0°. It can easily be verified that the curvature is positive at 0° from Eq. (D.23).

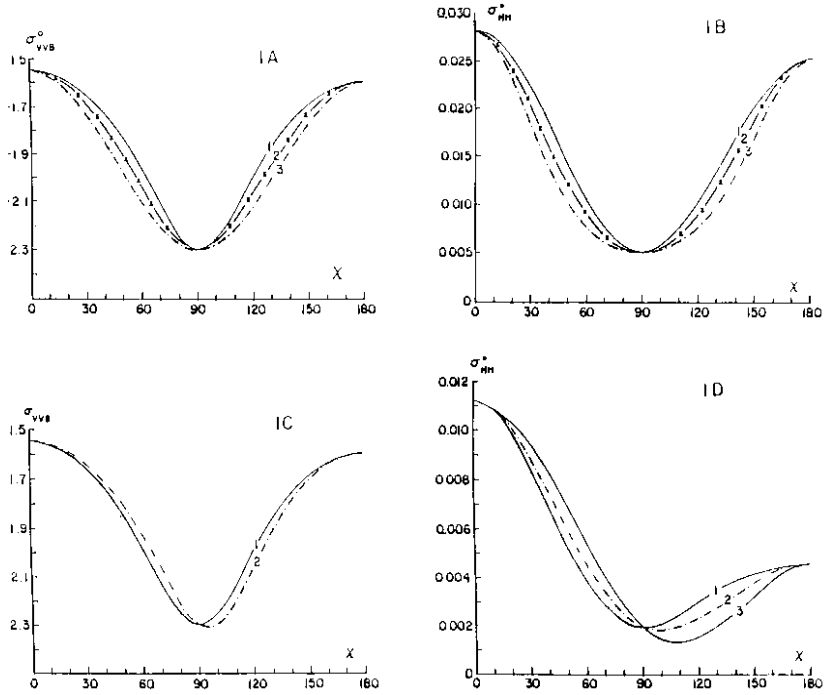

Figure D.1. Candidate natural and logarithmic plots to describe azimuthally modulated backscatter. Fitted at upwind, downwind and crosswind with a minimum to be at χ_M.

Curve	
A1	Natural fit; logarithmic plot.
A3	Logarithmic fit; logarithmic plot.
A2	Average of the logarithmic values.
B1	Natural fit; natural plot.
B3	Logarithmic fit; natural plot.
B2	Average of the natural values.
C1	Natural fit; logarithmic plot; minimum at 90°.
C2	Natural fit; logarithmic plot; Minimum at 100°.
D1	Natural fit; natural plot; minimum at 90°.
D2	Natural fit; natural plot; minimum at 100°.
D3	Natural fit; natural plot; minimum at 110°.

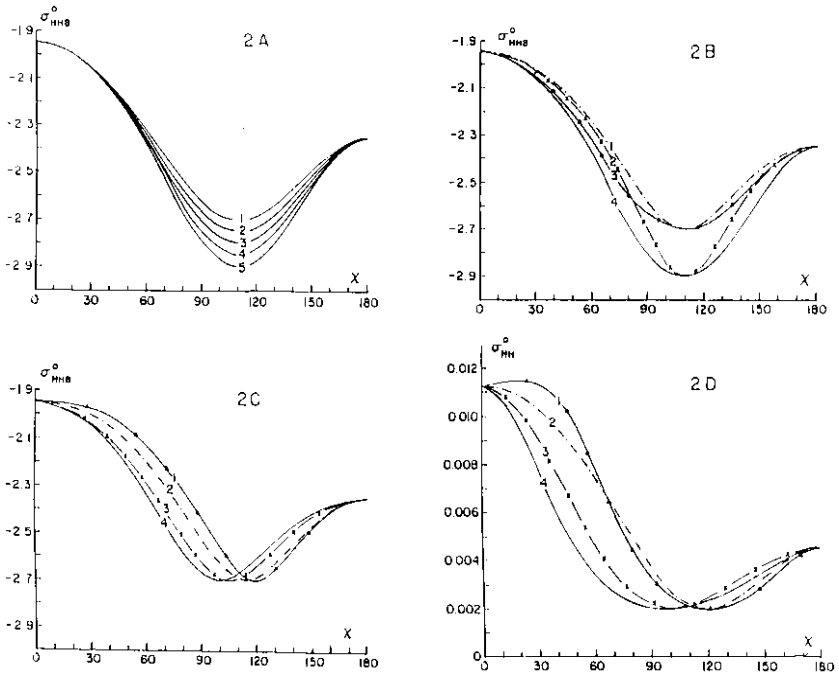

Figure D.2. Candidate natural and logarithmic plots to describe azimuthally modulated backscatter fitted at upwind and downwind and for a minimum value at an assigned angle.

Curve

A1-A5 Logarithmic fit; logarithmic plot; minimum at 110°.

B1 Natural fit; logarithmic plot; minimum at 110°.
B2 Natural fit; logarithmic plot; minimum at 110°.
B3 Logarithmic fit; logarithmic plot; minimum at 110°.
B4 Logarithmic fit; logarithmic plot; minimum at 110°.

C1 to C4 Natural fit; logarithmic plot; minimum at 100°, 105°, 115° and 120°.

D1 Logarithmic fit; natural plot; minimum at 120°.
D2 Natural fit; natural plot; minimum at 120°.
D3 Logarithmic fit; natural plot; minimum at 100°.
D4 Natural fit; natural plot; minimum at 100°.

E. Threshold wind speed and temperature dependance: recent results

The following is a brief summary of recent results obtained by Drs. W.J. Plant and M.A. Donelan.

An ideal scatterometer would yield a direct measure of the near surface wind (or stress) vector so that, carried by a satellite, it would be the ultimate global marine anemometer. However the normalized radar cross section, sigma-0 of a wind excited water surface depends on the dominant scattering mechanism and the response of the scatters to many properties of the air-sea interface. The principal source of energy for the scattering waves is the wind, although the breaking of larger waves will also generate centimetric scale waves. The principal dissipation mechanisms are wave breaking and viscosity. Wave breaking limits the slope of all waves and is by far the dominant mechanism for strongly forced waves. In light winds, on the other hand, the wave slopes may be too gentle to cause breaking and the dominant dissipation mechanism is the viscosity of the surface waters. In clean water viscosity is principally a function of water temperature, but the effective viscosity may be modified by dust on the surface or the presence of surfactants. Finally the longer waves can modulate the energy density of the short waves and tilt the surface, thereby changing the effective reflectivity to incident microwave radiation.

In this preliminary report we examine the results of a laboratory experiment on radar backscatter conducted during April 1996 at the Canada Centre for Inland Waters. The Ku-band radar response looking upwind and downwind (in turn) at 35°, 45°, and 55° incidence angle was explored at various wind speeds and water temperatures.

i. Experimental Set-up

The "Gas Transfer Flume" used has a working section of 32 m length and 76 cm width. The water depth was 22.5 cm and the air channel height was 62.5 cm. A 1.5 m section of the tunnel roof was made of Teflon through which the microwave signals passed. Looking upwind the microwave footprint on the water was at fetch of 10, 10 and 9.7 m for incidence angles of 35°, 45°, and 55°. Looking downwind, the corresponding fetches were 12.1, 12.4 and 12.5 m. At the end of the experiment these fetches were reduced by 5 m by the addition of a floating extension of the floor of the wind tunnel. Water temperature was varied between 8° C and 30° C and the wind speed from 0 to 16 m/s as measured about 20 cm above the surface.

ii. Threshold wind speed

The glassy appearance of the sea surface in very light winds indicates that the slopes of the centimetric waves, which are largely responsible for the microwave reflectivity, are vanishingly small. This clearly indicates that there is a "cut-off" or threshold wind speed below which Bragg scatterers are simply not generated nor sustained. If this threshold wind speed is determined by a balance between wind forcing and viscous dissipation -- it being intuitively obvious that in very light winds wave breaking contributes little to wave dissipation -- the minimum speed required to sustain waves will depend on the water viscosity and the wavenumber of the Bragg waves. The former depends on the water temperature and the latter on the incidence angle of the Ku-band radar.

a.Dependence of threshold wind speed on temperature

Figure E.1a (Run 29) shows sigma-0 at 45° incidence for various wind speeds (measured at 3 cm above the surface) and water temperature of 8° C, while Figure E.1b (Run 100) shows the response at water temperature of 29.4° C. The sharp change in sigma-0 at wind speeds around 2 m/s clearly indicates the threshold wind speed. This threshold wind speed is about 0.35 m/s lower at the higher temperature. This is just what would be expected, since water viscosity decreases with increasing temperature.

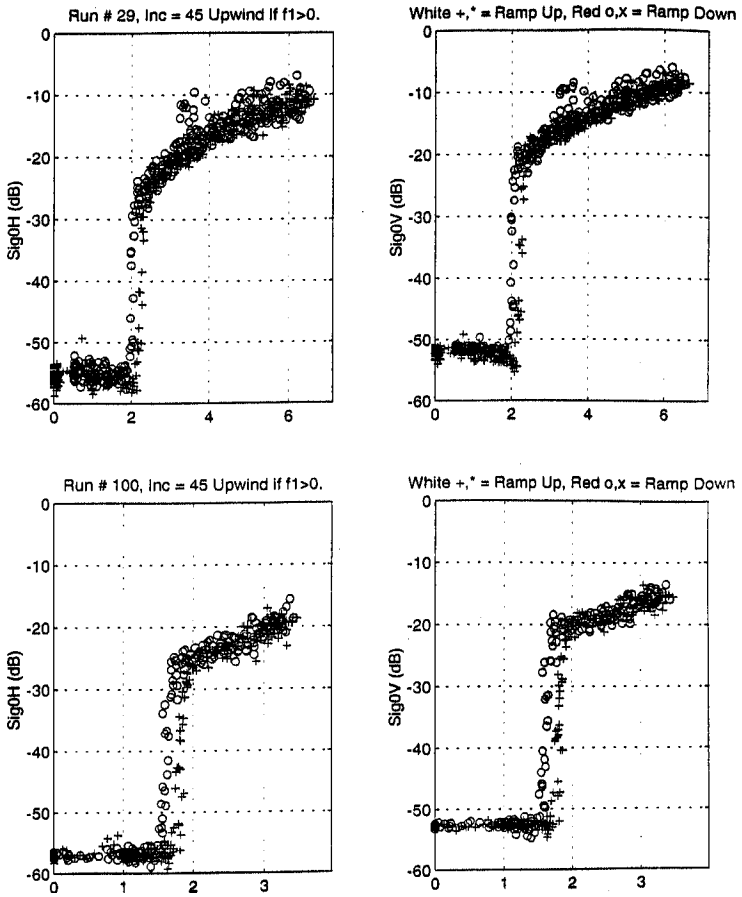

Figure E.1. Sigma-0 versus wind speed at Ku-band looking upwind at 45° incidence. The abscissa is the mean wind speed measured at 3 cm above the mean water level. (a) Top panels: air temperature = 18° C and water temperature = 8° C. (b) Bottom panels: air temperature = 22.7° C and water temperature = 29.4° C.

In Figure E.1, two sets of symbols appear designated as "ramp up" and "ramp down." This refers to the sign of the rate of change of wind speed with time. In order to explore the response of sigma-0 to changes in wind speed in a very narrow range near the threshold speed, we controlled the fan speed by computer in which the speed was made to increase from zero to some preset value ("ramp up") or to decrease to zero from some preset value ("ramp down"). In the latter case the wind was held steady until the wave field at 14 m fetch had come to equilibrium. Consequently, the disappearance of energy in any wavenumber range as the wind speed is reduced suggests that particular wavenumber could not be *sustained* by the wind at that level. In the case of the "ramp up" tests, on the other hand, the first appearance of waves at the Bragg wavelength requires the initiation of some surface disturbances by the breakdown of the shear layer in the water. Since this breakdown is a function of fetch -- occurring at lower wind speeds at longer fetch -- the sudden rise in sigma-0 with increasing wind reflects this breakdown. The fact that the "ramp down" sigma-0 values in the cut-off regions always lie at a lower wind speed than in the corresponding "ramp up" cases means that centimetric waves can be sustained at a lower wind speed than that required to initiate them -- at least at short typical wind-tank fetches. Thus, the "ramp down" cases more closely reflect what may happen at open ocean fetches and, unless otherwise stated, it is these that we will discuss.

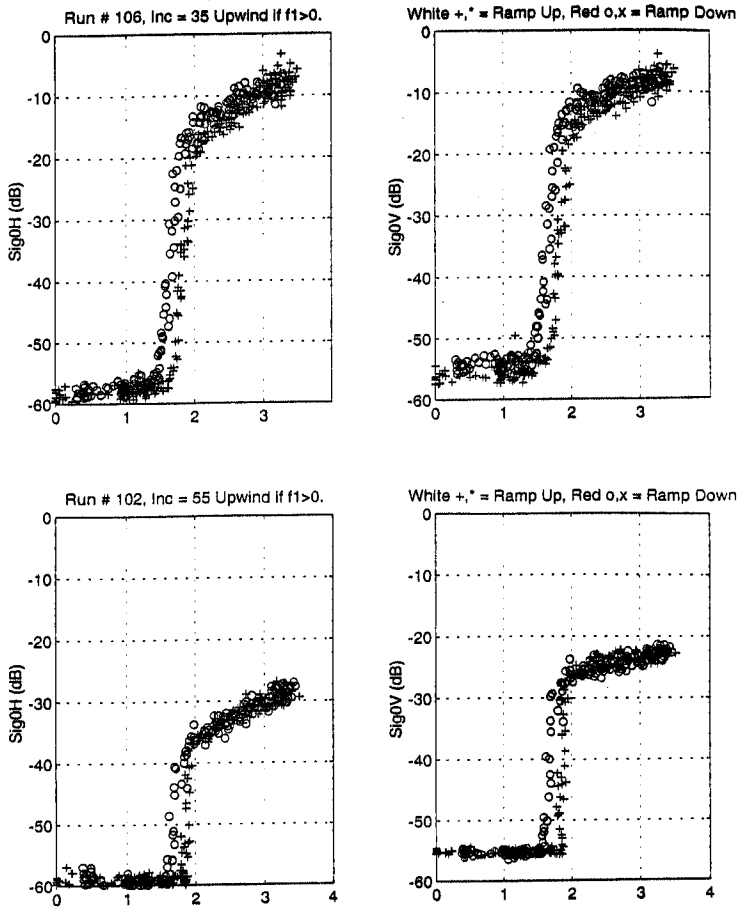

Figure E.2. Sigma-0 versus wind speed at Ku-band looking upwind. The abscissa is the mean wind speed measured at 3 cm above the mean water level. (a) Top panels: incidence angle = 35°, air temperature = 23.8° C and water temperature = 26.7° C. (b) Bottom panels: incidence angles = 55°, air temperature = 24.0° C and water temperature = 27.8° C.

b. Dependence of threshold wind speed on incidence angle

Figure E.2 (Runs 106 and 102) show the sigma-0 response to wind for 35° and 55°, respectively. The corresponding Bragg wavenumbers are 3.6 and 5.1 cm^{-1}. Thus, the Bragg wavenumber at 55° incidence is only 43% larger than that at 35° incidence. The cut-off speed is certainly larger in Figure E.2b (Run 102) at 55° incidence than in Figure E.2a (Run 106) at 35° incidence. Figure 4 and equation (13) of *Donelan and Pierson* (1987) give the cut-off ("threshold") wind speeds for Ku-band at various incidence angles. The speeds are given at one half wavelength or approximately 1 cm. In Figure E.2, the speeds were measured at 3 cm and so would be somewhat larger than those in *Donelan and Pierson* (1987). These are 1.29 and 1.50 m/s for 35° and 55°, respectively. Using a roughness length of 0.002 cm, the speeds at 3 cm would be 1.55 and 1.92 m/s. The threshold speeds from Figure E.2 (when sigma-0 just rises above the noise level of about -57 dB) are 1.4 and 1.65 m/s.

iii. Conclusions

These results establish that at moderate incidence angles the microwave radar return quickly decreases below a "threshold" wind speed. For steady winds, this represents the low limit of usefulness of scatterometers as anemometers. When the winds are variable, curves such as those shown in the above figures (but on linear scales) must be multiplied by the probability distribution of the wind speed and integrated to determine what cross section will be measured in any particular case. This means that such precipitous drops in cross section will be smoothed by wind variability and that the threshold wind speed at which a relatively stable cross section can be obtained may be somewhat higher than the stable wind values. The threshold wind speeds for steady winds decrease with increasing water temperature and increase with incidence angle or Bragg wavenumber as predicted by *Donelan and Pierson* (1987). Further analysis is continuing to explore the relative effects of long waves and the behavior of sigma-0 versus u_*, $U_{(\lambda/2)}$ or U_{10}.

iv. References

Donelan, M. A., and W.J. Pierson, Jr., "Radar Scattering and Equilbrium Ranges in Wind-Generated Waves with Application to Scatterometry," *J. Geophys. Res.*, Vol. 92, pp. 4971-5029, 1987.